ADVANCED HEALTHCARE MATERIALS
www.advhealthmat.de

Design and Properties of Antimicrobial Biomaterials Surfaces

Babak Mehrjou, Yuzheng Wu, Pei Liu, Guomin Wang,* and Paul K. Chu**

Emergence of antibiotic-resistance pathogens has caused serious health issues and if the current trend is to continue, treatment of the infection will become complicated and even unsuccessful due to new antimicrobial resistance (AMR). Therefore, there is a global drive to identify new methods to treat infection and develop better antibacterial materials and therapy. Although new and more potent antibiotics have aided the fight against microbes, they only offer a temporary solution because future bacteria strains may become resistant to these antibiotics and drugs. Recently, application of non-biological methods such as, electrical currents and photothermal/dynamic therapies to kill bacteria, reveal new approaches to design antimicrobial biomaterials, as complications stemming from drug-resistant bacteria can be obviated. Furthermore, recent research has focused on mimicking the surface patterns on plants and insects such as lotus leaves and dragonfly wings. Bio-inspired micro/nano patterns have been replicated on a variety of biomaterials to improve the bacterial resistance and other properties with good success. This is an exciting research area with immense practical and clinical potentials. In this review, recent advances in the application of chemical/biological approaches to combat bacterial infection and AMR are summarized and the related mechanisms are discussed.

1. Introduction

Human beings have been dealing with bacteria for as long as people exist. Some bacteria are vital, for example, those in the gastrointestinal system,[1–4] but others may cause infection to threaten human health. Primitive antiseptic methods include boiling in water, salts, and herbal medicine.[5] As medical technologies advance, antibiotics are frequently used to treat infection but extensive usage and abuse of antibiotics reduce the susceptibility of bacteria strains toward some antibiotics and drugs leading to the emergence of antimicrobial resistant (AMR) bacteria such as methicillin-resistant *staphylococcus aureus* (MRSA).[6,7] There are two solutions. The first approach is to develop new and more powerful antibiotics[8] but it may only be temporary because new super bacteria may evolve as a consequence. The second strategy is to develop biomaterials and implants that can kill bacteria upon contact.[9]

Researchers have been designing biomaterials that can avoid bacteria attachment, kill bacteria, and mitigate the formation of biofilms by modifying the surface properties.[10,11] Antibacterial polymeric coatings,[12] incorporation of antibacterial metallic nanoparticles,[13,14] biomimetic antibacterial surfaces,[15] and stimulation by electrical signal,[16] magnetic field,[17] and photon irradiation[18] have been proposed. For example, metallic nanoparticles[19,20] and antibacterial polymeric peptides[21,22] have been developed to combat AMR and antibacterial biomimetic design has garnered much interest.[23–25] Inspired by the intrinsic antibacterial and antifouling properties of some plants and insects such as lotus leaves,[26] rose petals,[27] insect wings,[28] gecko skin,[29] and others,[30–32] micro/nanopatterns have been replicated on biomaterials to achieve bacterial killing. Besides learning from nature, photons have been used to kill bacteria either directly or thermally[33] and electrical and magnetic stimuli have also been proven to have antimicrobial effects[34] and mitigate biofilm formation.[35]

To design antibacterial surfaces, various methods have been implemented based on the nature of the biomaterials and expected final features.[36,25] For example, in the case of biomimicking micro/nanopatterns found in the nature such as animals and plants, the common method is molding by pouring the molding materials, in most cases polymers like poly(dimethylsiloxane) (PDMS), on the patterns followed by peeling.[37,38] The complexity of the pattern and vulnerability under harsh mechanical/chemical conditions are the main reasons why the molding method is frequently chosen as the replication technique. In this way, by preserving most of the details in the pattern, high-quality replication can be accomplished. Lithographic methods,[39]

B. Mehrjou, Y. Wu, P. Liu, G. Wang, P. K. Chu
Department of Physics
Department of Materials Science and Engineering
and Department of Biomedical Engineering
City University of Hong Kong
Tat Chee Avenue, Kowloon, Hong Kong China
E-mail: bmehrjou2-c@my.cityu.edu.hk; guomiwang2-c@my.cityu.edu.hk; paul.chu@cityu.edu.hk
G. Wang
Shanghai Tenth People's Hospital, School of Medicine
Tongji University
Shanghai 200072, China

The ORCID identification number(s) for the author(s) of this article can be found under https://doi.org/10.1002/adhm.202202073

DOI: 10.1002/adhm.202202073

hydrothermal processing,[40] laser surface treatment,[41] and 3D printing[42,43] have been utilized to produce patterns resembling natural micro/nano patterns. Hydrothermal processing is mainly used for metallic biomaterials, whereas the other techniques are mainly used on metallic and polymeric biomaterials. Regarding photon-activated or electrically stimulated antibacterial surfaces, the active components are normally introduced to the surface by ion implantation, deposition, and coating techniques.[35,44–46] The choice also depends on the depth or thickness of the antibacterial layer.

In this review, recent advances pertaining to the design of biomimetic biomaterials and emerging methods such as photon irradiation and electrical stimulation are discussed and the various techniques are compared comprehensively in **Table 1**. This review aims at providing guidance to future research in this important field.

2. Biomimetic Surfaces Inspired by Nature

Many structures existing in nature[131–134] repel bacteria and have antimicrobial effects, for example, lotus leaves,[26] insect wings,[135] shark skin,[32] and gecko skin.[29] These structures have been analyzed and artificial micro/nano patterns resembling them have been fabricated on artificial biomaterials.[136] It has also been shown that micro/nanopatterned surfaces can regulate immune systems by macrophage polarization toward the repair-like state.[137,138] To improve the effectiveness, nature-inspired techniques can be combined with other common bactericidal methods like conjugation of antimicrobial peptides and polymeric brushes[139–142] or loading of antimicrobial metals.[143–145] However, because these traditional bactericidal agents and techniques are quite well known and some of them are prone to causing bacterial resistance, they are excluded from this review.

2.1. Biomimetic Micro/Nano Topography

Ivanova, et al.[47] were among the first reporting nanopatterns on the surface of cicada wings (*Psaltoda claripennis*) (**Figure 1**a–c). The superhydrophobic structure consisting of closely packed nanoarrays with a high aspect ratio kills bacteria swiftly (within 3 min) and provides a surface that is bacteria-free and antireflective as well (Figure 1d,e). The effects are not chemical as coating the surface of wings with gold shows the same effects. However, cicada wings are only effective against gram negative strains, whereas gram positive ones can survive and adapt better to the physical environment.[28] There have been a lot of efforts to mimic and replicate these structures on artificial biomaterials to kill gram positive strains and widen the scope to other applications such as food packaging. The wings of different cicada species have different surface structures[146] in terms of the spacing, height, and width and can be replicated with high resolution by molding biopolymers. In addition, mask-less reactive ion etching,[147–149] electron beam lithography,[150] fabrication of scalable hexagonally close-packed arrays of nanospheres with different dimensions by colloidal lithography,[39,151,152] spin coating,[153] and reactive ion etching have been demonstrated to produce these patterns on biopolymers.[48]

Hydrophobic and superhydrophobic surfaces repel bacteria and living organisms[154–156] but the low surface energy also reduces cell attachment,[49] although surfaces that are not hydrophobic have been used to foster cell proliferation in biomedical applications.[157–161] Kim, et al.[49] have shown that hydrophobic (water contact angle = 114°) nanopatterned poly(methyl methacrylate) prepared by photolithography and molding not only repels bacteria (*P. aeruginosa*), but also reduces attachment of C2C12 myoblast cells. This is related to the surface energy and the size difference between mammalian cells and bacteria. Therefore, nanopatterns which can repel and kill bacteria remain harmless to cells. Mammalian cells can tolerate surface topographies varying from 50 to 500 nm in diameter and 0.5 to 2 μm in height by engulfing the structure without rupturing or cell wall damage.[162] Superhydrophobic surfaces can be prepared by etching biomaterials with a fluorinated gas to repel both gram-negative and gram-positive bacteria.[149,163,164] However, surface chemistry is not the only factor determining the antibacterial properties, as the nanofeature dimensions, type of bacteria strains, and biomaterials properties impact bacteria attachment and antibacterial properties as well.[165] Nanopatterns are normally more effective on gram-negative bacteria than gram-positive ones due to the different cell walls.[29,47,166,52] Arias et al.[51] have shown that if bacterial cellulose (BC) is etched by low-energy argon ions, the formed nanopatterns with a high aspect ratio kill gram-positive bacteria (*B. subtilis*) more effectively than gram-negative bacteria (*E. coli*). However, in spite of the success against *B. subtilis*, it is ineffective against another gram-positive strain (*S. aureus*). Even though *E. coli* has a thinner membrane, it is more resilient and can spread the mechanical force more efficiently to avoid rupturing. It was revealed that by applying a force with the AFM cantilever tip, a smaller force is needed to rupture the *B. subtilis* cell membrane compared to *E. coli*, that is, 0.74 nN compared to 1.04 nN, respectively (**Figure 2**a).

Although hydrophobic or superhydrophobic surfaces repel bacteria, the small surface energy prohibits the surface friendly to mammalian cells. Hence, they can be implemented on food packaging,[165] coatings on non-implantable biomedical tools,[167,168] and anti-stain fabrics,[169] but not suitable for implantable biomaterials. Pham et al.[53] have used black silicon (bSi) with a high bactericidal potential[170] to realize cell attachment and proliferation on a pre-infected surface if the antibacterial efficacy is adequate. Reactive ion etching using a mixture of SF_6 and oxygen forms nanoarrays of bSi which is bactericidal against *S. aureus* and *P. aureginosa*. Although this structure mimics the cicada wing, it is not superhydrophobic and therefore, COS-7 cells can attach and proliferate on the pre-infected samples (for 6 h) (Figure 2b). In vivo implantation into CD-1 mice shows that after 15 days, only minimal bacterial infection is observed. Inspired by this study, nanocones are fabricated on a silk substrate by oxygen plasma etching to produce a hydrophilic surface with both antibacterial and cell supporting characteristics. The surface energy increases after plasma etching.[50] Although the silk nanocones can be evaded by bacteria subsequently escaping the fatal destiny, the main achievement is that mammalian cells win in the fight against bacteria and the bacteria-free surface facilitates cell attachment and growth (Figure 2c–n). Another cell-friendly antibacterial platform has been prepared by Mo et al.[54] Various nano/micro structures are fabricated by

Table 1. Summary of recent results obtained from antibacterial platforms based on AMR-free strategies, biomimetic surfaces, photon-based therapies, and electrical stimuli.

No.	Strategy	Antibacterial features	Functional components	Bacteria	Substrates	Refs.
1	Biomimetic surface	Naturally occurred nanostructures	–	*P. aeruginosa* *B. subtilis* *B. catarrhalis* *P. maritimus* *P. fluorescens* *E. coli* *S. aureus*	Cicada wing	[28, 47]
2	Biomimetic surface	Nanopyramids	–	*E. coli*	PS	[48]
3	Biomimetic surface	Nanopatterns	–	*P. aeruginosa* *E. coli*	PMMA	[49]
4	Biomimetic surface	Nanocones	–	*E. coli* *S. aureus*	Silk	[50]
5	Biomimetic surface	Nanopatterns	–	*E. coli* *S. aureus* *B. subtilis*	Bacterial cellulose	[51]
6	Biomimetic surface	Nanopattern	–	*P. aeruginosa*	Diamond	[52]
7	Biomimetic surface	Nanopattern	–	*S. aureus* *P. aeruginosa*	Black silicon	[53]
8	Biomimetic surface	Micro/nanopatterns	–	*E. coli*	PEEK	[54]
9	Biomimetic surface	Nanopatterns	–	*E. coli* *S. aureus*	PDMS	[55]
10	Biomimetic surface	Micellar, vertical, and parallel cylindrical	–	*E. coli* *S. aureus*	Poly(styrene-block-2-vinylpyridine)	[56]
11	Biomimetic surface	Nanoripple	–	*S. aureus*	PLA	[57]
12	Biomimetic surface	Nanoripple	–	*E. coli*	PET	[58]
13	Biomimetic surface	Nanopatterned	–	*E. coli*	Aluminum	[59]
14	Biomimetic surface	Nanopatterned	–	*P. aeruginosa* *S. aureus*	VACNTs	[60]
15	Biomimetic surface	Nanospikes	–	*E. coli*	Ti	[61]
16	Biomimetic surface	Nanoarrays	–	*E. coli* *S. aureus*	Ti	[62]
17	Biomimetic surface	Nanopattern	–	*P. aeruginosa* *S. aureus*	Ti	[63]
18	Biomimetic surface	Nanopattern	–	*S. aureus* *P. aeruginosa*	Ti	[64]
19	Biomimetic surface	Nanopattern	–	*S. aureus*	Ti	[65]
20	Biomimetic surface	Nanoflake	–	*E. coli* *S. aureus*	Mg	[66]
21	Biomimetic surface	Nanopattern	–	*E. coli* *S. aureus*	AZ31	[67]

(*Continued*)

Table 1. (Continued).

No.	Strategy	Antibacterial features	Functional components	Bacteria	Substrates	Refs.
22	Biomimetic surface	Nanopattern	–	*E. coli*	PDMS	[68]
23	Biomimetic surface	Micro/nanostructure	–	*E. coli*	Silicon	[26]
24	Biomimetic surface	Rose petals micro/nano structures	–	*S. epidermidis* *P. aeruginosa*	PDMS	[69]
25	Biomimetic surface	Rose petal micro/nano structures	–	*Micromonospora purpurea* *Serinicoccus chungangensis* *Kocuria marina* *Bacillus licheniformis*	Supramolecular gelator G1 and G2	[27]
26	Biomimetic surface	Rice leaf pattern	–	*E. coli* *S. aureus*	Polypropylene (PP)	[70]
27	Biomimetic surface	*Laminaria japonica*	–	*E. coli*	PDMS	[37]
28	Biomimetic surface	Moth eye	–	*E. coli* *S. aureus*	PEG	[71, 72]
29	Biomimetic surface	Shark skin	–	*E. coli* *S. aureus*	Chitosan/GO	[73]
30	Biomimetic surface	Urchin	–	*E. coli*	PLLA	[31]
31	Biomimetic surface	Nanoholes	–	*E. coli* *S. aureus*	MoS_2	[74]
32	Biomimetic surface	Nanospike	–	*E. coli* *S. aureus*	Ti	[75]
33	PDT	High $^1O_2$ quantum yield	Methylene blue	*MRSA*	Cyclodextrin modified hyaluronic acid	[76]
34	PDT	Synergy of ROS and Cu^{2+}, Zn^{2+}	Cu2O/ZnO	*S. aureus*	Indium tin oxide conductive glass	[77]
35	PDT	Physical action and enhanced ROS production	GO/AgNPs/Collagen	*E. coli* *S. aureus*	Ti	[78]
36	PDT	ROS generation	Ce6	*E. coli* *S. aureus*	PVDF/PTFE; GelMAc/MPDA	[79, 80]
37	PDT	Enhanced ROS generation and IPCE	TiO2/BTO/Au heterojunction	*E. coli* *S. aureus*	TiO2/BTO/Au	[81]
38	PTT	ROS generation, increased temperature, low cytotoxicity	Vertical graphene	*E. coli* *S. aureus*	Ti	[82]
39	PTT	ROS generation, increased temperature, charge affinity toward bacteria cell wall, low cytotoxicity	Carboxyl graphene	*E. coli* *S. aureus* *MRSA*	Glycol chitosan	[83]
40	PTT	NIR-responsive TiOx	TiOx	*E. coli* *S. aureus*	Ti	[44, 84]
41	PTT	Sterilization by mild PTT	ZnL2-modified BPs	*E. coli* *S. aureus*	3D-printed scaffold	[85]
42	PTT	Synergy of AuNPs and MXene	MXenes with various shapes	*E. coli* *S. aureus*	Chitin sponges	[86]

(*Continued*)

Table 1. (Continued).

No.	Strategy	Antibacterial features	Functional components	Bacteria	Substrates	Refs.
43	PTT	Spatial separation reduces cell damage from PTT	Micro-featured thermal-responsive hydrogel embedded with Au nanostars	*S. aureus*	PDMS film	[87]
44	Synergy strategy	PTT and enhanced PDT	PB and PCN-224 heterojunction	*S. aureus*	PB-PCN-224	[88]
45	Synergy strategy	Synergy of PDT, PTT, and antibiotic	PDA, IR820, Daptomycin	*S. aureus*	Ti	[89]
46	Synergy strategy	PDT and enhanced PTT	Au nanoparticles, carbon quantum dots	*E. coli* *S. aureus*	Ti	[90]
47	Synergy strategy	ROS production via PTT and SDT	S-doping TiO_{2-x}	*S. aureus*	Ti	[91]
48	UST	ROS generation	Au@$BaTiO_3$; HNTM-Pt@Au; HNTM-MoS_2; ZTNs; Pd@Pt-T790	*S. aureus* *E. coli* *MRSA* *E. faecium*, *K. pneumoniae*, *A. baumannii*, *P. aeruginosa*, *K. aerogenes*	–	[92–96]
49	UST	ROS generation	Red phosphorus	*MRSA*	Ti	[97]
50	Electrical Stimulus	Low current	Silver positive electrode	*E. coli* *S. aureus*	–	[98, 99]
51	Electrical Stimulus	Lontophoresis	Gold, carbon, and platinum electrodes	*E. coli* *Candida albicans* *P. aeruginosa* *P. mirabilis* *K. pneumoniae*	–	[100]
52	Electrical stimulus	Direct current (DC)	Carbon-containing electrodes	Normal microorganisms on human intact skin	–	[101]
53	Electrical stimulus	Novel electrochemical reactor	Carbon-cloth Electrodes	*E. coli*	–	[102]
54	Electrical stimulus	Electrical stimulus with biocide	Platinum wire	*P. aeruginosa* biofilms	–	[103]
55	Electrical stimulus	AC and DC electrical stimulation	–	*E. coli* *P. aeruginosa* *S. aureus*	–	[104]
56	Electrical stimulus	High voltage pulsed current	Stainless-steel wires	*S. aureus* *E. coli* *P. aeruginosa*	–	[105]
57	Electrical stimulus	DC	ITO	*S. salivarius* *A. naeslundii*	Glass plates	[106]
58	Electrical stimulus	DC	Stainless steel	*S. epidermidis*	–	[107]
59	Electrical stimulus	Electromagnetic field	Stainless steel	Bacteria in river water	–	[108]

(*Continued*)

Table 1. (Continued).

No.	Strategy	Antibacterial features	Functional components	Bacteria	Substrates	Refs.
60	Electrical stimulus	Low-frequency electromagnetic fields	Copper wire	*H. pylori* Biofilm	–	[109]
61	Electrical stimulus	Magnetic field-induced shape changes	Magneto responsive LM	Biofilms of *P. aeruginosa, S. aureus, and E. coli*	Gallium-based LM droplets	[110, 111]
62	Electrical stimulus	Magnetoelectric conversion	TD/P(VDF-TrFE)	*S. aureus* *E. coli*	Stainless steel	[112]
63	Electrical stimulus	Magneto-thermal conversion	Fe_3O_4–ZnO, Fe_3O_4@SiO_2, $CoFe_2O_4$@$MnFe_2O_4$, Fe_2C@Fe_3O_4-PEG nanozymes	*S. aureus, E. coli* and their biofilms	Nanomaterials	[113–116]
64	Electrical stimulus	Polycationic groups	DMAEMA	*E. coli*	PET film	[117]
65	Electrical stimulus	Polycationic groups	PDMAEMA	*E. coli*	PP	[118]
66	Electrical stimulus	Quaternary ammonium	Quaternary ammonium monomers on DMAEMA	*E. coli* *S. aureus*	Polystyrene	[119]
67	Electrical stimulus	Quaternary ammonium	Quaternary ammonium silane	*E. coli*	Polyurethane catheters	[120]
68	Electrical stimulus	Quaternary ammonium	*N*-(2-ethoxy-2-oxoethyl)*N*,*N*-dimethylprop-2yn-1-aminiumbromide(edmpabr)	*E. coli*	Cellulose	[121]
69	Electrical stimulus	Cationic peptide	Plectasin-derived peptide MP1106	*S. aureus*	–	[122]
70	Electrical stimulus	Cationic peptide	Cationic antimicrobial peptides	*E. coli* *S. aureus* *K. pneumoniae* *A. baumannii* *E. faecalis* *P. aeruginosa*	–	[123]
71	Electrical stimulus	Cationic peptide	Tripeptides	*Candida albicans*	–	[124]
72	Electrical stimulus	Positive charge	Ethylenediamine	*S. mutans*	Graphene oxide nanosheets	[125]
73	Electrical stimulus	Micro-galvanic	Silver nanoparticles	*S. aureus* *E. coli*	Ti	[45, 126]
74	Electrical stimulus	Electron transfer	Silver nanoparticles	*E. coli*	Ti	[127]
75	Electrical stimulus	Electron transfer	Graphene oxide	*E. coli*	Zn, Ni, Sn, and steel	[128]
76	Electrical stimulus	Electron transfer	Gold nanoparticles	*S. aureus* *E. coli*	Titania nanotubes	[129]
77	Electrical stimulus	DC charge	Silver nanoparticles	*S. aureus*	Polypyrrole	[130]
78	Electrical stimulus	Capacitance	Carbon-doped titania nanotubes	*S. aureus* *E. coli*	Titanium	[35]
79	Electrical stimulus	Electron transfer	Gold coated ZnO nanorod	*S. aureus* *E. coli*	Titanium	[46]

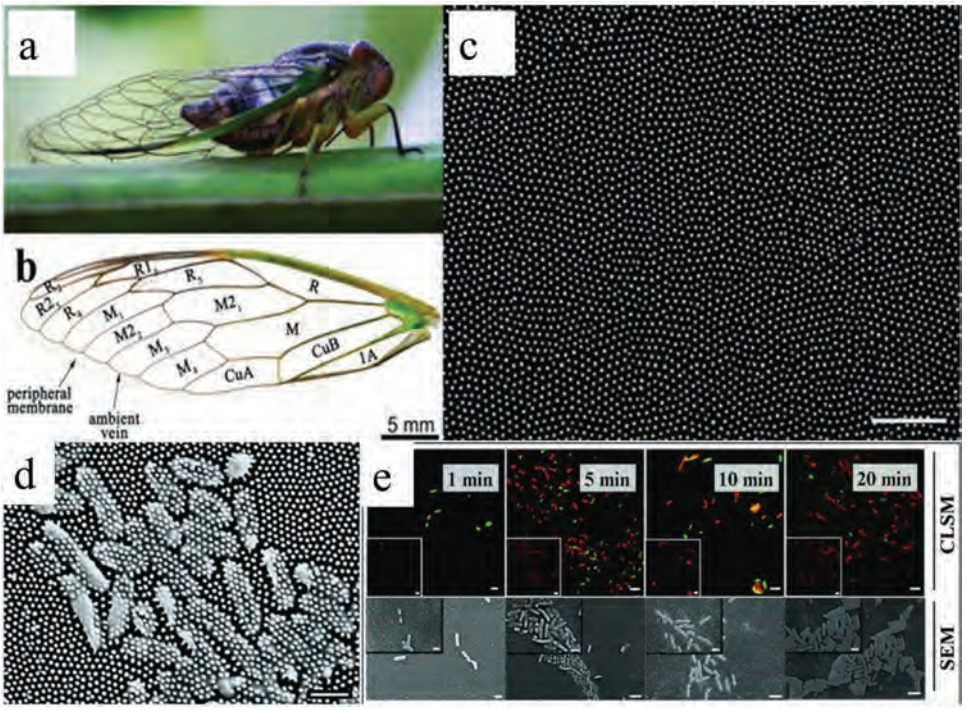

Figure 1. a) Photograph of cicada (*Psaltoda claripennis*). b) Wing of the cicada wing. c) SEM image of the cicada wing (scale bar = 2 µm). d) SEM image of *Pseudomonas aeruginosa* on the cicada wing showing the bacteria cell walls clearly penetrated by the nanopillars (scale bar = 1 µm). e) Confocal laser scanning microscopy (CLSM) images of the bacteria cultured on the cicada wing after 1, 5, 10, and 20 min with dead and live bacteria indicated by red and green color, respectively (scale bar = 5 µm). Reproduced with permission.[47] Copyright 2012, Wiley-VCH GmbH.

colloidal lithography and reactive ion etching. The results show that micropillars have better antibacterial properties than the other micro/nanostructures due to the 2D lateral plates on the edge of the pillars and high adhesion tendency of bacteria. The higher surface hydrophilicity after oxygen plasma etching distorts the *E. coli* cell wall as the bacteria try to anchor on the surface. In contrast, owing to the more restricted contact with nanocones, the only bactericidal force occurs by penetration of sharp tips into the cell wall and so they can bend the nanocones or modify their own cell wall shape to overcome the harsh environment.

Besides bio-mimicked surfaces designed according to insect wings, nanostructured surfaces which are not representative of natural ones can also reduce bacteria attachment. Molding,[55] block co-polymer assembly,[56] and laser treatment[57–58,171] can be utilized to fabricate surface nanofeatures with antibacterial properties. These platforms show distinctive behavior regarding bacteria and mammalian cells. They are harmless to cells and promote their attachment and proliferation while offering antimicrobial effects.[55,56] In the treatment of poly-lactic acid (PLA),[57] the laser parameters affect the surface hydrophilicity/hydrophobicity but not the surface chemistry. The nanofeatures reduce bacteria attachment and orient mesenchymal stem cells (MSCs) proliferation along the grooves. Nanoripples fabricated on poly(ethylene terephthalate) (PET) foils by the laser treatment[58] exhibit different surface chemistry and increased hydrophilicity. The nanoripples reduce *E. coli* attachment and the effect stems from repulsion rather than direct killing. Laser surface treatment is also effective for metallic materials.[172–175] Boinovich et al.[59] have produced superhydrophilic and superhydrophobic structures. The former is more effective against *E. coli* due to stronger adhesion between the rough laser-treated surface and bacteria cell wall, which results in high tension and cell wall rupturing. The nanostructures fabricated by the laser surface treatment can be coupled with other techniques to produce enhanced antibacterial properties. Doll et al.[176] have prepared nanospikes by a laser treatment and then covered them with a fluorinated polymer to form a slippery liquid-infused porous surface to prohibit biofilm formation of *S. oralis*. However, the surface also repels human cells and may not be suitable for some applications.

Polymeric biomaterials are widely used but most of them do not have adequate bacterial resistance and hence, nanofeatures are created to improve the properties as discussed above. The same strategy can be applied to metallic biomaterials. Titanium, magnesium, and their alloys are common in implants. Ti and Ti alloys do not have inherent antibacterial properties and Mg alloys suffer from easy corrosion despite having favorable bactericidal properties. Moreover, it is difficult to administer antibiotics after surgical insertion of Ti implants because of AMR and therefore, alternative measures must be implemented to mitigate bacterial infection.

Thermal and chemical treatment,[40,61,177–181] sand blasting,[182] electrochemical additive manufacturing,[183] sputtering,[184,185] and imprinting followed by hot water treatment[186] have been proposed to alter the surface topography of metallic substrates to improve the antibacterial properties. By forming nanospikes on Ti alloys by thermal oxidation,[61] bone[187] and dental implants[188] have been designed. Fabrication of TiO_2 nanotubes

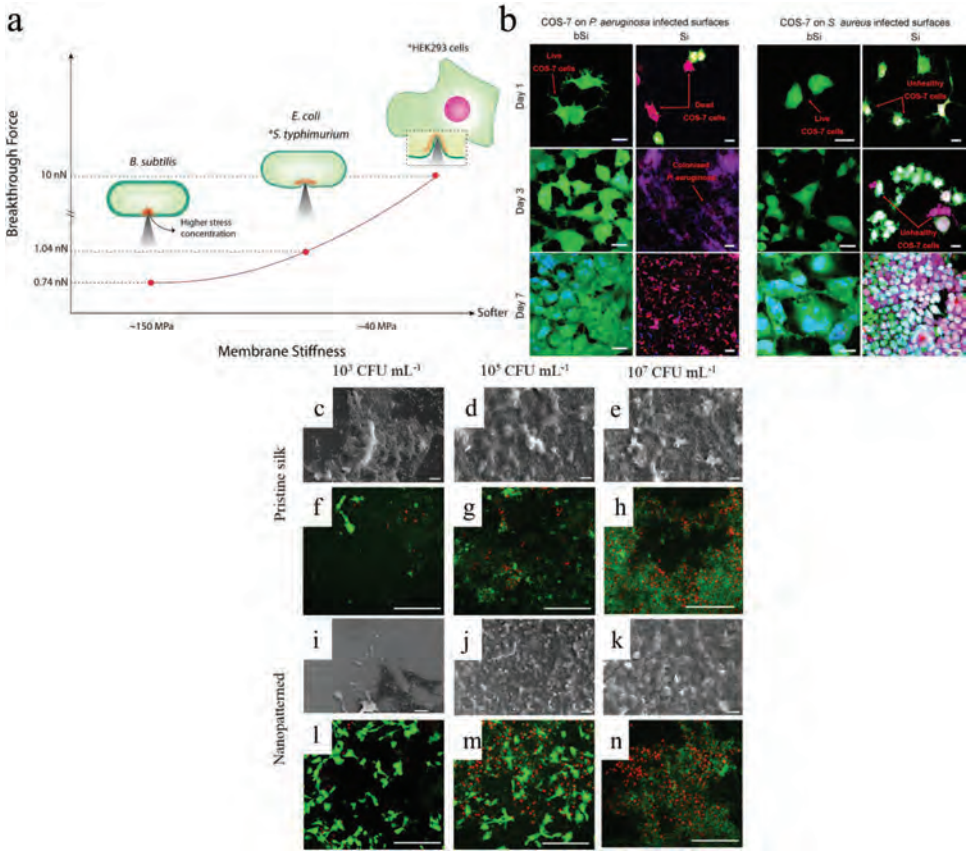

Figure 2. a) Schematic diagram of the needed force to rupture *B. subtilis*, *E. coli*, *S. typhimurium*, and HEK293 cells membrane. Reproduced with permission.[51] Copyright 2020, ACS publishing. b) Confocal laser scanning microscopy images of COS-7 cells on the pre-infected surfaces for both bSi and Si with *S. aureus* and *P. aeruginosa* after culturing for 1, 3, and 7 days. The live cells, dead cells, and viable bacteria are stained green, red, and blue, respectively, and the scale bars is 20 µm. Reproduced with permission.[53] Copyright 2016, ACS publishing. c–n) Fluorescent and SEM images of the pre-infected silk substrate with different concentrations (10^3, 10^5, and 10^7 CFU mL^{-1}) of *S. aureus* cultured for 6 h, followed by culturing with MC3T3 cells for 24 h. The red and green signals are the dead and live microorganisms and the scale bars in the SEM and fluorescent images are 10 and 250 µm, respectively. Reproduced with permission.[50] Copyright 2019, ACS publishing.

with a tunable distance, height, and diameter can also impede bacteria development. Ge et al.[62] have shown that although arrays of TiO_2 cannot killed bacteria (both *E. coli* and *S. aureus*), bacteria development such as cell division can indeed been hampered. The optimal implants should offer sufficient bacteria resistance while allowing cells to grow during healing. Bright et al.[63] have introduced nano-roughness to biomedical grade titanium (Ti-6Al-4 V) by hydrothermal etching and assessed bacteria survival and biofilm formation for *P. aeruginosa* and *S. aureus* for 21 days. The biocompatible and hydrophilic surface not only supports macrophage (RAW 264.7) attachment and proliferation, but also suppresses bacteria and biofilm formation. In the case of the gram-negative strain, *P. aeruginosa*, the survival suppression rate is more than 90% after 21 days as manifested by a thick layer of dead bacteria, although small colonies of live bacteria are found on the dead ones. The observation from *S. aureus*, gram positive bacteria, is different from that from *P. aeruginosa*. The maximum bactericidal effect is observed on the 3rd day and rebound in bacteria colonization is detected afterward. This difference stems from the different cell walls and cell division time which can alter the cell membrane integrity, vulnerability, and so on leading to expression of the extracellular death factor. Wandiyanto et al.[64] have demonstrated that by introducing nano-roughness to pure Ti by hydrothermal treatment, Mg-63 cells can attach to the surface pre-infected with *S. aureus* and *P. aeruginosa* for 6 h. The bacteria are repelled from the surface in the first 3 h and it is more prominent for *P. aeruginosa*, as it takes a longer time for *S. aureus*. In both cases, the MG-63 cells find the bacteria-free space which is not available on the untreated Ti. Hydroxyapatite (HA) nanofeatures incorporated with strontium (Sr) and fluorine (F) fabricated on Ti have good antibacterial properties against *S. aureus* even after 28 days.[65] By doping with 5% F, cell adhesion and proliferation are not affected significantly but the bactericidal properties improve remarkably. To verify the in vitro results, in vivo tests conducted on rabbits reveal osteogenesis and antibacterial effects after 8 weeks.

Magnesium alloys degrade naturally in the physiological environment and implants made of Mg alloys do not require a second operation for removal. They also possess good antibacterial properties, but the corrosion resistance is poor due to dissolution in body fluids and Mg ions leached from implants can cause toxic effects and inflammation. A hydrothermal treatment can improve the corrosion properties of pure Mg while preserving the antibacterial properties by forming nanoflakes on the surface.[66] After

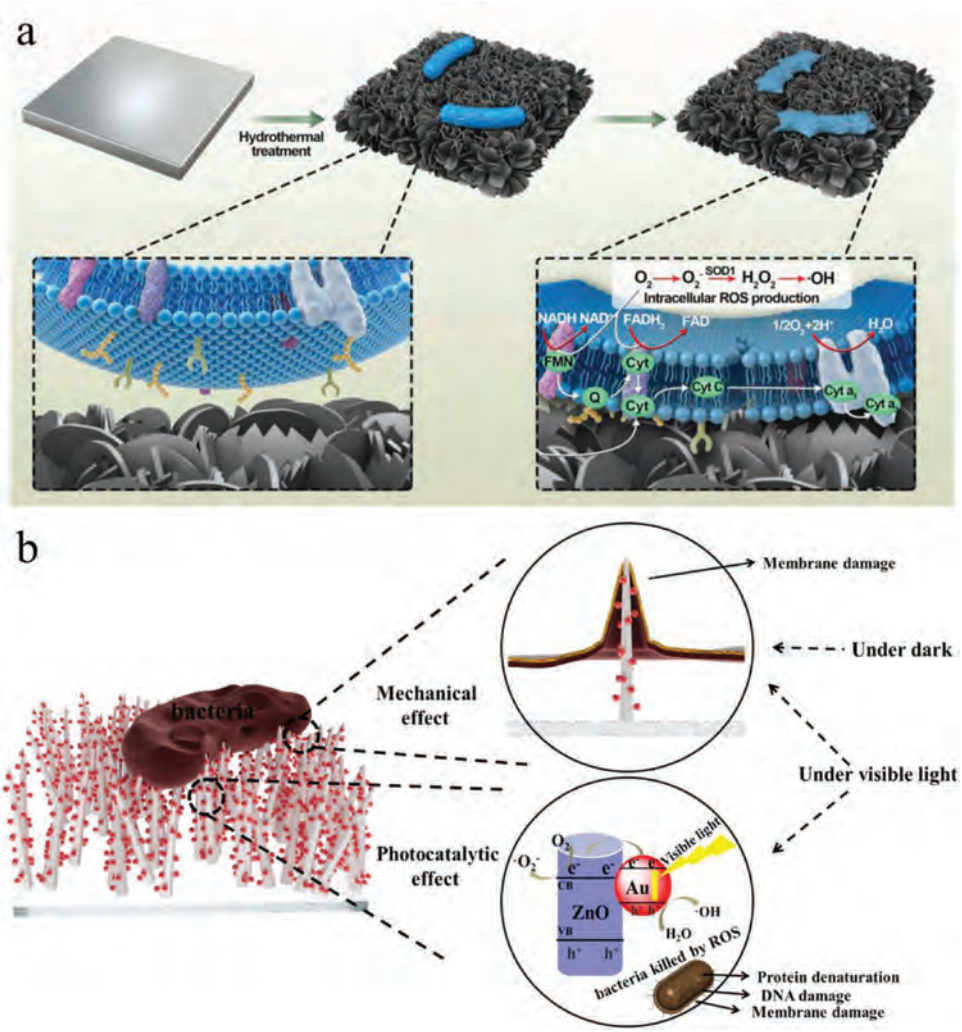

Figure 3. a) Proposed antibacterial mechanism for the hydrothermally treated pure Mg showing the nanoflakes exerting stress on the bacteria cell membrane and the changing oxidation–reduction potential causing secretion of ROS resulting in bacteria killing. Reproduced with permission.[66] Copyright 2020, Wiley-VCH GmbH. b) Schematic illustration of dual-antibacterial functions rendered by the physical barrier of the sharp ZnO nanorods and photocatalytic effects of Au nanoparticles. Reproduced with permission.[68] Copyright 2020, Elsevier.

the 12-h hydrothermal treatment, the corrosion current, I_{corr}, of pure Mg decreases by 97% and furthermore, more than 99% of bacteria are killed in 3 h after introducing 100 µL of the bacteria suspension. The bactericidal properties can be attributed to stretching of the cell membrane and production of reactive oxygen species (ROS) (**Figure 3**a). This technique is helpful to overcome inflammation triggered by leaching of Mg ions as indicated by the in vivo results. Polymeric coatings can mitigate magnesium corrosion but most polymeric materials do not have intrinsic antibacterial properties. However, the silk coating with nanopatterns mimicking the cicada wing nanostructure formed on AZ31 Mg shows both reduced corrosion and enhanced antibacterial properties.[67]

Another strategy is to combine different AMR-free antibacterial techniques. For example, nanopatterning can be combined with photon-based therapy.[68] ZnO nanorods can be prepared on the surface of PDMS to mimic the cicada wing nanostructure in conjunction with loading Au nanoparticles to produce photocatalytic effects (Figure 3b). The same concept has been applied to TiO_2. Although the photocatalytic properties and ROS generation efficiency of TiO_2 is poor, they can be improved by introducing a 50 nm thick TiO_2 coating on the dense array of SiO_2.[189] Fabrication of nanospikes on Ti and Ti alloys shows good potential in bactericidal applications and combination with other techniques yields better results. Coating Ti nanospikes with an antibacterial peptide (catechol-ended Pep (cPep)) shows remarkable improvement against *E. coli* and *S. aureus* and they are also non-toxic to MC3T3 cells.[75] Peptides with a cationic structure provide the suitable affinity between anionic bacteria cell walls and nanospikes to enhance the antimicrobial efficacy as shown by a killing rate of more than 99% against both gram-positive and gram-negative bacteria. In comparison, without the coating, only gram-negative bacteria are affected. Long-lasting bactericidal effects are observed in vivo after implantation for 5 days as indicated by more than 6-log reduction in the bacteria level compared to the control group.

2.2. Biomimicking Micro/Nano Nanofeatures of Plants

Similar to insect wings, plants have evolved to adapt to different environments. Superhydrophilic surfaces assure plants to be wet, while superhydrophobic surfaces help plants like lotus to remain dry by sliding water droplets or rose petals to capture and trap water to remain wet. Superhydrophobic structures reduce bacteria attachment and have been imitated in antibacterial and self-cleaning applications. The mechano-bactericidal effects of the nanostructures of plants are different from those of insect wings. For example, bacteria on a lotus leaf are stretched to death rather than pierced by nanofeatures on the cicada wing.[26]

The unique micro/nano structures of lotus leaves reduce the surface energy and provide the conditions to be clean even in muddy water. This structure[190] results in an antibacterial or antibiofouling surface[191] and has been adopted by oil separation membranes,[192] food packaging,[193,194] and wound healing gauze.[195] However, exact duplication is not an easy task,[196] specifically the hair-like nanostructure which is mainly responsible for the superhrdophobicity of lotus leaves.[197,198] Huang et al.[199] have proposed a 2-step protocol to replicate the structure on polypropylene (PP). The structure not only retains the characteristics of lotus leaves for a long time, but also resists change in hot water (Figure 5a). A 3-step process comprising plasma etching, hydrothermal processing, and fluorination has been proposed by Jiang et al.[26] The structure is fabricated on silicon by first forming microscale pillar arrays and then spin-coating ZnO nanoneedles on top by a hydrothermal process (**Figure 4**b,c). After fluorination, a larger water contact angle of 174° is observed from the sample in comparison with the lotus leaf (154°). The bactericidal effects of the biomimicked micro/nano structure are physical and leaching of Zn or other chemical factors have no impact because the gold coating shows the same bactericidal behavior and absence of inhibition zones in the agar-plate antibacterial test. On the natural lotus leaf, almost all the bacteria are repelled within the first 3 h, but the bactericidal efficacy degrades with time because the air cushion formed destabilizes bacteria repulsion[200] and the dead bacteria reduce the roughness of the nanofeatures.[26] On the other hand, the biomimicked structure retains not only the mechanobiocidal properties, but also the antibacterial capability even after 24 h (Figure 4d–i). The durability is demonstrated by the unchanged bactericidal properties after exposure to bacteria. However, the lack of cell culture results does not confirm the biocompatibility. There have been few reports describing the behavior of lotus leaves[201,202] and some of them are in fact contradictory.[203] For instance, Li et al. have shown the inescapable inhibitory impact of human umbilical vein endothelial cells (HUVECs) attachment on the surface of PDMS modified with the heparin-like polymer, but no study has been performed on antibacterial behavior of the structure.[204] By fabricating lotus-like poly(L-lactide-*co*-ϵ-caprolactone) by casting on PLCL using an aluminum oxide template followed by heparin conjugation, the blood compatible biomaterials are shown to decrease protein absorption.[205] Although the surface chemistry such as superhydrophilicity or superhydrophobicity is important,[206] more investigation of cell-friendly lotus-inspired structures is needed.

The nanopatterns on rose petals are another example of the natural bactericidal pattern. Apart from the bactericidal properties on a wide range of bacteria, fungi, and other microorganisms,[207,208] the unique pattern is hydrophobic and different from that on the lotus leaf. The superhydrophobic structure consists of microscale hemispherical micropapillae and nanoscale folds across the micropapillae.[209] The replica of rose petal made from PDMS has the micro/nano structure with micropapillae about 23 µm in diameter and nanofolds about 700 nm (**Figure 5**a–c).[69] The materials are exposed to *S. epidermidis* and *P. aeruginosa* to assess the antibacterial and antibiofilm formation capability. After culturing for 2 h, most of the bacteria of both strains are seen from the valleys between the micropapillae and isolated bacteria are seen on top. This structure prohibits and delays biofilm formation after 2 days. Compared to the flat surface, the bacteria colonies are isolated from one another without forming filamentous fibrils that are an indication of mature biofilms. The rose petal structure in comparison with the periodic nanostructure (500 nm, 1 µm, and 2 µm, diameter, center-to-center and height, respectively) shows that it can isolate bacteria from each other to avoid contact and inhibit biofilm formation. The size of the bacteria is similar to the nanofold structure and although the bacteria can place themselves inside the nanofolds with time, they cannot contact each other (Figure 5d). Dou et al.[27] have shown that by altering the surface chemistry on the same rose petal micro/nano structure, different attachment of gram-positive ones is seen. Mimicking the rose petal micro/nanostructure on substrates with superhydrophilic, superhydrophobic and mixed states leads to different bacteria attachment trends similar to the adsorption behavior on peptidoglycan (PGN), the main component in the gram-positive bacteria cell membrane. Lower PGN adsorption on the superhydrophilic or superhydrophobic rose petal mimicked surface shows that in the superhydrophilic and superhydrophobic states, the bond between water and the substrate and presence of relatively stable air cushion between PGN and the substrate hamper bacteria attachment (**Figure 6**e–h). However, this trend is not observed from gram-negative bacteria as they have different components in the outer cell membrane which is lipopolysaccharide. Incorporation of the honey/silk scaffold with the rose petal surface micro/nano structure is a suitable strategy against MRSA and MSCs proliferation.[210]

In addition to the two aforementioned micro/nanopatterns found on the lotus leaf and rose petal, molding of the rice leaf[70] and *Laminaria japonica*[37] produces superhydrophobic antibacterial structures. Switchable properties of different micro/nano structures on plants such as rose petals, lotus leaves, and rice leaves have been reported.[215–218] These works address the fabrication process and switchability between different states and impart information about the design of smart biomaterials. In spite of the good prospect, more results are needed to address the biocompatibility in vivo.

2.3. Biomimicking Micro/Nano Features of Animals

Similar to plants, animals have evolved with micro/nano patterns according to their needs and natural habitats. For instance, the moth eye structure has low reflectivity and antifog properties[219,220] and the antibacterial properties have attracted scientists' attention recently. Minoura et al.[71] have shown that the moth-eye imprinted hydrophilic resin based on PEG has

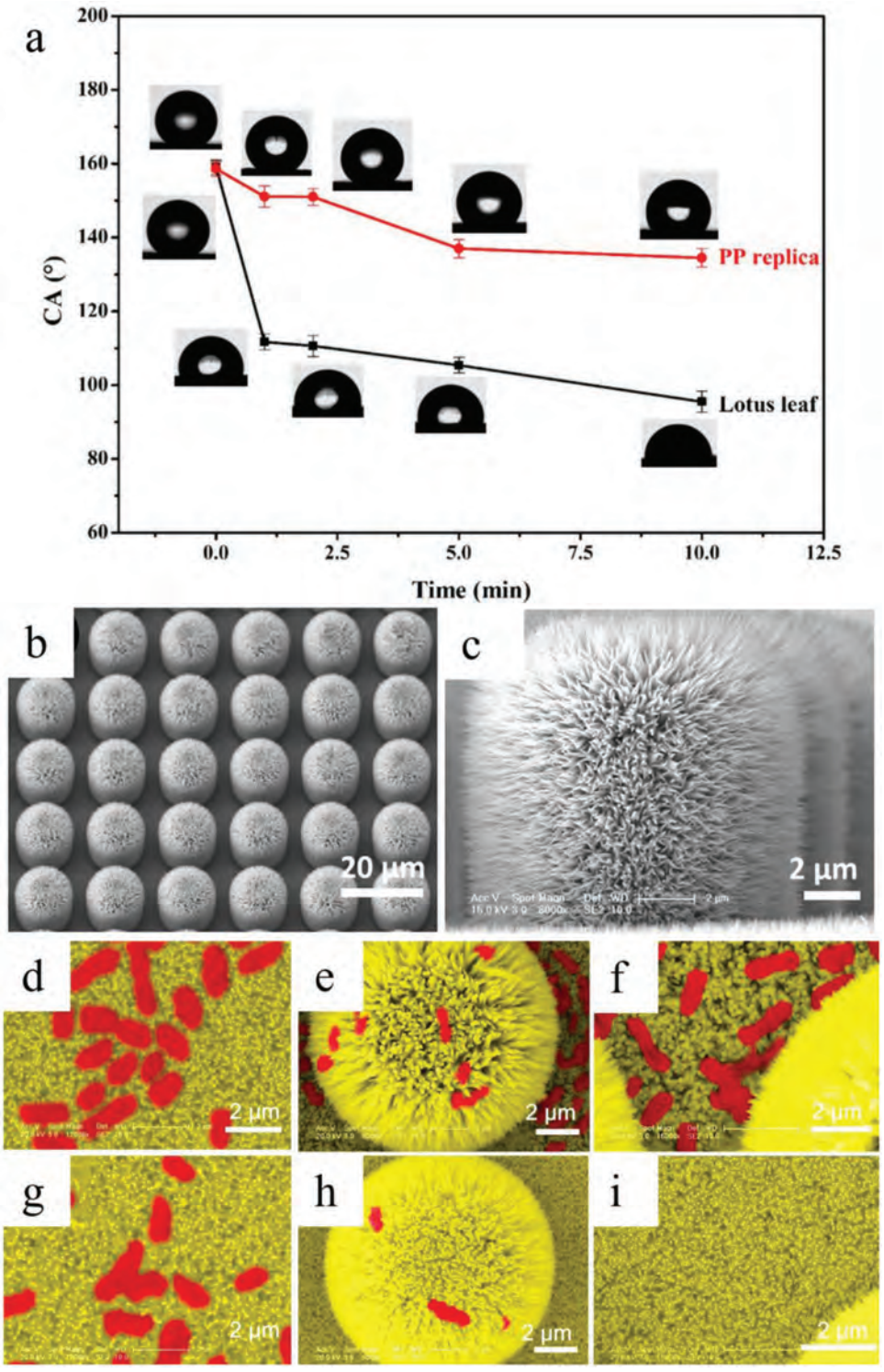

Figure 4. a) Water contact angles on the lotus leaf and replication on PP after immersing in hot water (100 °C) for different time. Reproduced with permission.[199] Copyright 2019, Elsevier. b,c) SEM images of the dual-scale micro/nanostructure biomimicked from the lotus leaf prepared on the silicon substrate. Artificial-colored SEM images of the d) nanostructure, e,f) dual-scale micro/structure, g) fluorinated nanostructure, and h,i) fluorinated micro/nanostructure. Reproduced with permission.[26] Copyright 2020, Elsevier.

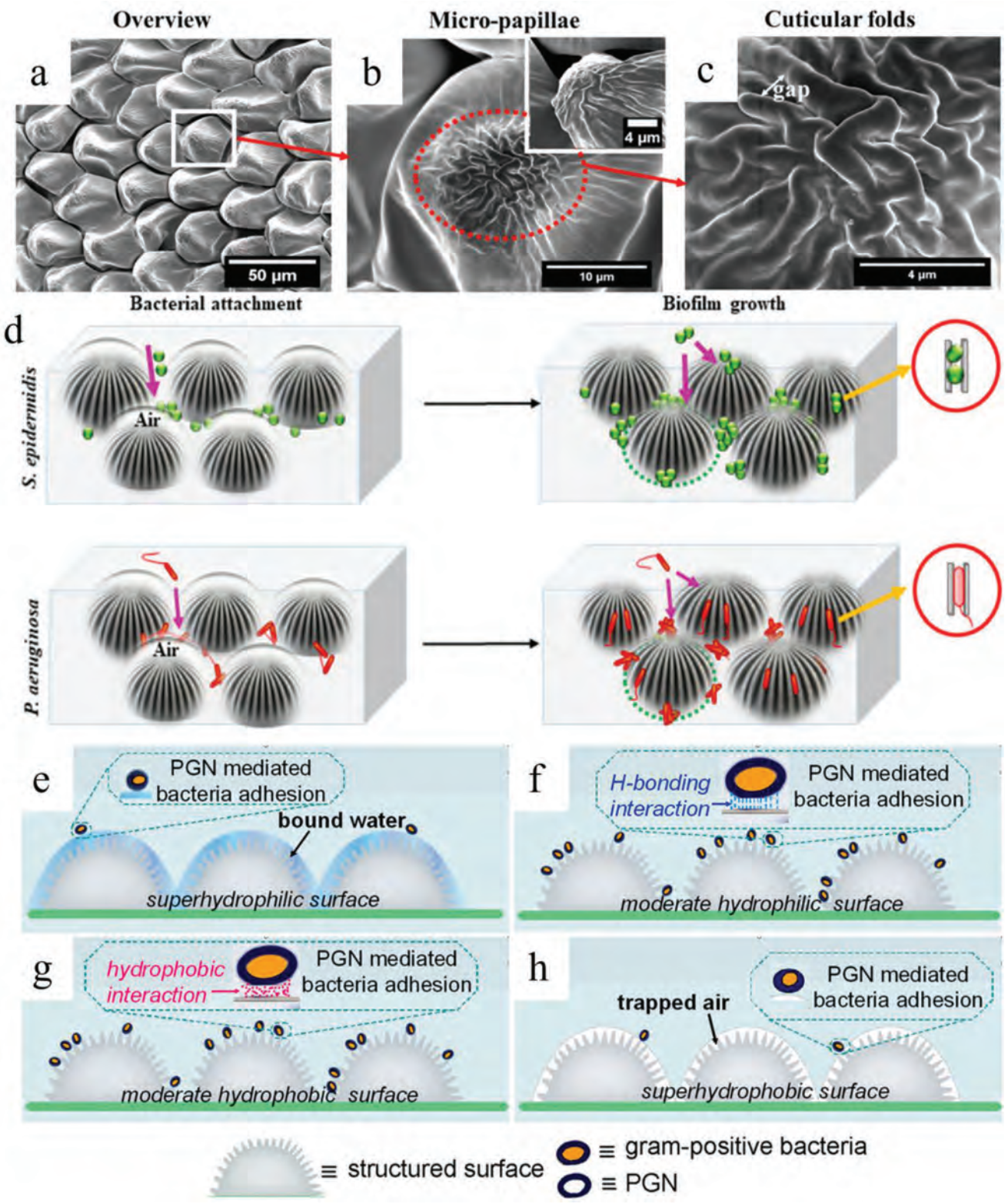

Figure 5. SEM images: a) Overview, b) micro papillae, and c) cuticular nanofolds of PDMS replicated from the rose petal. d) Postulated mechanism for the antibacterial behavior of the rose petal replica by separating bacteria on the nanofolds and isolating bacteria attachment in the valleys alongside the micro papillae. Reproduced with permission.[69] Copyright 2019, ACS publishing. e–h) Proposed mechanism for PGN adsorption on the rose petal replica with different surface chemical states of being superhydrophilic, moderately hydrophilic, moderately hydrophobic, and superhydrophobic, respectively. Reproduced with permission.[27] Copyright 2015, ACS publishing.

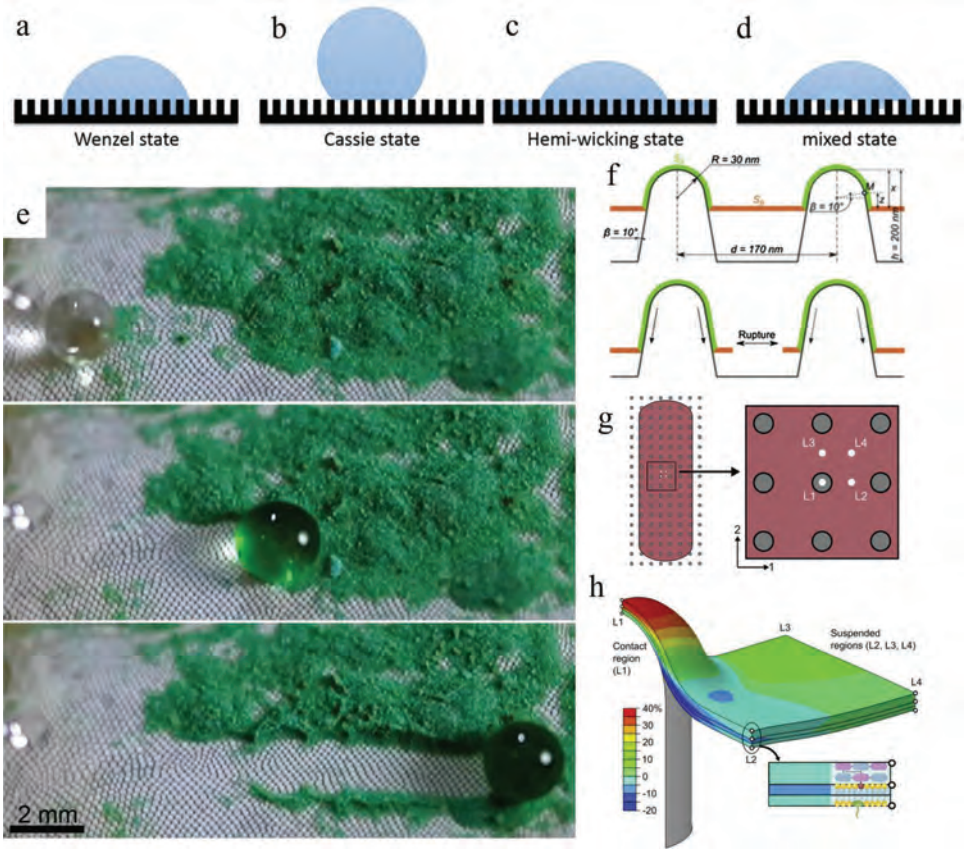

Figure 6. a) Wenzel, b) Cassie-Baxter, c) Hemi-wicking, and d) mixed state of wetting surfaces. Reproduced with permission.[211] Copyright 2015, AIP Publishing. e) Photographs of gecko skin contaminated with silica particles dyed green for better illustration. The water droplet with a diameter of about 2 mm collects the contaminants with a small roll-off angle (≈2°). Reproduced with permission.[212] Copyright 2015, Elsevier. f) Biophysical model showing the interaction between the cicada wing nanostructure and rod-shape bacteria. The cell wall is divided into two regions, that in contact with the pillar (green line) and levitated layer (orange line). As the bacteria try to maximize the contact area, the cell wall, specifically in the orange section, experience extreme tension which may result in rupture. Reproduced with permission.[213] Copyright 2013, Elsevier. g) Biophysical model showing the top view of the interaction between the rod-shape bacteria and pillar arrays with defined points: pillar tip (L1), midpoint between the pillar and next longitudinal and circumferential pillar (L2, L3), and midpoint to any peripheral pillar (L4). h) Contour plot of the strain distribution of the L1, L2, L3, and L4 points of the bacteria cell wall showing the maximum strain applied to the contact area of the tip and bacteria cell wall. Reproduced with permission.[214] Copyright 2021, Elsevier.

better antibacterial properties than the flat surface. In the early stage, leaching from the resin kills bacteria but as time elapses, the leaching effect diminishes and the superhydrophilic imprinted substrate dominates in the bacterial resistance. The superhydrophilic structure disperses the bacteria solution on the surface and fast drying is fatal to bacteria. Moreover, bacteria have little chance to avoid contact with nanopatterns during drying. Consequently, *E. coli* cannot survive for more than 20 min on the nanostructured surface but can live for more than 100 min on the flat surface. More obvious results are observed from *S. aureus*. By wiping the surface with ethanol-soaked paper, the bactericidal effects on the flat surface diminish as the leached compounds are removed, while the nanopatterned one still shows some bactericidal effects after wiping for 4000 times. The moth-eye imprinted sample shows reduced *S. aureus* attachment and growth compared to the flat surface as manifested by less attached bacteria and secreted proteins but more work for a longer time should be conducted. The materials have been applied to basins in universities and cafeteria.[72] Besides being antibacterial against *E. coli*, *S. aureus*, and *P. aeruginosa*, Viela et al.[30] have revealed good biocompatibility on the imprinted moth-eye nanostructure against HaCaT human cells.

Another natural micro/nanopatterned structure is shark skin which reduces drag in water and has antifouling properties.[32,221,222] The riblet-like structure on shark skin provides hydrophobic properties and air-trapping cushion for antifouling. Rostami et al.[73] have shown that by molding hydrophilic chitosan on shark skin and incorporation with graphene oxide, compatibility with human cells is observed. The nanotopography plays a more prominent role on bacteria adhesion reduction for both gram-negative and gram-positive bacteria, although both chitosan and graphene oxide have good bactericidal capability.[223] The biomimicked shark skin shows significantly lower bacteria adhesion, even though there is no significant difference in bacteria adhesion among similar morphologies but with different chemistry. Urchin has also inspired scientists to design biomaterials. Gao et al.[31] have fabricated an urchin-like structure on PLLA that exhibits long-lasting

superhydrophobicity even after immersing in water and PBS for 24 and 12 h, respectively. The structure repels *E. coli* and provides a bacteria-free zone at the gas–liquid–solid interface to inhibit bacteria attachment.

Besides the animals mentioned above, the structures found on enamel or mussels have provided clues to reduce bacteria attachment. Laser-assisted biomimetic techniques have been utilized to form antibacterial fluoride-incorporated apatite on dentin[224] and sintered HA[225] to reduce attachment of *S. mutans* due to release of fluoride ions. However, in most of these experiments, some chemical bactericidal agents are incorporated into the structures but the structural effects have not been investigated solely.[223,226,227]

Nanoholes are also quite effective against bacteria attachment and biofilm formation.[74,228–229] Small nanoholes 10 to 25 nm in size fabricated in aluminum by anodization reduce bacteria attachment albeit being hydrophilic. The electrostatic repulsion exerted by the side walls of the nanoholes repel *E. coli*, *S. aureus*, *L. monocytogenes*, and *S. epidermidis*.[229] Shi et al.[74] have formed nanoholes in MoS_2 nanosheets and the antibacterial behavior is different from the conventional mechanism by affecting the critical active sites of bacteria. Biofilm formation of *S. aureus* and *E. coli* is inhibited but without the nanoholes, the bacteria cover the surface entirely. After culturing for 24 h with Caco-2 cells and bacteria, the nanoholes impede adhesion and invasion of *S. aureus* of cells. The in vivo ocular and intestinal evaluations confirm the efficiency from AMR prospective. Mice administered with 3 different antibiotics of tetracycline, methicillin, and ciprofloxacin exhibit a surge in the bacteria colonies of *S. aureus* after a few rounds of infection/treatment, unless higher doses are administered in the next round. However, with regard to the nanohole samples, no surge is observed after 20 cycles of infection/treatment, but more in-depth studies are still needed.

2.4. Bactericidal Mechanisms of Nanopatterned Surfaces

Bacteria attach to materials to communicate with others, obtain nutrients, perform vital metabolic activities like respiration, and defend against mechanical, chemical, and biological stresses.[230]. The bacteria-surface interactions, especially in the early stage, determine the fate of the biomaterials and the best strategy to combat infections by either repelling or killing them before or upon attachment. In the later stage, if thick and mature biofilms are formed, it will be almost impossible to eradicate them. Antibiotic resistance in bacteria mainly stems from the formation of biofilms and secretion of ECM with unique physical and biological features. Consequently, penetration of biocides into biofilms are impeded and moreover, the bacteria phenotype can change from the planktonic state called the "biofilm phenotype."[231–233] The complex phenomena result in big resistance to antibiotics and even biocides. Nevertheless, there have been few reports about development of resistance on micro/nanopatterned surfaces but systematic studies are required in the future to elucidate the potential effects. The mechanisms for bacteria repelling and killing on biomimetic nonpatterned surfaces are discussed in this section.

Bacteria assess and sense the surface for the suitability to form colonies.[234–236] The surface energy and electrostatic charge of the biomaterials determine the affinity to bacteria and higher surface energy and positive charge generally lead to higher bacteria attachment. The reversible process can happen as fast as a minute and up to a few hours.[237–241] In this step, bacteria try to modify themselves with regard to the position and morphology to achieve the maximum contact area and after finalizing the position, start to secrete ECM, colonize, and develop biofilms.

In most cases, bacteria reach the surface through a liquid medium and therefore, the wetting properties are crucial. Surface can be categorized into 4 states: Superhydrophilic, hydrophilic, hydrophobic and superhydrophobic, and wetting follows the Wenzel, Cassie-Baxter, Hemi-wicking, or mixed models (Figure 6a–d).[211] On the nanopatterned surfaces, the superhydrophobic state is beneficial because air cushions are formed between nanofeatures and in the valleys to inhibit full wetting and reduce contact between the bacteria and biomaterials. In most superhydrophobic systems, the surface energy is too low for bacteria or other foreign objects to firmly attach and hence, loose objects can be washed away or detached (Figure 6e).[26,198,242,212] In some superhydrophobic systems, water droplets are pinned to the surface so that they cannot roll off and the contact angle is large.[69] Based on these models and that superhydrophobic surfaces repel bacteria and delay biofilm formation, efforts have been made to design antibacterial biomaterials. The common example is the superhydrophobic surface of the cicada wing with sharp arrays with a large aspect ratio.

The bactericidal mechanisms of nanopatterned surfaces have been studied experimentally and theoretically.[243] The bacteria membrane experiences stress and tension resulting in rupture and death.[213–214,244–248] Besides the applied stress, a model suggests that gravity and non-specific forces such as van der Waals forces play crucial roles in stretching the cell wall.[249] Rupturing commonly occurs at the contact area between the tips and bacteria or the cell membrane trapped between two adjacent tips. Rupturing is the main killing mechanism for gram-negative bacteria (Figure 6f–h).[213,214] Gram-positive bacteria have thicker cell walls thereby requiring higher stress for rupturing. The situation with eukaryotic cells is different as they are usually much bigger than these nanofeatures and they also have support from their cytoskeleton to preserve the structural integrity. The size, dimension, distribution, aspect ratio, and mechanical energy of nanofeatures are critical to the bactericidal efficacy.[60,250–251] As for the influence of the surface roughness in the hydrophobic state, the valleys are not as important as the asperity size. Therefore, by increasing the asperity size, bacteria adhesion increases due to the lower energy barrier.[246] Micro/nanofeatures with suitable dimensions are important.[244,252–254] Bacteria can avoid contact with the sharp areas on big features and so a size smaller than that of the bacteria has better effects.[244] However, if the nanofeatures are too small, the tension is dispersed due to too many contact points dropping below the critical value required for cell membrane rupturing. In both cases, more uniform and less extensive distribution of the applied stress gives rise to lower bactericidal efficiency. Velic et al.[255] have studied the impact of various physical parameters of the nanopatterns on the bactericidal efficacy using *B. subtilis* as the model bacteria. A smaller nanopillar diameter increases the bactericidal efficacy, while the center-to-center distance and nanopillar height do not have a significant impact. These findings contradict some experimental

results which show that a smaller pillar spacing and larger pillar height enhance the bactericidal efficacy.[60,256,257] Based on the accepted notion gram-positive bacteria are less susceptible to rupturing on sharp nanopatterns compared to gram-negative ones due to different cell wall thickness, however, *E. coli* is more adaptable to nanopatterns than *B. subtilis* as the former is more deformable.[51] More experimental studies and better theoretical models are required to settle the controversy.

Linklater et al.[60] have prepared vertically aligned carbon nanotubes (VACNTs) with a very large aspect ratio to kill bacteria by storing and releasing mechanical energy. VACNTs with heights of 30 and 1 µm have the superhydrophobic state showing a water contact angle of about 150°. Different heights and surface chemistry have different effects on different types of bacteria and the bactericidal platform should be designed according to needs. Surface functionalization with either CF_4 or O_2 increases bacteria attachment and after attaching bacteria to the forest of VACNTs, the bacteria membrane ruptures. Experiments have been performed to understand how tall these nanofeatures should be and whether or not taller is better.[251] Although taller ones with a larger aspect ratio may store more mechanical energy, the bactericidal efficacy decreases due to irreversible deflection by the nanofeatures. Nanopillars with heights of 220, 360, and 420 nm are compared and the highest bactericidal efficiency is observed from the 360 nm one, that is, 95 ± 5% and 83 ± 12% against *P. aeruginosa* and *S. aureus* as the gram negative and gram-positive strains, respectively.

These platforms are normally not suitable for cell growth for the same reason that they are not suitable for bacteria growth, because the low surface energy reduces the affinity to microorganisms. One of the main components in superhydrophobic systems is the air cushion which is responsible for the large contact angle and low/unstable bacterial attachment. However, the surface can be dynamic and bacteria attachment can change with time.[200] Superhydrophobic antibacterial surfaces that do not require cell attachment are used in food packaging, marine applications, non-implantable biomedical tools, door handles and knobs, and basins so that the use of disinfectants can be minimized. Meanwhile, superhydrophobic biomaterials may not be appropriate for biomedical implants in vivo and researchers have started to consider introducing bactericidal properties to hydrophilic biomaterials. The bactericidal mechanism of hydrophilic and superhydrophilic nanopatterned biomaterials is more or less the same, that is, rupture of the cell membrane[50,54] but the approach is different. Boinovich[59] et al. have shown that superhydrophilic structures can kill bacteria by the strong adhesive force between the surface and bacteria arising from the nanopatterns. The attraction between bacteria and hydrophilic surfaces exerts intolerable tension to the bacteria cell wall due to the top or edge of nano features.[54] Valiei, et al.[258] have suggested that the large capillary force at the interface of liquid–air surface on superhydrophilic materials enhances the bactericidal properties compared to the superhydrophobic surface as bacterial repulsion dominates. According to their model, the generated force between the hydrophilic surface and *P. aeruginosa* is not enough[258,259] and the capillary force generated during liquid evaporation or movement of air bubbles creates significant tension in the bacteria membrane, but the situation is different on a flat surface.

Another nanofeatures of interest are nanoholes.[228,260] Nanoholes with diameters between 10 and 100 nm have been studied and the best antibacterial performance is observed for 10 and 25 nm. They are the most hydrophilic ones against *E. coli*, *L. monocytogenes*, *S. aureus*, and *S. epidermidis*. Based on the model developed to explain the exceptional antibacterial behavior of small pores, additional electrostatic repulsion by the vertical sidewalls of densely distributed nanoholes is responsible.[229] In another study, nanoholes are introduced to the surface of MoS_2 nanosheets and the mechanism is different from that of traditional methods like piercing or ROSs production.[74] By interfering with the bacteria electron transfer chain, the active sites of bacteria such as polysaccharide intercellular adhesion (PIA) and extracellular DNA are targeted and the corresponding contents decrease significantly. In the presence of ethanol, glucose, and NaCl, biofilm formation is enhanced on the MoS_2 nanosheets without pores. By introducing nanoholes, reduction of biofilm formation ensues as evidenced by downregulation of specific genes such as S*ig*B and R*sb*U factors responsible for the formation of PIA.

The wettability and surface roughness are sometimes interdependent from the viewpoint of the bactericidal action. Surface roughness shows the combined effects of the micro/nano feature dimensions (height and width), center-to-center distance (density, homogeneity and heterogeneity of micro/nano patterns, rigidity, etc.), and geometry of the tip (tapered, round, sharp, etc.).[15,251] A high surface roughness does not always reduce bacterial attachment,[261] as the size of the micro/nanofeatures and whether they are comparable with the size of the bacteria are important factors. In addition, sharp and pointy features are usually bactericidal, but other factors such as the density, height, and homo/heterogeneity should be considered.[248,254] Pointy micro/nanofeatures with different heights and densities can produce different degrees of bacterial attachment, regardless of whether the surface is hydrophilic or hydrophobic because bacteria can bend to accommodate the structure or modify their position to avoid contacting a rough surface. Sharp edges on micro/nanofeatures[262] can introduce antibacterial effects, for example, graphene oxide nanosheets[263] and they can be combined with micro/nanocones[54] to elevate the bactericidal effects. Surface roughness does not arise from perturbances alone and micro/nanopores have attracted scientists' attention. All in all, it is still difficult to predict in general the bactericidal efficacy of micro/nanofeatures and all the aforementioned factors must be considered when designing the appropriate surfaces.

3. Photon-Activated Surfaces

Stimulus-responsive biomaterials can carry out extra functions in tissue regeneration and bacterial elimination. Du et al.[264] have studied the response to physical stimuli as one of the essential factors in the design of biomedical implants. Exposing biomaterials to light can lead to physical/chemical changes to affect bacteria. Photo-activated surfaces have been developed to monitor the antibacterial performance using different electromagnetic waves. Specifically, a photo-activated surface is able to respond to external light stimuli to develop bactericidal properties. Compared to the passive antibacterial strategies such as ion release, drug releasing, and nanostructured surfaces, photon-based methods

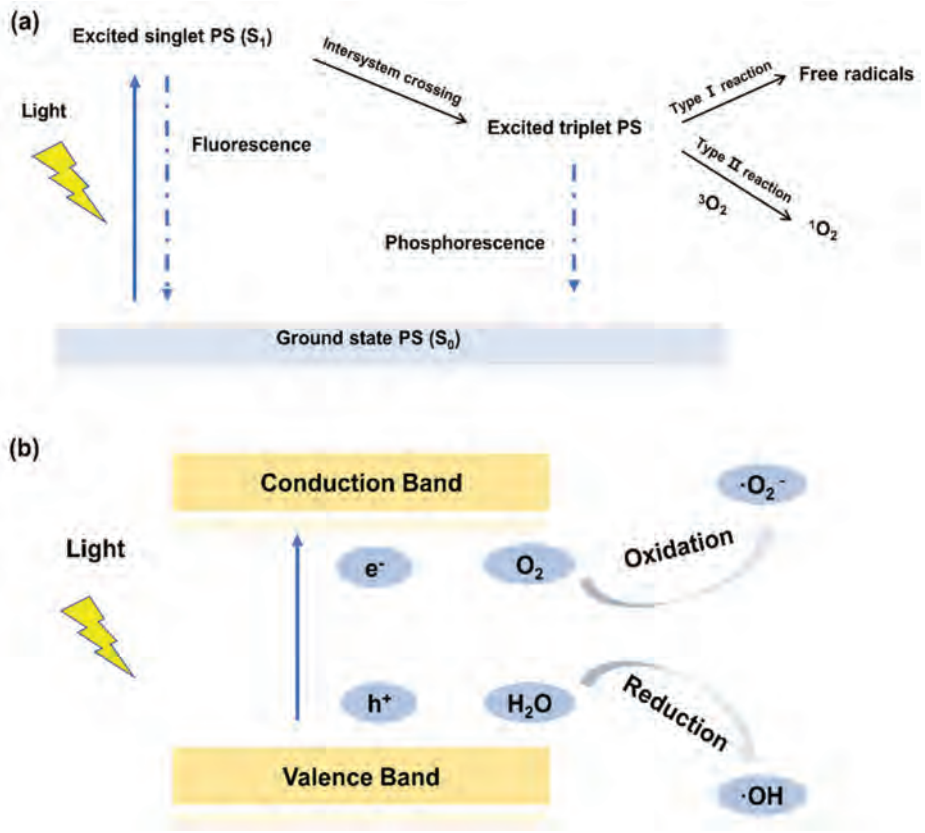

Figure 7. Schematic illustration of a) fluorescence-based and b) photocatalytic-based PSs.

using radio waves, microwaves, infrared, visible light, ultraviolet (UV), X-rays, and gamma rays are effective as well.[265] Infrared, visible, and ultraviolet light is frequently used in photon-based antibacterial strategies on account of the moderate energy and tissue penetration. For example, photothermal therapy (PTT) and photodynamic therapy (PDT) are promising. In PTT and PDT, photo-response is necessary and photo-sensitive agents must be incorporated into the biomaterials by techniques such as self-assembly,[266] hydrothermal processing,[44] electrostatic adsorption,[76] and physical wrapping.[85] The main killing mechanisms are production of ROSs and heat generation. Since bacteria develop some resistance against heat, application of pressure in conjunction with high temperature has been proposed.[267,268] ROS are also recognized to be highly effective[269–271] but it is known that some bacteria have find specific ways to thwart the impact of ROSs by secretion of enzymes, proteins, and toxins.[272] Therefore, attention must be paid to detect early signs of resistance and the use of multiple antibacterial methods can be more efficient. Recently, it has been observed that mitochondrial ROS plays an important role in the antimicrobial immune response[273–275] and therefore, production of ROS is highly desirable for antimicrobial purposes.

3.1. Photodynamic Surfaces

PDT has been approved by the United States Food and Drug Administration (FDA) for cancer treatment.[276] PDT requires a light source, photosensitizers (PSs), and ROS. PSs commonly show little cytotoxicity without illumination but absorb energy in the presence of light forming ROS such as hydroxyl radicals (·OH), superoxide anions ($\cdot O_2^-$), singlet oxygen ($^1O_2$), and hydrogen peroxide (H_2O_2) to cause irreversible oxidative damage on biomolecules such as membrane lipids, proteins, and cellular DNA[277] (**Figure 7**). Antibacterial PDT exploits oxidative damage of microbes and the broad antibacterial spectrum results in less drug resistance while offering advantages such as remote controllability, good selectivity, negligible systemic toxicity, and effectiveness on drug-resistance bacteria.[278–282]

Near-infrared (NIR) light is usually used due to deeper tissue penetration and less harm to normal tissues.[283] PSs like porphyrin-based and macrocyclic compounds convert the optical energy to cytotoxic ROS by absorbing photons to go from the ground state to the excited state. Upon relaxation, the absorbed energy generates toxic ROS. However, traditional PSs tend to self-aggregate due to strong π–π stacking and hydrophobic interactions inducing fluorescent quenching, which in turn reduces the quantum yield of ROS. Immobilization of PSs is a priority and dispersion methods such as self-assembly,[266] host-guest assembly driven by electrostatic or hydrophobic interactions,[3] metal-organic frameworks[277] (MOFs) stabilized by coordination, and conjugating biomaterials have been applied.[284] For example, a fluorinated mesoporous silica membrane is loaded with methylene blue (MB) to form the PSs. Because of the low surface energy of fluorination, the membrane disperses methylene blue to enhance ROS generation and the antibacterial activity against both

S. aureus and *E. coli*.[285] In addition, aggregation-induced emission (AIE) fluorogens improve generation of ROS and as a result of AIE, this kind of antimicrobial PDT has image-guided properties for more accurate therapy.[286,88] For example, Xie et al.[287] have designed an amino acid/berberine hydrogel activated by AIE for enhanced photodynamic antibacterial and anti-biofilm activity under white light irradiation with no obvious cytotoxicity and low haemolytic behavior for normal cells.

In addition to fluorescence-based PSs, photosensitive agents and photocatalytic agents have been explored. Unlike fluorescence-based PSs, photocatalytic agents generate electron-hole (e^-/h^+) pairs by absorbing light energy. The resulting reduction and oxidization abilities generate ROS when they reach the surface.[288] Semiconductor-based photocatalysts such as titanium dioxide (TiO_2)[288] and zinc oxide (ZnO)[289] have been proposed, but recombination of e^-/h^+ pairs decreases the quantum yield and photocatalytic efficiency. New structures are designed with the objective of inhibiting recombination of e^-/h^+ pairs and longer wavelengths. Energy band alignment is utilized to construct the heterostructures. For example, piezoelectric nanomaterials commonly used in electrical modulation and MOFs can promote charge transfer.[88,290] For instance, the ferroelectric $BaTiO_3$ nanolayer inserted between TiO_2 nanorods and gold nanoparticles enhances $\cdot O_2^-$ and ·OH generation due to the piezophototronic and plasmonic properties and the antibacterial efficiency is 99.9% upon illumination with simulated sunlight.[81]

Besides PSs, combined methods have been explored to eradicate the intractable biofilm which is a self-produced polymeric matrix by microorganisms causing infection and high resistance to antibiotics.[291] Combined methods are usually used to eradicate biofilms noninvasively. The traditional antibiotic,[89] PTT,[292] and superhydrophobic surfaces are common approaches to eliminate and restrain biofilms.[293] For example, biocompatible polydopamine is used as an immobilizer for both daptomycin (DAP) and IR820. After releasing DAP to damage the bacterial membrane and inhibit bacteria growth, $^1O_2$ generated by IR820 is capable of eradicating the biofilm further after NIR irradiation.[89]

Antibacterial PDT is a new method that is less likely to give rise to antibiotic resistance due to the low demand for targets sites of the bacteria. Conventional PSs and novel semiconductor-based photocatalytic materials both trigger oxidative damage in bacteria. The technique reduces the use of antibiotics, eradicates biofilms, and is a more powerful tool to combat drug-resistant bacteria. Moreover, PDT can be combined with other methods such as PTT, targeting components like antimicrobial peptide, and traditional chemical therapy to enhance the therapeutic efficacy. At present, PDT is performed the NIR region because of absorbance of PSs. In order to expand the application of antibacterial PDT, the usable wavelength should be expanded and a higher sensitivity is also necessary.

3.2. Photothermal Surfaces

In antibacterial therapy, photothermal approaches utilize hyperthermia-induced bacterial ablation upon photon-heat conversion of specific materials to treat multidrug-resistant bacterial infection.[294] Materials with photothermal properties have some common features. Photothermal materials should be able to absorb and trap photons, meaning low emissivity and high light-heat conversion efficiency. The photothermal materials should be harmless to human tissues. There are four common photothermal materials, namely, carbonaceous nanomaterials, narrow bandgap semiconductors, plasmonic nanomaterials, and MXenes.[295]

3.2.1. Carbon-Based Materials

Carbon-based photothermal materials have drawn enormous attention and CNTs, graphene and its derivatives, graphite, and carbon black have excellent photothermal properties. However, debris shed from carbon-based photothermal materials can lead to inflammatory responses in vivo.[296,297] Moreover, some 2D materials like graphene generate ROS upon irradiation with visible light[298] thus increasing the risk of normal tissue damage. As biocompatibility is essential to biomaterials, these side effects should be minimized. Graphene grown vertically on medical titanium shows no obvious cytotoxicity and the photothermal antibacterial performance is outstanding as reflected by sterilizing rates of 93.3% against *E. coli* and 99.1% against *S. aureus* upon NIR irradiation.[82] Because of the low cytotoxicity,[299] graphene oxide (GO) is another candidate. The functional groups on GO make it reactive in binding with bioactive molecules. In this way, the photothermal properties are preserved while biosafety is enhanced. For example, carboxyl graphene conjugated with glycol chitosan eradicates *E. coli*, *S. aureus*, and MRSA completely upon 0.75 W cm^{-2} NIR irradiation for 10 min while exhibiting negligible cytotoxicity toward fibroblasts at a concentration of 1 mg mL^{-1}.[83] Similarly, modification with double bond *N*-dodecylated or quaternized chitosan produces the GO derivative with photothermal antibacterial capability and biocompatibility.[300,301] The reactive carboxyl and hydroxyl groups on GO provide crosslinking sites to connect with macromolecules. In the cellulose-GO nanosheet hydrogel network, the GO nanosheets not only act as a photothermal agent to sterilize bacteria upon NIR irradiation, but also strengthen the mechanical properties of the hydrogel by absorbing and dissipating energy due to the rigid characteristics.[302]

3.2.2. Narrow Bandgap Semiconductors

In a semiconductor, a smaller bandgap produces the better capability to absorb photons in a wider range thus enhancing the photothermal performance.[303] TiO_2 is a potential photothermal candidate for medical Ti implants because of the good biocompatibility, mechanical properties, corrosion resistance, and photo-sensitivity.[304] However, the large bandgap (≈3 eV) requires UV irradiation of wavelengths less than 400 nm. Since UV light is harmful to human tissues, the light absorption range of TiO_2 should be broadened for safer PTT. Doping, hydrogenation, and Al reduction have been utilized to narrow the bandgap of TiO_2. Well aligned nano TiO_2 structures also enhance the NIR sensitivity.[44,84] Yang et al. have fabricated a TiO_2/TiO_{2-x} metasurface on the Ti alloy implant by a topochemical conversion-based alkaline–acid bidirectional hydrothermal method. NIR absorption and near-field distribution of the TiO_2/TiO_{2-x}

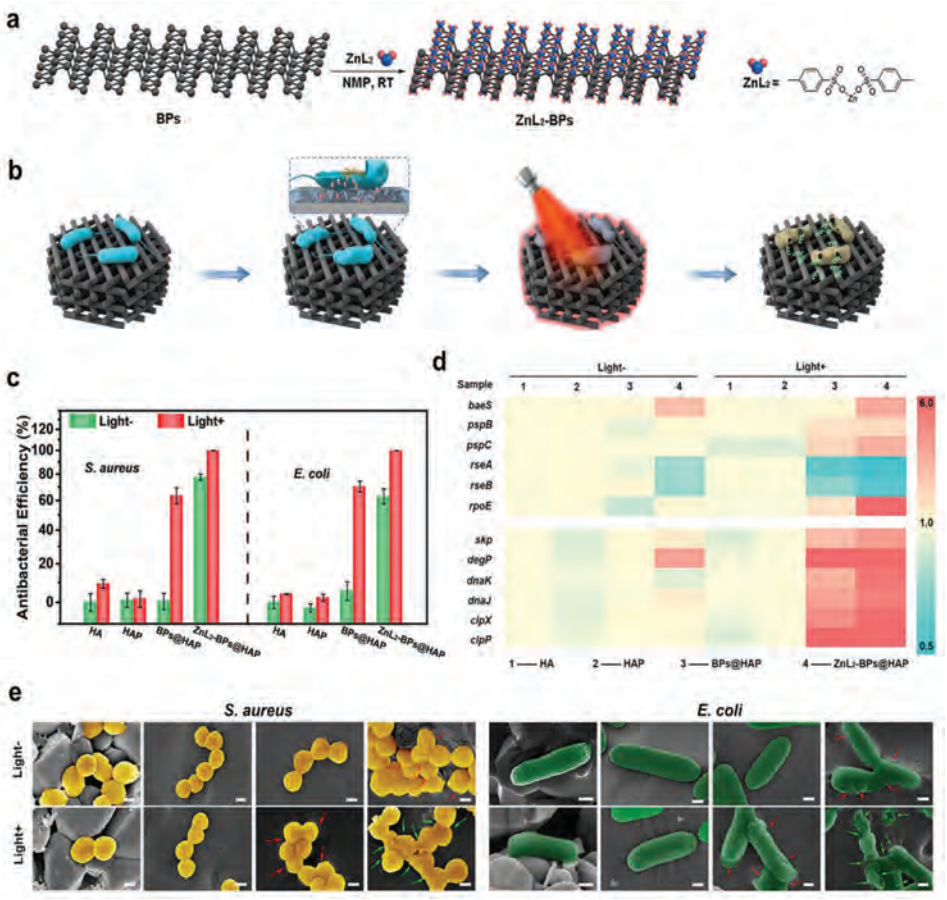

Figure 8. a) Surface coordination of ZnL_2 to BPs. b) Schematic illustration of the antibacterial mechanism of the ZnL_2-BPs@HAP+Light group. c) Antibacterial efficiency of the scaffolds with/without NIR irradiation. d) Heat map depicting the gene expressions of *E. coli* on different scaffolds with/without NIR irradiation. e) SEM images of the bacteria on different scaffolds with/without NIR irradiation (scale bar = 400 nm). Reproduced with permission.[85] Copyright 2021, ACS publishing.

meta-surface can be tailored by altering the arrangement and dimensions of the nanostructure. After low-power NIR irradiation for 10 min, bacteria are eliminated on the meta-surface in vitro and in vivo.[44] Zhang et al. have reported that TiO_2 nanorod arrays on Ti possess the capability of light-heat conversion and ROS generation upon NIR irradiation due to the synergistic effects of photothermal anti-biofilm therapy.[84]

Besides Ti oxide, emerging 2D narrow bandgap materials such as MoS_2,[305–307] Bi_2Te_3,[308] and black phosphorus (BP) have been studied as photothermal antibacterial agents. BP has excellent photothermal properties and biosafety and in the presence of oxygen and water, BP is oxidized to soluble phosphate[309] which is harmless in vivo. In fact, the degradation products of BP can promote bone regeneration[310] and so it is popular in PTT for bone-related bacterial elimination. Nevertheless, rapid degradation makes BP unstable and the photothermal effects can deteriorate. Strategies have been developed to stabilize BP, for example, physical wrapping,[311] macromolecules modification,[312] and metal coordination.[313–315] Recently, Wu et al.[85] have fabricated zinc sulfonate ligand (ZnL_2) coordinated BP nanosheets (ZnL_2-BPs) (**Figure 8**a) with better oxygen resistance and bioactivity. The ZnL_2-BPs modified and 3D-printed scaffold delivers stable photothermal performance and eliminates more than 99% of the bacteria at a mild photothermal temperature (<50 °C) boding well for in vivo antibacterial therapy (Figure 8b,c). Upon NIR irradiation, hyperthermia and zinc ions produce envelope stress leading to physiological disorder in the bacteria (Figure 8d). The dual stimulation destroys the bacterial membrane and kills the bacteria (Figure 8e). After antibacterial therapy, milder weekly PTT (40–42 °C) is applied to the implantation site to foster regeneration of bone because the mild heat stimulation promotes new bone formation,[316] thus giving rise to a photothermal-regulated win-win strategy.

3.2.3. Plasmonic Nanomaterials

The photothermal effects of plasmonic nanomaterials stem from localized surface plasmon resonance (LSPR) caused by collective oscillations of electrons in metallic nanomaterials during light irradiation at certain frequencies leading enhanced absorption of the incident light and light-heat conversion.[317–319] Nanostructured Au,[320] Ag,[321,322] and Cu[323] particles have been developed to produce photothermal effects. Au nanomaterials are

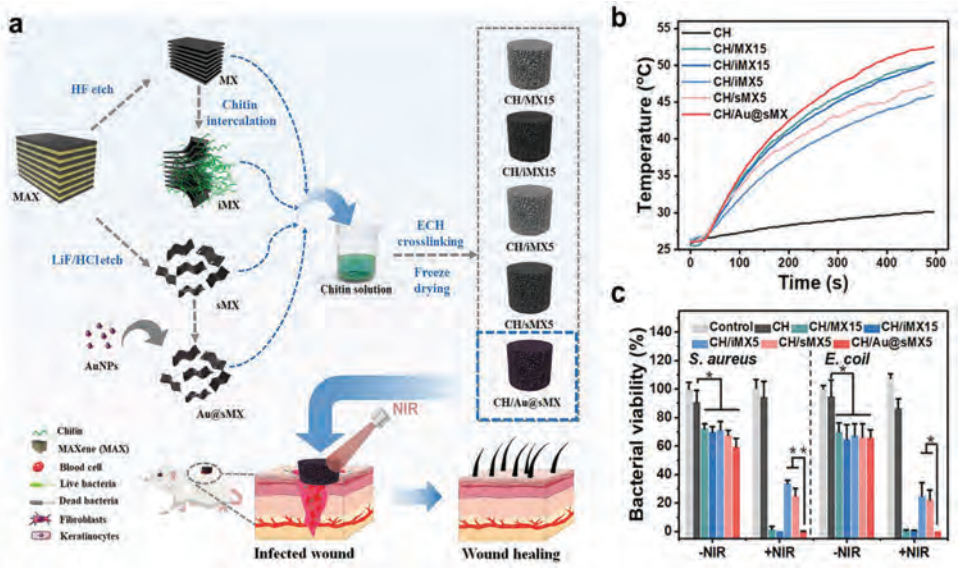

Figure 9. a) Schematic illustration of chitin/MXene composite sponges for bacteria-infected wound healing. b) Photothermal heating curves of the composite sponges irradiated by a NIR laser (808 nm, 2 W cm^{-2}). c) Bacterial viabilities of *E. coli* and *S. aureus* on different composite sponges with/without NIR irradiation. Reproduced with permission.[86] Copyright 2022, Wiley-VCH GmbH.

frequently used in photothermal antibacterial therapy because of the chemical stability and biocompatibility.[324–327] Biomaterials modified with nanostructured Au such as nanostars,[328,329] nanoshells,[330] nanorods,[331] and nanoparticles have been reported to possess the ability to photothermally eliminate bacteria/biofilms upon light illumination.[90,332–333] To produce the antibacterial surface, Jin et al. have fabricated TiO_2 nanotubes incorporated with Au nanoparticles and carbon quantum dots on Ti.[90] Upon NIR irradiation, the carbon quantum dots convert NIR into 500–600 nm light causing electron transfer to activate the TiO_2 nanotubes to produce ROS. Meanwhile, local heating is generated by the NIR-responsive Au nanoparticles and carbon quantum dots. By combining ROS and PTT, more than 95% of *E. coli* and *S. aureus* can be eliminated after NIR irradiation for 15 min.

3.2.4. MXenes

MXenes is a collective name of 2D transition metal carbides, carbonitrides, and nitrides, in which the M stands for the metal and X represents carbon or nitrogen. The general formula of MXenes is $M_{n+1}X_nT_x$ (n = 1, 2, or 3) because in the sheet of 2D MXenes, n+1 layers of M are interleaved with n layers of carbon or nitrogen, and the outer M layer is terminated by O, OH, F, and/or Cl.[334,335] The strong light absorption and LSPR effect endow MXenes with outstanding photothermal properties[336–339] which have been studied for biomedical purposes.[335,340,341] As prospective photothermal nanomaterials to replace antibiotic treatment, MXenes have been modified with different materials to improve the therapeutic effects, for instance, Au incorporation,[342] copper sulfide integration,[343] heterojunction constructions[344,345] and cerium oxide.[346] As for bulk biomaterials, MXenes serve photothermal antibacterial functions in textiles,[347,348] sponges,[86] and hydrogels.[349–351] Li et al. have fabricated a series of chitin/MXenes composite sponges with accordion-shaped MXene, polymer-intercalated MXene, single-layer MXene, and AuNPs-loaded MXene (**Figure 9**a).[86] The sponge modified by AuNPs-loaded MXene exhibit enhanced efficiency in light-heat conversion (Figure 9b) and more than 99% of *E. coli* and *S. aureus* can be killed after NIR irradiation for 8 min (Figure 9c). Compared to other 2D materials such as graphene and black phosphorus, MXene is an emerging material that needs more exploration. In addition to the bioactivity of MXenes, the safety and stability are critical.[352] Zhang et al.[353] have found that the MXene nanosheets cultured with HUVECs exhibit no obvious toxic effects even at a relatively high concentration (0.5 mg mL^{-1}). Nevertheless, at such a concentration, functional disorder of mitochondria and inhibition of tricarboxylic acid cycle are detected from the HUVECs exposed to MXenes. The symptoms include enhanced ROS production, glycolysis, fatty acid biosynthesis, and lipid accumulation. Therefore, application of MXenes to the biomedical field remains challenging.

PTT is seldom used alone as an antibacterial method and needs to be combined with other antibacterial methods to produce promising results. Unlike the treatment of tumors, the side effects of PTT must be considered because the bacteria and host cells have different hyperthermia tolerance. Although a high temperature can sterilize bacteria, the antibacterial efficiency reaches an acceptable level only if the photothermal temperature is beyond 88 °C.[354] However, it has been suggested that the photothermal temperature applied in vivo should not exceed 50 °C or the host cells will be damaged and the healing time will be lengthened.[85,355] Therefore, the photothermal surface usually contains other materials or drugs to produce a more effective and biocompatible strategy for antibacterial purposes. To minimize cell damage caused by excessive heat, Hu et al.[87] have designed a PDMS dressing with the topography mimicking shark skin to mitigate intercellular cohesion loss (**Figure 10**a). The

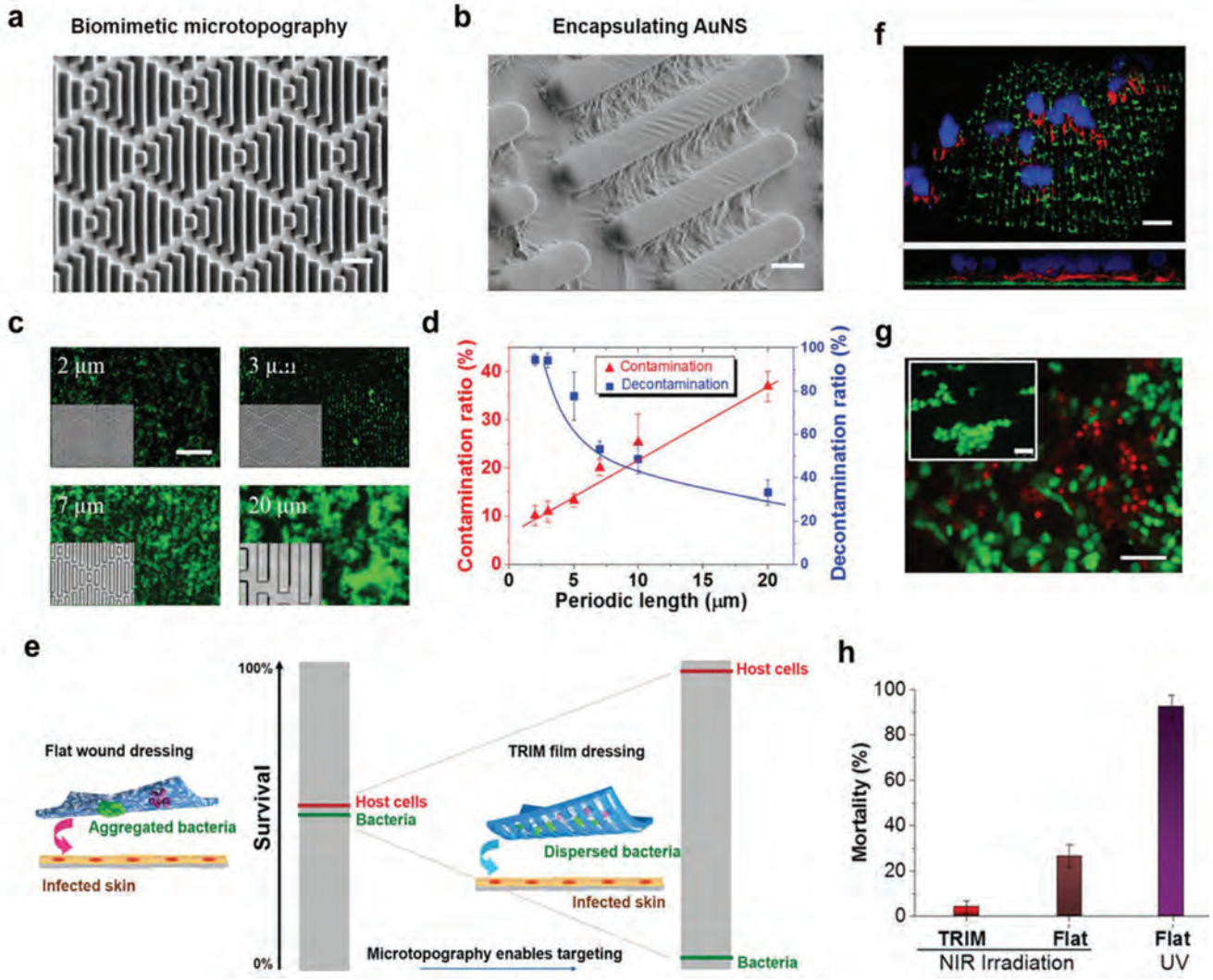

Figure 10. PDMS film with topography mimicking the feature of shark-skin a) before and b) after (b) integration with AuNS. Scale bars: a) 10 μm and b) 3 μm. c) Fluorescence images showing that *S. aureus* (green) attach within feature gaps when dispersed on films with different topography features. The inset in (c) are from one measurement representative of the contamination experiments. Scale bar = 50 μm. d) Graph showing films with a larger periodic length of surface features enhancing bacterial growth and biofilm formation (red curve). Bacteria in the biofilms are more difficult to decontaminate (blue curve). e) Illustration showing the survival dichotomy of bacteria and host cells during phototherapy due to the biomimetic topography. f) Confocal fluorescence microscopy images of the top view (top) and sectional view (bottom) showing that MDCK cells are suspended above the depressed regions. The surface features are labeled with FITC-conjugated nanoparticles (green), cell nucleus is stained with DAPI (blue), and cytoskeleton (F-actin) is stained with phalloidin (red). Scale bar = 20 μm. g) MDCK cells survival on the thermal-disrupting interface inducing mitigation (TRIM) films (inset) and flat films under NIR irradiation (70 mW cm^{-2}). The cells are co-stained with calcein AM and propidium iodide to differentiate the live cells (green) from dead cells (red). Scale bars = 50 μm. h) Mortality assay of MDCK cells on the biomimetic surfaces and flat surfaces upon NIR irradiation. The UV-irradiated flat surface is the positive control. Reproduced with permission.[87] Copyright 2020, Wiley-VCH GmbH.

thermal-responsive hydrogel encapsulating Au nanostars (AuNS) endows the dressing with the desirable photothermal capacity in which the volume is reduced by heating (Figure 10b). As shown in Figure 10c,d, the dimensions of the surface features are larger than the cut-off size of the bacteria but smaller than those of the host cells (3 μm). The biomimetic topography-decorated wound dressing leads to survival dichotomy of bacteria and host cells during phototherapy (Figure 10e). Upon NIR irradiation, the bacteria adhering to the thermal-sensitive hydrogel fall into the depressed regions, while the host cells stay in the raised regions because of spatial confinement (Figure 10f,g). In this way, accurate topical antibacterial PTT reduces normal cell mortality by keeping the cells away from the heat source (Figure 10h).

Although photon-based antibacterial therapy has developed quickly in recent years, obstacles still exist because of the limited depth of light penetration into tissues.[356] For example, most photo-responsive biomaterials are NIR-triggered but NIR can only penetrate about 7 mm of human tissues at a power of 1.0 W cm^{-2}.[316] Hence, many photon-based antibacterial studies require NIR irradiation with longer or maximally permittable

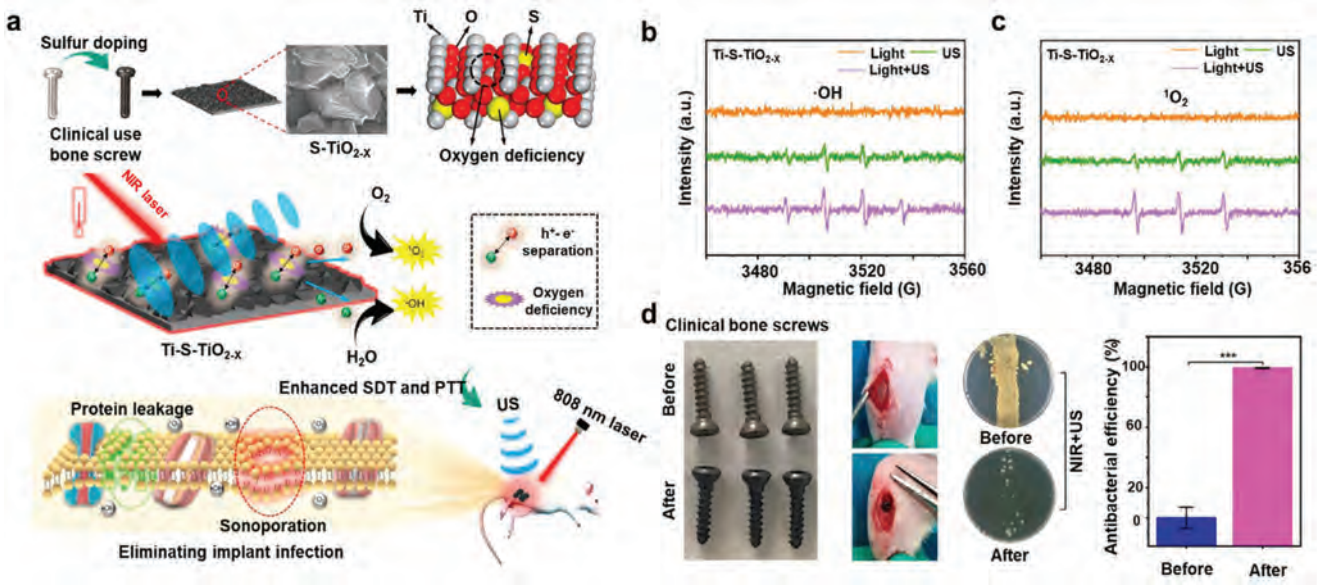

Figure 11. a) Schematic illustration showing that the sulfur-doped Ti bone screw exhibits enhanced sonocatalytic-photothermal ability in bone infection therapy. b) ·OH and c) $^1O_2$ signals detected from Ti-S-TiO_{2-x} in the magnetic field. d) Antibacterial characteristics of clinical bone screws before and after S doping. Reproduced with permission.[91] Copyright 2020, ACS publishing.

exposure (0.4 W cm^{-2} at 850 nm, 0.33 W cm^{-2} at 808 nm) as stipulated by the American National Standards Institute,[357,358] even though these experimental animals are much smaller than human beings.[85,355] Therefore, better photon delivery is necessary to minimize tissue damage by the laser. Recently, an optical fiber that can precisely perform PTT at deep-seated lesion in situ without body invasion and tissue damage has been proposed[359] and the precision therapy strategy may become another research focus in this burgeoning field.

3.3. Other Physical Strategies

There are other methods that can offer out better, safer, and smarter antibacterial functions in addition to nanostructured surface and photo-activation. For example, owing to excellent tissue penetration and biosafety, ultrasound (US) can be used. In this section, alternative physical antibacterial approaches are discussed and more details are shown in Table 1.

3.3.1. Uultrasound-Based Therapy

Ultrasound (US) triggered therapy has superiority due to deep tissue penetrability and precise energy delivery without affecting surrounding normal tissues in vivo.[360,361] It is also non-invasive and non-ionizing, thus enabling repetitive treatment with minimal systemic toxicity.[362,363] Therefore, US-based approaches have been studied for antibacterial treatment, drug release, and sonodynamic therapy (SDT). In US-triggered drug release systems, drugs are usually encapsulated into the US-sensitive vehicles like liposome or integrated with carriers by dynamic covalent linkage.[364,365] In the US treatment, the vehicles collapse and the dynamic covalent bond is broken resulting in controlled release of the antibacterial agent. Delaney et al.[366] have prepared a polyether ether ketone (PEEK) antibiotic reservoir that achieves bolus release of vancomycin upon US excitation. The vancomycin loaded in PEEK is encapsulated by the PLA membrane to form an antibiotic reservoir. In the in vitro and within tissue ex vivo evaluation, high-dose release of vancomycin is triggered by US-triggered rupture of the PLA membrane, which reduces adherent bacteria on the implant after surgery.

SDT driven by low-frequency US is a physical antibacterial process utilizing US and sonosensitizers to generate ROS. Compared to US-triggered drug release, the sonodynamic strategy is more suitable for antibacterial therapy because ROS are highly lethal to nearly all kinds of bacteria but exhibit very little drug resistance.[367,368] In the aqueous environment, US excitation gives rise to nucleation, growth, and implosive collapse of gas-filled bubbles, a process known as acoustic cavitation.[369] Bubble implosion causes rapid light emission and higher local temperature and pressure to activate the sonosensitizers to produce ROS.[370–372] Sonosensitizers in the form of nanomaterials composed of piezoelectric ceramic,[92] MOFs,[93–95] and nanoenzymes have been developed for sonodynamic antibacterial therapy.[96] However, the US-sensitive surface for SDT of bulk biomaterials has rarely been reported. Su et al.[91] have fabricated a S-doped TiO_2 layer on Ti (Ti-S-TiO_{2-x}) with good photothermal and sonocatalytic characteristics (**Figure 11**a). Under US excitation, ·OH and $^1O_2$ signals are detected from the Ti-S-TiO_{2-x} + US and Ti-S-TiO_{2-x} + Light + US groups due to the enhanced separation of electrons and holes in S-TiO_{2-x} (Figure 11b,c). After NIR exposure for 15 min and the US treatment, more than 99.99% of *S. aureus* are eliminated in vivo due to hyperthermia and excessive ROS (Figure 11d). Moreover, the Ti-S-TiO_{2-x} layer improves osseointegration of Ti and the stable structure and antibacterial efficiency are retained after immersion in water for 6 months.

Besides controlled drug release and SDT, novel US-based antibacterial processes are being studied because of the excellent tissue penetrability of US. For example, sonothermal therapy mediated by red phosphorus – coated Ti in combination with US excitation provides localized hyperthermia to synergistically sterilize MRSA resulting in enhanced release of NO.[97] Similar to other physical approaches, an excessively high US power causes hyperthermia in body fluids to possibly damage normal tissues.[373] What's more, the hypoxic environment at the infection site limits gas-filled bubble production in SDT.[374] Therefore, a surface with high sensitivity to US should be explored in order to achieve safer and better therapeutic efficiency.

4. Antibacterial Properties at the Interface Stimulated by Electrical Interaction

Device-related infection is highly resistant to conventional antimicrobial treatment and novel therapeutic approaches are called for. Bioelectricity is attracting attention in the research of the interactions between man-made devices and the living body, especially attempts to figure out the surface modification strategy that disturbs the bioelectrical balance in the intracellular and extracellular components in bacteria.[375] Electricity can provoke immune response to combat malady.[376–378] Furthermore, electrical stimulation can increase immune cytokines secretion, enhance uptake of immunomodulatory agents, and increase growth factor secretion and cell proliferation.[379–381] In this section, the electrical impact on bacteria and how the electrical factors influence bacterial metabolism are discussed. Moreover, studies utilizing bioelectrical approaches to kill and eradicate bacteria are described.

4.1. Bioelectrical Activities in Bacteria

A biological cell is analogous a battery, as both depend on redox reactions and movement of ions. In the biological cell, the membrane partitions ions and charged molecules giving rise to a membrane potential to move ions. This is the core theory and bioelectrical conceptualization of biological cells. Eukaryotic cells rely on the potential across the cellular and mitochondrial membrane to couple external bioelectrical stimuli to the corresponding internal cell states including gene expression and physiological responses. Despite the simpler cellular structure, we are just starting to understand the intracellular responses to external bioelectrical stimulation. Recently, electrophysiology of bacteria has become a new discipline to study the currents across a bacterial membrane sustained by an ion flux, which can report the real-time states of the proteins in the membrane (**Figure 12**).[382,383] The bacteria membrane potential is dynamic in cell division,[384] signaling, and metabolic coordination after stressful stimulation or antibacterial treatment.[385,386] On the other hand, extracellular electron transfer (EET) is related to the membrane potential,[387] which bridges the external electrophysical signal and intracellular physiological responses.

Recent research activities have focused on how electrical stimuli can influence the bacterial membrane potential and how the changed potential was transduced to gene regulation. Up to now,

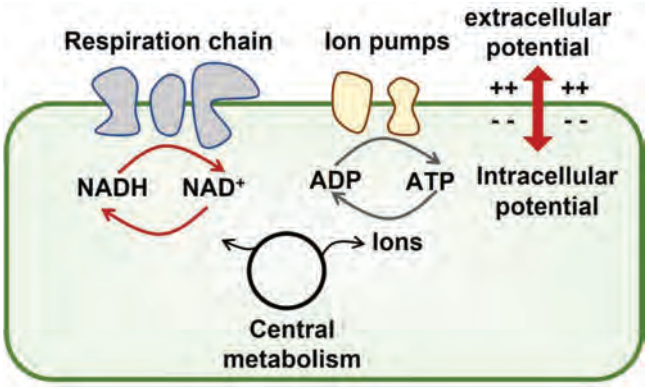

Figure 12. Bioelectrical conceptualization of bacteria.

the following two pathways have been identified. First, electrochemically activated bacteria can inspire the redox-coupled electrical sensing system such as Arc (anoxic redox control) to alter the expression of metabolic genes.[388] Moreover, the post-electrically stimulated bacteria can respond on the gene level via the ion flux across the membrane. For instance, the expression of K^+ and Ca^{2+}-related proteins is altered by external bioelectrical disturbance, which plays a vital role in the bacteria physiology.[389] Given the aforementioned nature of bioelectricity in bacteria, electrical stimuli can be employed to engineer bacteria to have the desired status. For instance, an altered membrane potential caused by an external electrical field can underpin the respiratory and fermentative status of bacteria thus determining the overall metabolic flux.[390] Bacteria proliferation can also be blocked by altering the membrane potential with an electric field.[389] As the bioelectrical signal is the heart in cell-cell communication, an external electrical field may cut off intra-biofilm signaling.[382] In the following section, the state-of-art antibacterial strategies based on external electrical stimulation are discussed. Generally, antibacterial strategies based on bioelectricity can be divided into ones depending on the external electric field, that is, materials carrying charged molecules or ions and surfaces that generate electron transfer based on capacitive or electron-storing materials. Regarding the first type of surfaces, external electrical stimulation produces a charged surface to deliver/snatch electrons to/from bacteria. As a result, bacterial metabolism is interrupted. For the second kind of surfaces, molecules or ions carrying charges produce the antibacterial surfaces and electrical damage is triggered in contact with bacteria. Moreover, antibacterial surfaces can be formed on energy-storing materials which are pre-charged prior to contact with bacteria. The external electricity produces rechargeable and instant antibacterial effects but repeated application is necessary. In this respect, materials that can store energy have advantages to reduce recharging and make the effects longer lasting.

4.1.1. Antibacterial Strategies Based on External Electric Fields

As bacteria depend on physical properties such as the membrane potential, it is rational that bacteria are affected by electric fields and currents trigger hyperpolarization or depolarization of the membrane potential. In the 1970s, Pareilleux et al.[98] and

Barranco et al.[99] investigated the inhibition effects of small currents on *E. coli* and *S. aureus* and demonstrated that a positive silver electrode produced the best antibacterial effects. The frequency of applied current, components, and metallic nature of the electrode were taken into consideration in their research. Afterward, scientists have attempted to explore the feasibility of using small currents as antibacterial strategy in clinical and environmental applications. The antibacterial and antifungal effects of these electrical measures have been validated for skin, catheters, and drinking water.[100–102] The underlying antibacterial mechanism of electrical stimulation is still not well understood, but the core antibacterial factors are attributed to the electrolytic products including ROSs, bacterial membranes, and respiratory rates.[391] Although the antibacterial ability of electrical currents has been verified, a small current is not effective and a high voltage is not suitable for biomedical applications. The research activities have turned to synergistic antibiofilm effects of physical treatment based on electrical and chemical measures based on antibiotics to enhance the efficacy. A series of in vitro studies have disclosed that antibiotics work better with the aid of a small current.[392] The reasons are related to changes in the binding between the biofilm and antimicrobials, altered membrane permeability, and oxygen or oxidizing agents produced by electrophysical reactions.[103,393–394]

Bacterial infection involving biofilms and AMR are threatening public health and antibiotics-free treatment is more desirable. Kincaid et al.[105] and Petrofsky et al.[104] have found that alternating currents and high voltage pulses can more effectively inhibit the growth of bacteria and researchers have tried to destroy biofilms with an electrical stimulus. Poortinga et al.[106] have found that a small DC current isolates adhered bacteria and Van der Borden et al.[107] have carried out a series of experiments and found that the electrical stimulus leads to biofilm detachment and poorer viability of the remaining bacteria. However, these conclusions need more in-depth verification and only a few ex vitro tests have been reported.

Recently, photothermal dynamic or magnetic therapy have been integrated to synergistically enhance the antibiofilm effects rendered by an electric field.[395,108] For instance, Campli et al.[109] have found that bacteria exposed to 50 Hz and 1 mT electromagnetic field show modified morphology and adhesion. Electrokinetic control of bacteria adherence has been investigated.[396] The antibacterial functions produced by a magnetic field can be divided into the direct and indirect types. In the direct type, the magneto-responsive materials are able to eliminate bacteria directly upon stimulation by an external magnetic field. For example, Elbourne et al.[110,111] have prepared magneto-responsive gallium-based liquid metal (LM) droplets which can be physically actuated to conform to the sharp edges when exposed to a rotating magnetic field. As a result, the moving liquid metal droplets with sharp edges damage the bacterial membrane and eradicate the biofilm effectively. As for the indirect mechanism, the antibacterial effect cannot be realized until the energy of the magnetic field is converted into electricity or heat, a process termed magnetoelectric and magnetothermal conversion.

To eliminate bacteria on stainless steel, Lai et al.[112] have prepared an electroactive $Tb_xDy_{1-x}Fe$ alloy/poly(vinylidene fluoride-trifluoroethylene) (TD/P(VDF-TrFE)) magnetoelectric coating which is responsive to a magnetic field (**Figure 13**a). After polarization by electric poling, the stainless steel magnetoelectric coating generates a micro-electric field with magnetic stimulation to produce ROS and H^+ consumption in the electrochemical gradient of the bacterial membrane (Figure 13d). Accumulation of intracellular OH^-, inhibition of ATP synthesis (Figure 13b,c), and hyperpolarization of the membrane potential are detected so that bacteria are sterilized. The strategies of using magnetothermal conversion to eliminate bacteria are similar to photothermal methods by producing hyperthermia or promoting drug release.[113–116] Wang et al.[115] have proposed a magneto-based synergetic therapy to destroy biofilms on orthopedic implants. The magnetically hard $CoFe_2O_4$ core and soft $MnFe_2O_4$ shell form the core-shell $CoFe_2O_4$@$MnFe_2O_4$ nanoparticles with excellent magnetic hyperthermia effects because of the exchange-coupled magnetism. The magnetothermal nanoparticles are coated with the thermosensitive NO donator (nitrosated mercaptosuccinic acid) and under an alternating magnetic field, the $CoFe_2O_4$@$MnFe_2O_4$ nanoparticles produce hyperthermia to loosen the dense biofilm and trigger NO release from nitrosated mercaptosuccinic acid, so that the nanoparticles with hyperthermia can penetrate the biofilm and release NO in the channels to synergistically eradicate the implant-associated infection. On the heels of clinical trial tests and advancement in electric field generation, the feasibility of electrical treatment has been validated for biomedical applications.

4.1.2. Antibacterial Interfaces with Charged Molecules or Ions

The susceptibility of bacteria to electrical stimuli has inspired the design of surfaces that carry charges and transport electrons to or deplete electrons from adhered bacteria. Multifunctional surfaces can be designed using materials with a nanostructure or surfaces grafted with functional species.

The most studied antibacterial surface based on cationic ions is the quaternary ammonium compound (QAC). Usually, these compounds are anchored on the surface of glass or silicon with or without a polymer spacer. Polymerization is used to bridge the substrate and QAC in the former case, while a simple physical coating is adopted in the latter case.[397] In the polymer spacer method, quaternization of DMAEMA on the PET film, PDMAEMA on PP, and PEI on glass slides can be achieved.[117,118] New methods to coat quaternary polymers on substrates are based on photocatalysis,[119] chemical linkage,[120] or direct covalent bonding.[121] The QACs kill bacteria based on ion exchange, in which cations on the membrane such as Mg^{2+} and Ca^{2+} are replaced by cations in the QAC thus destabilizing the ionic equilibrium and causing lethal effects in the bacteria.[398] The charge density plays the main role in enhancing the antibacterial efficiency.[399] While both positive and negative currents can kill bacteria by applying an electric field, the positive charge of the QAC is essential to antibacterial surface construction. The thresholds for the outer layer charge density vary from 1×10^{14} to 5×10^{15} charges/cm^{-2}.[400]

Cationic peptides are biocides found in the natural defending system of most living organisms. They usually possess amino acids arginine and lysine which are positively charged at a neutral pH due to localized polarization. The peptides are divided into four classes according to the folding modes, of which the

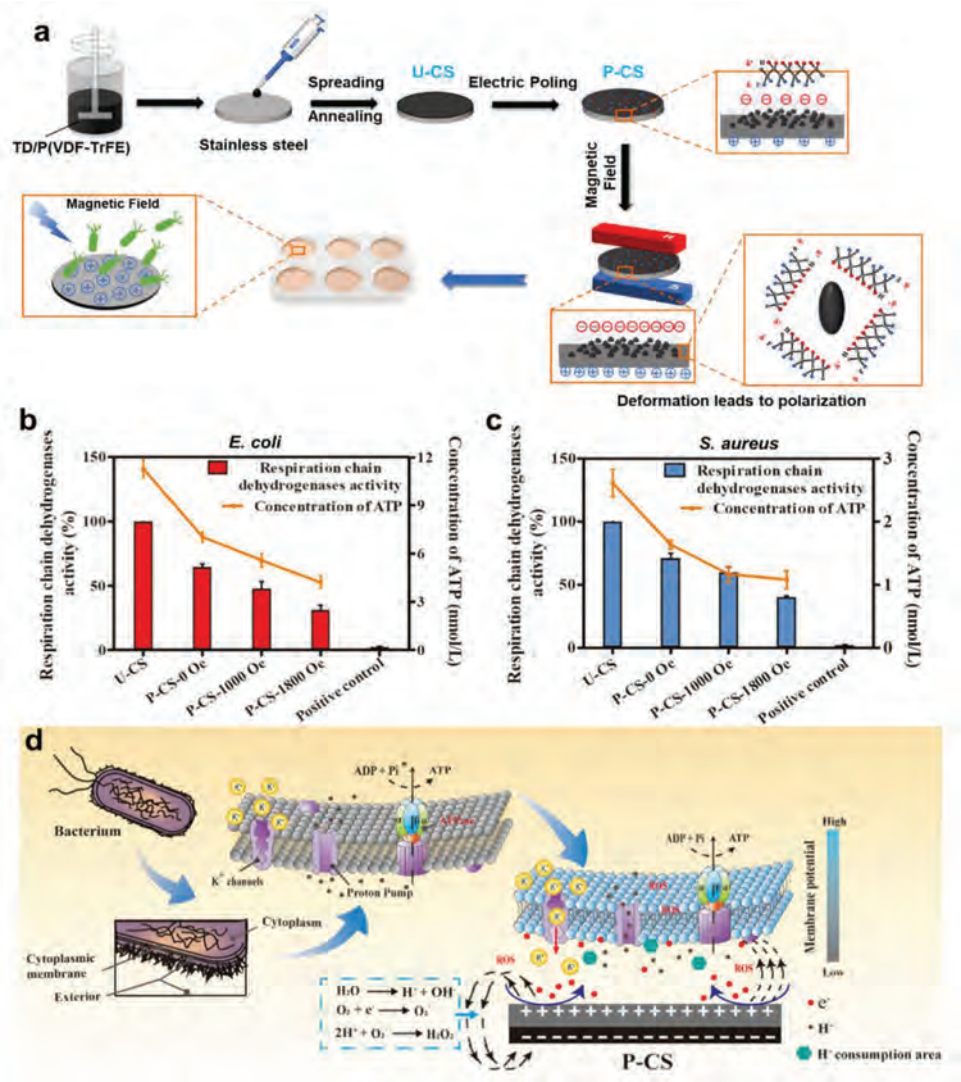

Figure 13. a) Illustration of the preparation and magnetoelectric effects of TD/P(VDF-TrFE) coatings. Respiratory chain dehydrogenase activity and ATP concentrations of b) *E. coli* and c) *S. aureus* after culturing for 24 h on the sample for different magnetic field strengths. d) Antibacterial mechanism of TD/P(VDF-TrFE)-assisted magnetoelectric stimulation. A micro-electric field is formed on the P-CS sample to produce ROS on the cathode and H^+ consumption due to the electrochemical gradient of the bacterial membrane. OH^- production and inhibition of ATP synthesis are detected. A K^+ efflux is also produced by TD/P(VDF-TrFE)-assisted electrical stimulation leading to hyperpolarization of the membrane potential in *E. coli*, thus causing rearrangement of the outer bacterial membrane. Reproduced with permission.[112] Copyright 2022, ACS Publishing.

α-helix class has been synthesized and optimized in laboratory. The antibacterial mode of cationic peptides is similar to the ion exchange mechanism for QACs. The positive charges on the peptides can easily replace Ca^{2+} and Mg^{2+} on the membrane as they have three times the affinity of lipopolysaccharide compared to the inherent cationic ions. Hence, the normal barrier of the membrane is disrupted and peptide undergoes transition forming clusters. Bacteria die from the destroyed membrane. The selectivity of bacteria instead of mammalian cells is attributed to the higher transmembrane potential of bacteria. Despite the broad-spectrum antibacterial properties and less toxicity, natural cationic peptides still need improvement as a larger charger density can produce higher antibacterial efficiency.[122] For example, the sliding window strategy has been developed to synthesize cationic peptides with 10 amino acid residues for higher antibacterial efficacy.[123] Stensen et al.[124] have designed and fabricated peptides with more positive charges with better anti-infection effects and Svenson et al.[401] have demonstrated that positively charged cationic peptides except arginine are simpler and less costly to make.

Despite the definite antibacterial efficiency and efforts people have made to decorate antibacterial interfaces with QACs or cationic peptides,[402–404] there are only a few products in the food industry and cleaning supply industry, but not biomedical applications due to the lack of toxicity and kinetics studies. One of the reasons for the limited application of QACs and cationic peptides is the uncertainty about bacterial resistance introduced by these chemical compounds.[405–408] Some compounds

like didecyldimethylammonium chloride can initiate allergic immune responses in the human body.[409,410] However, the combination of QACs and antimicrobial peptides with other methods such as biomimetically designed surfaces may reduce the needed quantity of QACs and deliver higher antimicrobial performance.[139–142,411] It is expected that antibacterial surfaces decorated with QACs and cationic peptides will be used clinically in the future.[125]

4.1.3. Antibacterial Surfaces on Capacitive or Electron-Storing Materials

Advances in functional materials and antibacterial theories spur the development of antibacterial materials. They are usually nanostructured materials with the ability to trigger charge transition upon contact with bacteria. Compared to the two main antibacterial methods, surfaces with a higher potential show higher efficacy. In this section, recent research related to antibacterial capacitive and electron-storage materials is summarized.

Metabolism of bacteria relies on many bioelectronic processes, among which EET plays a big part. EET is a fundamental mechanism for bacteria to generate energy to support cell growth.[412] Reguera et al.[413] have found that EET through pili of *G. sulfurreducens* may serve as biological nanowires to transport electrons. Microorganisms with the EET ability have been used in pollution treatment, biofuels, and biomineralization.[414–416] Antibacterial platforms based on electron transfer have been proposed by Cao et al.[126] Ag nanoparticles are introduced to titanium by plasma immersion ion implantation. The micro-galvanic couple composed of embedded Ag nanoparticles as the cathode and the Ti substrate as the anode is activated during immersion in a solution containing bacteria. The proton-depleted regions may disrupt the proton electrochemical gradient in the intermembrane space of the bacteria thus interfering with the energy supply system causing lethal effects. Subsequently works include optimizing the size of the electron-storing Ag nanoparticles to achieve the best antibacterial efficiency[45] and understanding the intracellular and extracellular mechanisms in the antibacterial process.[127] The electron transfer mediated antibacterial properties are not limited to Ag or Ti because other electron storing materials such as monolayer graphene can also kill bacteria by charge transfer.[417] Panda et al.[128] have revealed the electron transfer directed antibacterial properties of graphene oxide prepared on metals. A similar phenomenon has been observed from semiconductors decorated with other noble metal nanoparticles.[129,418–419]

Surfaces that kill bacteria based on electron transfer are superior to the ones based on photocatalysis or photothermal dynamics as no light is needed. Wang et al.[35] have designed a capacitive surface which can be charged to trigger electron transfer upon contact with bacteria. By adjusting the capacitance of the surface, the amount of charges can be tailored to achieve different antibacterial efficiency, which can be elevated to more than 90% by recharging. The antibacterial properties depend on the conducting or semiconducting substrate, which in theory can be extended to wearable devices by means of conductive polymers. Wu et al.[130] have found that Ag decoration improves the antibacterial ability of PPy, while it is not antibacterial in the pristine state. The bacterial current is found to be proportional to the number of bacteria as reported by Wang et al.,[46] who have proposed a quantitative bacterial killing and monitoring platform based on electron transfer at the interface (**Figure 14**).

Attempts to utilize electron transfer to treat or monitor bacterial infection forebode promising applications of the novel bioelectric antibacterial strategy applicable to implantable and wearable devices, because both wireless charging and the mechanical energy of the body can be utilized to trigger the electric interactions. However, this field is in the infancy stage and more work is necessary. Issues such as the effects of the charging current and impact on the functions of mammalian tissues and cells, platforms that can integrate the power supply and antibacterial components, and preclinical and clinical trials for implantable and wearable devices should be addressed.

5. Conclusion and Prospective

In this review, recent research progress pertaining to the design of antimicrobial surfaces without evolving microbial resistance is described. There are three major strategies to accomplish this purpose by killing and inhibiting bacteria from attaching to the surfaces: 1) Biomimetic design by fabricating micro/nanopatterns inspired by nature such as lotus leaves, shark skin, and insect wings. 2) Killing bacteria by sound and light waves using techniques such as ultrasound therapy and photothermal/dynamic therapy. 3) Disrupting and killing bacteria by electrical and other external stimuli.

These approaches, especially those based on light and electrical stimulation, have been demonstrated to be effective for other purposes such as cancer therapy and[276] cell differentiation.[420] Although most of these techniques do not introduce drug and antibiotics resistance, practical implementation is still challenging and more work is needed to bring the technology to clinical fruition.

Despite recent advances in human hygiene and living conditions, bacterial infection continues to be one of the primary causes of AMR and post-surgical complications.[421] Strategies such as new antibiotics and incorporation of antibacterial agents into biomaterials are the most common.[422,423] However, these approaches may give rise to super bacteria[139–145] that can exacerbate AMR. Therefore, other methods such as fabrication of surface micro/nanopatterns, phototherapy, and electrical stimulation have attracted research interests.

In spite of significant breakthroughs, most of the techniques described in this review have only shown success in the laboratory and clinical adoption is still challenging. For example, platforms making use of hydrophobic or superhydrophobic surfaces may be difficult to implement on implants in vivo because other biological and mechanical concerns must also be addressed. In some orthopedic and dental applications, cell attachment and proliferation are also necessary for proper healing. Surfaces that require cleaning and disinfection with alcohol, UV, plasma, and so on may lose some of the antibacterial efficacy afterward and the durability and stability of the modified surfaces must be improved.[71,424] In this respect, encouraging results have been obtained from hydrophilic antibacterial platforms. As aforementioned, besides the surface properties, the interactions between the stimuli and human cells must be well understood. For

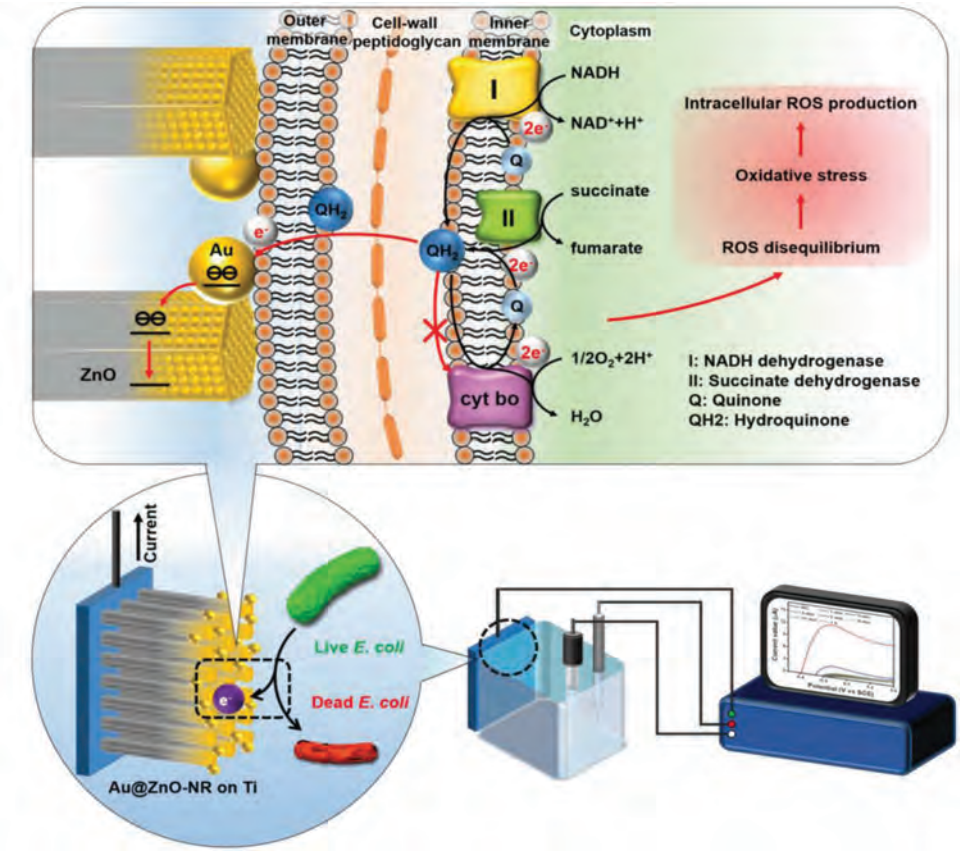

Figure 14. Illustration of electron transfer from *E. coli* to Au@ZnO resulting in bacteria death and the detection method of generated current using an electrochemical workstation. Reproduced with permission.[46] Copyright 2020, Wiley-VCH GmbH.

instance, electrical stimulation may alter the cell fate[425] and in the application of phototherapy for antibacterial purposes, the impact of generated heat, ROSs, and others on the cellular behavior should be examined and optimized carefully,[85,355] otherwise the adverse effects may outweigh the gain in the antibacterial capability.

Another important factor is the longevity and stability of the modified materials. For instance, how long biomimetic nanopatterns remain effective during storage and after surgical implantation is critical to clinical implementation. PTT has been shown to be effective in cancer therapy and no AMR is expected. Although different photon wavelengths have been experimented to improve the penetration depth and biocompatibility of PDT and PTT, it may be difficult to implement in deep tissues without endoscopic techniques and inadvertent heating of adjacent healthy tissues must be mitigated.[87,359] In the case of electrical bacteria killing, means to provide electrical currents inside the body and in situ monitoring techniques must be developed to monitor the healing process.[35,98,99,120,413] Most of the antimicrobial methods work by disrupting the cell walls and functions of bacteria and hence, the underlying mechanisms must be well understood to expedite clinical adoption. Although researchers are eager to find the panacea to eliminate AMR, we must also be realistic. Each platform is different and multiple factors such as bacterial resistance, biofilm formation, cytotoxicity, stability, durability, tissue growth, mechanical properties, cost, clinical difficulty, and others must be considered to identify the best solution which may require one or more techniques. Obviously, there is still much room for improvement pertaining to materials design and fabrication/operational protocols. A better understanding of the fundamental mechanisms will also be necessary for future development.

Acknowledgements

This work was financially supported by City University of Hong Kong Donation Research Grant (DON-RMG 9229021), City University of Hong Kong Strategic Research Grant (SRG 7005505), City University of Hong Kong Donation Grant (9220061), Hong Kong PDFS—RGC Postdoctoral Fellowship Scheme (PDFS2122-1S08 and CityU 9061014), Hong Kong HMRF (Health and Medical Research Fund) (2120972 and CityU 9211320).

Conflict of Interest

The authors declare no conflict of interest.

Keywords

antimicrobial resistance, biomimicked nanopatterned surfaces, electron transfer, photodynamic/thermal therapy

Received: August 17, 2022
Revised: October 12, 2022
Published online: November 1, 2022

[1] J. O. Lundberg, E. Weitzberg, J. A. Cole, N. Benjamin, *Nat. Rev. Microbiol.* **2004**, *2*, 593.
[2] M. Salami, *Front Neurosci* **2021**, *15*, 613120.
[3] H. Wang, C.-X. Wei, L. Min, L.-Y. Zhu, *Biotechnol Biotechnol Equip* **2018**, *32*, 1075.
[4] S. L. Gorbach, *Ann. Med.* **1990**, *22*, 37.
[5] R. I. Aminov, *Front Microbiol* **2010**, *1*, 134.
[6] K. A. Davis, J. J. Stewart, H. K. Crouch, C. E. Florez, D. R. Hospenthal, *Clin. Infect. Dis.* **2004**, *39*, 776.
[7] H. Hanberger, S. Walther, M. Leone, P. S. Barie, J. Rello, J. Lipman, J. C. Marshall, A. Anzueto, Y. Sakr, P. Pickkers, P. Felleiter, M. Engoren, J.-L. Vincent, *Int. J. Antimicrob. Agents* **2011**, *38*, 331.
[8] J. S. Bertino, *Clin Ophthalmol* **2009**, *3*, 507.
[9] C. Ghosh, P. Sarkar, R. Issa, J. Haldar, *Trends Microbiol.* **2019**, *27*, 323.
[10] A. K. Epstein, B. Pokroy, A. Seminara, J. Aizenberg, *Proc. Natl. Acad. Sci.* **2010**, *108*, 995.
[11] H. Vlamakis, Y. Chai, P. Beauregard, R. Losick, R. Kolter, *Nat. Rev. Microbiol.* **2013**, *11*, 157.
[12] W. Shen, P. He, C. Xiao, X. Chen, *Adv. Healthcare Mater.* **2018**, *7*, 1800354.
[13] S. M. Dizaj, F. Lotfipour, M. Barzegar-Jalali, M. H. Zarrintan, K. Adibkia, *Mater. Sci. Eng., C* **2014**, *44*, 278.
[14] J. A. Lemire, J. J. Harrison, R. J. Turner, *Nat. Rev. Microbiol.* **2013**, *11*, 371.
[15] D. P. Linklater, V. A. Baulin, S. Juodkazis, R J. Crawford, P. Stoodley, E P. Ivanova, *Nat. Rev. Microbiol.* **2021**, *19*, 8.
[16] J. L. Del Pozo, M. S. Rouse, J. N. Mandrekar, M. F. Sampedro, J. M. Steckelberg, R. Patel, *Antimicrob. Agents Chemother.* **2009**, *53*, 35.
[17] C. Piyadasa, T. R. Yeager, S. R. Gray, M. B. Stewart, H. F. Ridgway, C. Pelekani, J. D. Orbell, *J. Chem. Technol. Biotechnol.* **2018**, *93*, 871.
[18] F. Cieplik, D. Deng, W. Crielaard, W. Buchalla, E. Hellwig, A. Al-Ahmad, T. Maisch, *Crit. Rev. Microbiol.* **2018**, *44*, 571.
[19] J. L. Hobman, L. C. Crossman, *J. Med. Microbiol.* **2015**, *64*, 471.
[20] B. Reddy, S. K. Dubey, *Environ. Pollut.* **2019**, *246*, 443.
[21] B. El Shazely, G. Yu, P. R. Johnston, J. Rolff, *Front Microbiol* **2020**, *11*, 103.
[22] H.-S. Joo, C.-I. Fu, M. Otto, *Philosophical Transactions B* **2016**, *371*, 20150292.
[23] J. Hasan, R. J. Crawford, E. P. Ivanova, *Trends Biotechnol.* **2013**, *31*, 295.
[24] K. Glinel, P. Thebault, V. Humblot, C. M. Pradier, T. Jouenne, *Acta Biomater.* **2012**, *8*, 1670.
[25] L. Luo, Y. Zhou, X. Xu, W. Shi, J. Hu, G. Li, Xi Qu, Y. Guo, X. Tian, A. Zaman, D. Hui, Z. Zhou, *Nanotechnol Rev* **2020**, *9*, 1562.
[26] R. Jiang, L. Hao, L. Song, L. Tian, Y. Fan, J. Zhao, C. Liu, W. Ming, L. Ren, *Chem. Eng. J.* **2020**, *398*, 125609.
[27] X.-Q. Dou, D. Zhang, C. Feng, L. Jiang, *ACS Nano* **2015**, *9*, 10664.
[28] J. Hasan, H. K. Webb, V. K Truong, S. Pogodin, V. A. Baulin, G. S. Watson, J. A. Watson, R. J. Crawford, E. P. Ivanova, *Appl. Microbiol. Biotechnol.* **2013**, *97*, 9257.
[29] X. Li, G. S. Cheung, G. S. Watson, J. A. Watson, S. Lin, L. Schwarzkopf, D. W. Green, *Nanoscale* **2016**, *8*, 18860.
[30] F. Viela, I. Navarro-Baena, J. J. Hernández, M. R. Osorio, I. Rodriguez, *Bioinspir. Biomim.* **2018**, *13*, 026011.
[31] A. Gao, Y. Yan, T. Li, F. Liu, *Mater. Lett.* **2019**, *237*, 240.
[32] M. Miyazaki, H. Moriya, A. Miyauchi, *J. Photopolym. Sci. Technol.* **2019**, *32*, 295.
[33] Y. Chen, Y. Gao, Y. Chen, L. Liu, A. Mo, Q. Peng, *J. Controlled Release* **2020**, *328*, 251.
[34] I. Gall, M. Herzberg, Y. Oren, *Soft Matter* **2013**, *9*, 2443.
[35] G. Wang, H. Feng, L. Hu, W. Jin, Q. Hao, A. Gao, X. Peng, W. Li, K.-Y. Wong, H. Wang, Z. Li, P. K. Chu, *Nat. Commun.* **2018**, *9*, 2055.
[36] W. Li, E. S. Thian, M. Wang, Z. Wang, L. Ren, *Adv. Sci.* **2021**, *8*, 2100368.
[37] L. Zhao, R. Chen, L. Lou, X. Jing, Qi Liu, J. Liu, J. Yu, P. Liu, J. Wang, *Appl. Surf. Sci.* **2020**, *511*, 145564.
[38] C. S. Sharma, K. Abhishek, H. Katepalli, A. Sharma, *Ind. Eng. Chem. Res.* **2011**, *50*, 13012.
[39] K. Nowlin, D. R. Lajeunesse, *Mol. Syst. Des. Eng.* **2017**, *2*, 201.
[40] R. Bright, A. Hayles, J. Wood, N. Ninan, D. Palms, R. M. Visalakshan, A. Burzava, T. Brown, D. Barker, K. Vasilev, *Nanomaterials* **2022**, *12*, 1140.
[41] S. Jin, Y. Wang, M. Motlag, S. Gao, J. Xu, Q. Nian, W. Wu, G. J. Cheng, *Adv. Mater.* **2018**, *30*, 1705840.
[42] F. Alam, M. Elsherif, B. Alqattan, A. Salih, S. M. Lee, A. K. Yetisen, S. Park, H. Butt, *ACS Biomater. Sci. Eng.* **2021**, *7*, 794.
[43] M. A. P Mahmud, A. Zolfagharian, S. Gharaie, A. Kaynak, S. H. Farjana, A. V. Ellis, J. Chen, A. Z. Kouzani, *Adv. Energy Sustainability Res.* **2021**, *2*, 2000045.
[44] M. Yang, S. Qiu, E. Coy, S. Li, K. Załęski, Y. Zhang, H. Pan, G. Wang, *Adv. Mater.* **2022**, *34*, 2106314.
[45] H. Cao, Y. Qiao, X. Liu, T. Lu, T. Cui, F. Meng, P K. Chu, *Acta Biomater.* **2013**, *9*, 5100.
[46] G. Wang, K. Tang, Z. Meng, P. Liu, S. Mo, B. Mehrjou, H. Wang, X. Liu, Z. Wu, P. K. Chu, *Adv. Mater.* **2020**, *32*, 2003616.
[47] E. P. Ivanova, J. Hasan, H. K. Webb, V. K. Truong, G. S. Watson, J. A. Watson, V. A. Baulin, S. Pogodin, J. Y. Wang, M. J. Tobin, C. Lobbe, R. J. Crawford, *Small* **2012**, *8*, 2489.
[48] K.-H. Tsui, X. Li, J. K. H. Tsoi, S.-F. Leung, T. Lei, W. Y. Chak, C. Zhang, J. Chen, G. S. P. Cheung, Z. Fan, *Nanoscale* **2018**, *10*, 10436.
[49] S. Kim, U. T. Jung, S.-K. Kim, J.-H. Lee, H. S. Choi, C.-S. Kim, M. Y. Jeong, *ACS Appl. Mater. Interfaces* **2015**, *7*, 326.
[50] B. Mehrjou, S. Mo, D. Dehghan-Baniani, G. Wang, A. M. Qasim, P. K. Chu, *ACS Appl. Mater. Interfaces* **2019**, *11*, 31605.
[51] S. L. Arias, J. Devorkin, J. C. Spear, A. Civantos, J. P. Allain, *ACS Appl. Bio Mater.* **2020**, *3*, 7974.
[52] L. E. Fisher, Y. Yang, M.-F. Yuen, W. Zhang, A. H. Nobbs, B. Su, *Biointerphases* **2016**, *11*, 011014.
[53] V. T. H. Pham, V. K. Truong, A. Orlowska, S. Ghanaati, M. Barbeck, P. Booms, A. J. Fulcher, C. M. Bhadra, R. A. Buividas, V. Baulin, C. J. Kirkpatrick, P. Doran, D. E. Mainwaring, S. Juodkazis, R. J. Crawford, E. P. Ivanova, *ACS Appl. Mater. Interfaces* **2016**, *8*, 22025.
[54] S. Mo, B. Mehrjou, K. Tang, H. Wang, K. Huo, A. M. Qasim, G. Wang, P. K. Chu, *Chem. Eng. J.* **2020**, *392*, 123736.
[55] L. Liu, B. Ercan, L. Sun, K. S. Ziemer, T. J. Webster, *ACS Biomater. Sci. Eng.* **2016**, *2*, 122.
[56] R. Fontelo, D. S. Da Costa, R. L. Reis, R. Novoa-Carballal, I. Pashkuleva, *Acta Biomater.* **2020**, *112*, 174.
[57] A. Daskalova, L. Angelova, E. Filipov, D. Aceti, R. Mincheva, X. Carrete, H. Kerdjoudj, M. Dubus, J. Chevrier, A. Trifonov, I. Buchvarov, *Polymers* **2021**, *13*, 2577.
[58] A. M. Richter, G. Buchberger, D. Stifter, J. Duchoslav, A. Hertwig, J. Bonse, J. Heitz, K. Schwibbert, *Nanomaterials* **2021**, *11*, 3000.
[59] L. B. Boinovich, E. B. Modin, A. V. Aleshkin, K. A. Emelyanenko, E. R. Zulkarneev, I. A. Kiseleva, A. L. Vasiliev, A. M. Emelyanenko, *ACS Appl. Nano Mater.* **2018**, *1*, 1348.
[60] D. P. Linklater, M. De Volder, V. A. Baulin, M. Werner, S. Jessl, M. Golozar, L. Maggini, S. Rubanov, E. Hanssen, S. Juodkazis, E. P. Ivanova, *ACS Nano* **2018**, *12*, 6657.
[61] T. Sjöström, A. H. Nobbs, B. Su, *Mater. Lett.* **2016**, *167*, 22.
[62] X. Ge, C. Ren, Y. Ding, G. Chen, X. Lu, K. Wang, F. Ren, M. Yang, Z. Wang, J. Li, X. An, B. Qian, Y. Leng, *Bioact. Mater.* **2019**, *4*, 346.
[63] R. Bright, D. Fernandes, J. Wood, D. Palms, A. Burzava, N. Ninan, T. Brown, D. Barker, K. Vasilev, *Mater. Today Bio* **2022**, *13*, 100176.

[64] J. v. Wandiyanto, V. K. Truong, M. al Kobaisi, S. Juodkazis, H. Thissen, O. Bazaka, K. Bazaka, R. J. Crawford, E. P. Ivanova, *Materials* **2019**, *12*, 1575.
[65] J. Zhou, B. Li, L. Zhao, L. Zhang, Y. Han, *ACS Biomater. Sci. Eng.* **2017**, *3*, 1437.
[66] G. Wang, W. Jiang, S. Mo, L. Xie, Q. Liao, L. Hu, Q. Ruan, K. Tang, B. Mehrjou, M. Liu, L. Tong, H. Wang, J. Zhuang, G. Wu, P. K. Chu, *Adv. Sci.* **2020**, *7*, 1902089.
[67] B. Mehrjou, D. Dehghan-Baniani, M. Shi, A. Shanaghi, G. Wang, L. Liu, A. M. Qasim, P. K. Chu, *Mater. Sci. Eng., C* **2020**, *116*, 111173.
[68] Y. Tang, H. Sun, Z. Qin, S. Yin, L. Tian, Z. Liu, *Chem. Eng. J.* **2020**, *398*, 125575.
[69] Y. Cao, S. Jana, L. Bowen, X. Tan, H. Liu, N. Rostami, J. Brown, N. S. Jakubovics, J. Chen, *Langmuir* **2019**, *35*, 14670.
[70] E. J. Nodoushan, N. G. Ebrahimi, M. Ayazi, *Appl. Surf. Sci.* **2017**, *423*, 1054.
[71] K. Minoura, M. Yamada, T. Mizoguchi, T. Kaneko, K. Nishiyama, M. Ozminskyj, T. Koshizuka, I. Wada, T. Suzutani, *PLoS One* **2017**, *12*, e0185366.
[72] M. Yamada, K. Minoura, T. Mizoguchi, K. Nakamatsu, T. Taguchi, T. Kameda, M. Sekiguchi, T. Suzutani, S. Konno, *PLoS One* **2018**, *13*, e0198300.
[73] S. Rostami, F. Puza, M. Ucak, E. Ozgur, O. Gul, U. K. Ercan, B. Garipcan, *Appl. Surf. Sci.* **2021**, *544*, 148828.
[74] T. Shi, X. Hou, S. Guo, L. Zhang, C. Wei, T. Peng, X. Hu, *Nat. Commun.* **2021**, *12*, 493.
[75] Q. Gao, T. Feng, D. Huang, P. Liu, P. Lin, Y. Wu, Z. Ye, J. Ji, P. Li, W. Huang, *Biomater. Sci.* **2020**, *8*, 278.
[76] T.-T. Yao, J. Wang, Y.-F. Xue, W.-J. Yu, Q. Gao, L. Ferreira, K.-F. Ren, J. Ji, *J. Mater. Chem. B* **2019**, *7*, 5089.
[77] Z. Liu, X. Liu, Z. Cui, Y. Zheng, Z. Li, Y. Liang, X. Yuan, S. Zhu, S. Wu, *J. Mater. Sci. Technol.* **2022**, *122*, 10.
[78] X. Xie, C. Mao, X. Liu, Y. Zhang, Z. Cui, X. Yang, K. W. K. Yeung, H. Pan, P. K. Chu, S. Wu, *ACS Appl. Mater. Interfaces* **2017**, *9*, 26417.
[79] Z. Wei, S. Teng, Y. Fu, Q. Zhou, W. Yang, *Prog. Org. Coat.* **2022**, *164*, 106703.
[80] Y. He, J. Leng, K. Li, K. Xu, C. Lin, Z. Yuan, R. Zhang, D. Wang, B. Tao, T. J. Huang, K. Cai, *Biomaterials* **2021**, *278*, 121164.
[81] X. Yu, S. Wang, X. Zhang, A. Qi, X. Qiao, Z. Liu, M. Wu, L. Li, Z. L. Wang, *Nano Energy* **2018**, *46*, 29.
[82] X. Zhang, J. Qiu, J. Tan, D. Zhang, L. Wu, Y. Qiao, G. Wang, J. Wu, K. W. K. Yeung, X. Liu, *Carbon* **2022**, *192*, 209.
[83] W. Qian, C. Yan, D. He, X. Yu, L. Yuan, M. Liu, G. Luo, J. Deng, *Acta Biomater.* **2018**, *69*, 256.
[84] X. Zhang, G. Zhang, M. Chai, X. Yao, W. Chen, P. K. Chu, *Bioact. Mater.* **2021**, *6*, 12.
[85] Y. Wu, Q. Liao, L. Wu, Y. Luo, W. Zhang, M. Guan, H. Pan, L. Tong, P. K. Chu, H. Wang, *ACS Nano* **2021**, *15*, 17854.
[86] S. Li, B. Gu, X. Li, S. Tang, L. Zheng, E. Ruiz-Hitzky, Z. Sun, C. Xu, X. Wang, *Adv Healthc Mater* **2022**, *11*, 2102367.
[87] B. Hu, C. Berkey, T. Feliciano, X. Chen, Z. Li, C. Chen, S. Amini, M. H. Nai, Q. L. Lei, R. Ni, J. Wang, W. R. Leow, S. Pan, Y. Q. Li, P. Cai, A. Miserez, S. Li, C. T. Lim, Y. L. Wu, T. W. Odom, R. H. Dauskardt, X. Chen, *Adv. Mater.* **2020**, *32*, 1907030.
[88] Y. Luo, X. Liu, L. Tan, Z. Li, K. W. K. Yeung, Y. Zheng, Z. Cui, Y. Liang, S. Zhu, C. Li, X. Wang, S. Wu, *Chem. Eng. J.* **2021**, *405*, 126730.
[89] J. Zeng, Y. Wang, Z. Sun, H. Chang, M. Cao, J. Zhao, K. Lin, Y. Xie, *Chem. Eng. J.* **2020**, *394*, 125017.
[90] C. Jin, K. Su, L. Tan, X. Liu, Z. Cui, X. Yang, Z. Li, Y. Liang, S. Zhu, K. W. K. Yeung, S. Wu, *Mater. Des.* **2019**, *177*, 107845.
[91] K. Su, L. Tan, X. Liu, Z. Cui, Y. Zheng, B. Li, Y. Han, Z. Li, S. Zhu, Y. Liang, X. Feng, X. Wang, S. Wu, *ACS Nano* **2020**, *14*, 2077.
[92] M. Wu, Z. Zhang, Z. Liu, J. Zhang, Y. Zhang, Y. Ding, T. Huang, D. Xiang, Z. Wang, Y. Dai, X. Wan, S. Wang, H. Qian, Q. Sun, L. Li, *Nano Today* **2021**, *37*, 101104.
[93] Y. Yu, L. Tan, Z. Li, X. Liu, Y. Zheng, X. Feng, Y. Liang, Z. Cui, S. Zhu, S. Wu, *ACS Nano* **2021**, *15*, 10628.
[94] X. Feng, L. Ma, J. Lei, Q. Ouyang, Y. Zeng, Y. Luo, X. Zhang, Y. Song, G. Li, L. Tan, X. Liu, C. Yang, *ACS Nano* **2022**, *16*, 2546.
[95] X. Pan, N. Wu, S. Tian, J. Guo, C. Wang, Y. Sun, Z. Huang, F. Chen, Q. Wu, Y. Jing, Z. Yin, B. Zhao, X. Xiong, H. Liu, D. Zhou, *Adv. Funct. Mater.* **2022**, *32*, 2112145.
[96] D. Sun, X. Pang, Y. Cheng, J. Ming, S. Xiang, C. Zhang, P. Lv, C. Chu, X. Chen, G. Liu, N. Zheng, *ACS Nano* **2020**, *14*, 2063.
[97] W. Guan, L. Tan, X. Liu, Z. Cui, Y. Zheng, K. W. K. Yeung, D. Zheng, Y. Liang, Z. Li, S. Zhu, X. Wang, S. Wu, *Adv. Mater.* **2021**, *33*, 2006047.
[98] A. Pareilleux, N. Sicard, *Appl. Microbiol.* **1970**, *19*, 421.
[99] S. D. Barranco, J. A. Spadaro, T. J. Berger, R. O. Becker, *Clin. Orthop. Relat. Res.* **1974**, *100*, 250.
[100] C. P. Davis, N. Wagle, M. D. Anderson, M. M. Warren, *Antimicrob. Agents Chemother.* **1991**, *35*, 2131.
[101] L. Bolton, B. Foleno, B. Means, S. Petrucelli, *Antimicrob. Agents Chemother.* **1980**, *18*, 137.
[102] T. Matsunaga, S. Nakasono, T. Takamuku, J. G. Burgess, N. Nakamura, K. Sode, *Appl. Environ. Microbiol.* **1992**, *58*, 686.
[103] S. A. Blenkinsopp, A. E. Khoury, J. W. Costerton, *Appl. Environ. Microbiol.* **1992**, *58*, 3770.
[104] J. Petrofsky, M. Laymon, W. Chung, K. Collins, T.-N. Yang, *J. Orthop.* **2008**, *31*, 43.
[105] C. B. Kincaid, K. H. Lavoie, *Phys Ther* **1989**, *69*, 651.
[106] A. T. Poortinga, R. Bos, H. J. Busscher, *Biotechnol. Bioeng.* **2000**, *67*, 117.
[107] A. J. Van Der Borden, P. G. M. Maathuis, E. Engels, G. Rakhorst, H. C. Van Der Mei, H. J. Busscher, P. K. Sharma, *Biomaterials* **2007**, *28*, 2122.
[108] A. Mercier, J. Bertaux, J. Lesobre, K. Gravouil, J. Verdon, C. Imbert, E. Valette, Y. Héchard, *Biofouling* **2016**, *32*, 287.
[109] E. Di Campli, S. Di Bartolomeo, R. Grande, M. Di Giulio, L. Cellini, *Curr. Microbiol.* **2010**, *60*, 412.
[110] A. Elbourne, S. Cheeseman, P. Atkin, N. P. Truong, N. Syed, A. Zavabeti, M. Mohiuddin, D. Esrafilzadeh, D. Cozzolino, C. F. Mcconville, M. D. Dickey, R. J. Crawford, K. Kalantar-Zadeh, J. Chapman, T. Daeneke, V. K. Truong, *ACS Nano* **2020**, *14*, 802.
[111] S. Cheeseman, A. Elbourne, R. Kariuki, A. V. Ramarao, A. Zavabeti, N. Syed, A. J. Christofferson, K. Y. Kwon, W. Jung, M. D. Dickey, K. Kalantar-Zadeh, C. F. Mcconville, R. J. Crawford, T. Daeneke, J. Chapman, V. K. Truong, *J. Mater. Chem. B* **2020**, *8*, 10776.
[112] S. Lai, Y. Wang, Y. Wan, H. Ma, L. Fang, J. Su, *ACS Appl. Mater. Interfaces* **2022**, *14*, 20139.
[113] S. Singh, K. C. Barick, D. Bahadur, *Powder Technol.* **2015**, *269*, 513.
[114] X. Zhang, C. Tian, Z. Chen, G. Zhao, *Adv. Ther.* **2020**, *3*, 2000001.
[115] J. Wang, L. Wang, J. Pan, J. Zhao, J. Tang, D. Jiang, P. Hu, W. Jia, J. Shi, *Adv. Sci.* **2021**, *8*, 2004010.
[116] C. Sun, W. Wang, X. Sun, W. Chu, J. Yang, J. Dai, Y. Ju, *Biomater. Sci.* **2021**, *9*, 8323.
[117] L. Cen, K. G. Neoh, E. T. Kang, *Langmuir* **2003**, *19*, 10295.
[118] J. Huang, H. Murata, R. R. Koepsel, A. J. Russell, K. Matyjaszewski, *Biomacromolecules* **2007**, *8*, 1396.
[119] G. Gozzelino, C. Lisanti, S. Beneventi, *Colloids Surf., A* **2013**, *430*, 21.
[120] S. Zanini, A. Polissi, E. A. Maccagni, E. C. Dell'Orto, C. Liberatore, C. Riccardi, *J. Colloid Interface Sci.* **2015**, *451*, 78.
[121] W. Z. Xu, G. Gao, J. F. Kadla, *Cellulose* **2013**, *20*, 1187.
[122] X. Cao, Y. Zhang, R. Mao, D. Teng, X. Wang, J. Wang, *Appl. Microbiol. Biotechnol.* **2015**, *99*, 2649.
[123] E. S. CÃ¢Ndido, M. H. Cardoso, L. Y. Chan, M. D. T. Torres, K. G. N. Oshiro, W. F. Porto, S. M. Ribeiro, E. F. Haney, R. E. W. Hancock, T.

K. Lu, C. De La Fuente-Nunez, D. J. Craik, O. V. L. Franco, *ACS Infect. Dis.* **2019**, *5*, 1081.
[124] W. Stensen, R. Turner, M. Brown, N. Kondori, J. S. Svendsen, J. Svenson, *Mol. Pharm.* **2016**, *13*, 3595.
[125] B.-Y. Lu, G.-Y. Zhu, C.-H. Yu, G.-Y. Chen, C.-L. Zhang, X. Zeng, Q.-M. Chen, Q. Peng, *Nano Res.* **2021**, *14*, 185.
[126] H. Cao, X. Liu, F. Meng, P. K. Chu, *Biomaterials* **2011**, *32*, 693.
[127] G. Wang, W. Jin, A. M. Qasim, A. Gao, X. Peng, W. Li, H. Feng, P. K. Chu, *Biomaterials* **2017**, *124*, 25.
[128] S. Panda, T. K. Rout, A. D. Prusty, P. M. Ajayan, S. Nayak, *Adv. Mater.* **2018**, *30*, 1702149.
[129] G. Wang, H. Feng, W. Jin, A. Gao, X. Peng, W. Li, H. Wu, Z. Li, P. K. Chu, *Appl. Surf. Sci.* **2017**, *414*, 230.
[130] Y. Wu, Q. Ruan, C. Huang, Q. Liao, L. Liu, P. Liu, S. Mo, G. Wang, H. Wang, P. K. Chu, *Biomater. Adv.* **2022**, *134*, 112701.
[131] L. M. Faulhaber, R. D. Karp, *Immunology* **1992**, *75*, 378.
[132] B. P. Lazzaro, *Curr. Opin. Microbiol.* **2008**, *11*, 284.
[133] J. P. Gillespie, M. R. Kanost, T. Trenczek, *Annu. Rev. Entomol.* **1997**, *42*, 611.
[134] M. Lamberty, D. Zachary, R. Lanot, C. Bordereau, A. Robert, J. A. Hoffmann, P. Bulet, *J. Biol. Chem.* **2001**, *276*, 4085.
[135] S. Cheeseman, S. Owen, V. K. Truong, D. Meyer, S. H. Ng, J. Vongsvivut, D. Linklater, M. J. Tobin, M. Werner, V. A. Baulin, P. Luque, R. Marchant, S. Juodkazis, R. J. Crawford, E. P. Ivanova, *ACS Omega* **2018**, *3*, 6039.
[136] D. Chopra, K. Gulati, S. Ivanovski, *Mater. Today Adv.* **2021**, *12*, 100176.
[137] T. U. Luu, S. C. Gott, B. W. K. Woo, M. P. Rao, W. F. Liu, *ACS Appl. Mater. Interfaces* **2015**, *7*, 28665.
[138] M. Shayan, J. Padmanabhan, A. H. Morris, B. Cheung, R. Smith, J. Schroers, T. R. Kyriakides, *Acta Biomater.* **2018**, *75*, 427.
[139] Q. Yu, J. Cho, P. Shivapooja, L K. Ista, G. P. López, *ACS Appl. Mater. Interfaces* **2013**, *5*, 9295.
[140] B. He, Y. Du, B. Wang, X. Wang, Q. Ye, S. Liu, *Prog. Org. Coat.* **2021**, *157*, 106298.
[141] Z. Liu, Y. Yi, L. Song, Y. Chen, L. Tian, J. Zhao, L. Ren, *Acta Biomater.* **2022**, *141*, 198.
[142] N. Vargas-Alfredo, A. Santos-Coquillat, E. Martínez-Campos, A. Dorronsoro, A. L. Cortajarena, A. del Campo, J. Rodríguez-Hernández, *ACS Appl. Mater. Interfaces* **2017**, *9*, 44270.
[143] M. Zhu, Y. Wang, M. Lou, J. Yu, Z. Li, B. Ding, *Nano Energy* **2021**, *81*, 105669.
[144] J. Li, G. Wang, Q. Meng, C. Ding, H. Jiang, Y. Fang, *Appl. Surf. Sci.* **2014**, *315*, 407.
[145] T. Ghoshal, M. C. Cruz-Romero, J. P. Kerry, M. A. Morris, *ACS Appl. Nano Mater.* **2019**, *2*, 6325.
[146] G. Reid, J. C. Mccormack, O. Habimana, F. Bayer, C. Goromonzi, E. Casey, A. Cowley, S. M. Kelleher, *Materials* **2021**, *14*, 1910.
[147] Y. Yang, M.-F. Yuen, X. Chen, S. Xu, Y. Tang, W. Zhang, *CrystEngComm* **2015**, *17*, 2791.
[148] K. Du, I. Wathuthanthri, Y. Liu, Y. T. Kang, C.-H. Choi, *Nanotechnology* **2014**, *25*, 165301.
[149] J.-H. Kim, C. Mun, J. Ma, S.-G. Park, S. Lee, C. S. Kim, *Nanomaterials* **2020**, *10*, 949.
[150] H. Shahali, J. Hasan, H. H. Cheng, S. Ramarishna, P. K. D. V. Yarlagadda, *Nanotechnology* **2020**, *32*, 065301.
[151] C. Cong, W. Junus, Z. Shen, T. Yu, *Nanoscale Res. Lett.* **2009**, *4*, 1324.
[152] Y. Wu, C. Zhang, Y. Yuan, Z. Wang, W. Shao, H. Wang, X. Xu, *Langmuir* **2013**, *29*, 14017.
[153] A. Chandramohan, N. V. Sibirev, V. G. Dubrovskii, M. C. Petty, A. J. Gallant, D. A. Zeze, *Sci. Rep.* **2017**, *7*, 40888.
[154] X. Zhang, L. Wang, E. Levãnen, *RSC Adv.* **2013**, *3*, 12003.
[155] M. N. Dickson, E. I. Liang, L. A. Rodriguez, N. Vollereaux, A. F. Yee, *Biointerphases* **2015**, *10*, 021010.
[156] J. Hasan, S. Raj, L. Yadav, K. Chatterjee, *RSC Adv.* **2015**, *5*, 44953.
[157] D. S. T. Chong, L.-A. Turner, N. Gadegaard, A. M. Seifalian, M. J. Dalby, G. Hamilton, *Eur J Vasc Endovasc Surg* **2015**, *49*, 335.
[158] S. Park, D. Kim, S. Park, S. Kim, D. Lee, W. Kim, J. Kim, in *Cutting-Edge Enabling Technologies for Regenerative Medicine* (Eds: H. J. Chun, C. H. Park, I. K. Kwon, G. Khang), Springer Singapore, Singapore **2018**, pp. 421–443.
[159] J. Carthew, H. H. Abdelmaksoud, M. Hodgsonâ-Garms, S. Aslanoglou, S. Ghavamian, R. Elnathan, J. P. Spatz, J. Brugger, H. Thissen, N. H. Voelcker, V. J. Cadarso, J. E. Frith, *Adv. Sci.* **2021**, *8*, 2003186.
[160] T.-H. Jung, E.-B. Chung, H. W. Kim, S. W. Choi, S.-J. Park, A. S. Mukhtar, H.-M. Chung, E. Kim, K. M. Huh, D. S. Kim, S.-W. Kang, S.-H. Moon, *PLoS One* **2020**, *15*, e0232899.
[161] S. Altuntas, H. K. Dhaliwal, N. J. Bassous, A. E. Radwan, P. Alpaslan, T. Webster, F. Buyukserin, M. Amiji, *ACS Biomater. Sci. Eng.* **2019**, *5*, 4311.
[162] L. Hanson, Z. C. Lin, C. Xie, Y. Cui, B. Cui, *Nano Lett.* **2012**, *12*, 5815.
[163] M. Gürsoy, H. Testici, E. Çıtak, M. Kaya, H. T. Dağı, B. Öztürk, M. Karaman, *Mater. Technol.* **2021**, *37*, 745.
[164] M. I. Kayes, A. J. Galante, N. A. Stella, S. Haghanifar, R. M. Q. Shanks, P. W. Leu, *React. Funct. Polym.* **2018**, *128*, 40.
[165] D. P. Linklater, S. Saita, T. Murata, T. Yanagishita, C. Dekiwadia, R. J. Crawford, H. Masuda, H. Kusaka, E. P. Ivanova, *ACS Appl. Nano Mater.* **2022**, *5*, 2578.
[166] A. Elbourne, R. J. Crawford, E. P. Ivanova, *J. Colloid Interface Sci.* **2017**, *508*, 603.
[167] A. Das, S. Ambastha, N. Priyadarshni, S. Samanta, Nagahanumaiah, *Proc. Inst. Mech. Eng., Part B* **2021**, *236*, 1093.
[168] D. Bains, G. Singh, J. Bhinder, P. K. Agnihotri, N. Singh, *ACS Appl. Bio Mater.* **2020**, *3*, 2092.
[169] L. Rong, H. Liu, B. Wang, Z. Mao, H. Xu, L. Zhang, Y. Zhong, X. Feng, X. Sui, *Carbohydr. Polym.* **2019**, *211*, 173.
[170] E. P. Ivanova, J. Hasan, H. K. Webb, G. Gervinskas, S. Juodkazis, V. K. Truong, A. H. F. Wu, R. N. Lamb, V. A. Baulin, G. S. Watson, J. A. Watson, D. E. Mainwaring, R. J. Crawford, *Nat. Commun.* **2013**, *4*, 2838.
[171] E. Stratakis, J. Bonse, J. Heitz, J. Siegel, G. D. Tsibidis, E. Skoulas, A. Papadopoulos, A. Mimidis, A.-C. Joel, P. Comanns, J. Kruger, C. Florian, Y. Fuentes-Edfuf, J. Solis, W. Baumgartner, *Mater. Sci. Eng., R* **2020**, *141*, 100562.
[172] L. Hu, L. Zhang, D. Wang, X. Lin, Y. Chen, *Colloids Surf., A* **2018**, *555*, 515.
[173] S. Li, Y. Liu, Z. Zheng, X. Liu, H. Huang, Z. Han, L. Ren, *Chem. Eng. J.* **2019**, *372*, 852.
[174] Q. Pan, Y. Cao, W. Xue, D. Zhu, W. Liu, *Langmuir* **2019**, *35*, 11414.
[175] X. Wu, H. Ao, Z. He, Q. Wang, Z. Peng, *Coatings* **2022**, *12*, 414.
[176] K. Doll, E. Fadeeva, J. Schaeske, T. Ehmke, A. Winkel, A. Heisterkamp, B. N. Chichkov, M. Stiesch, N. S. Stumpp, *ACS Appl. Mater. Interfaces* **2017**, *9*, 9359.
[177] B. Valdez-Salas, E. Beltrán-Partida, N. Nedev, R. Ibarra-Wiley, R. Salinas, M. Curiel-Álvarez, Y. Valenzuela-Ontiveros, G. Pérez, *Mater. Sci. Eng., C* **2019**, *96*, 677.
[178] D. T. Elliott, R. J. Wiggins, R. Dua, *J. Biomed. Mater. Res., Part B* **2021**, *109*, 973.
[179] M. Lorenzetti, I. Dogša, T. Stošicki, D. Stopar, M. Kalin, S. Kobe, S. Novak, *ACS Appl. Mater. Interfaces* **2015**, *7*, 1644.
[180] J. Li, X. Liu, Y. Qiao, H. Zhu, J. Li, T. Cui, C. Ding, *RSC Adv.* **2013**, *3*, 11214.
[181] A. Hayles, J. Hasan, R. Bright, D. Palms, T. Brown, D. Barker, K. Vasilev, *Mater Today Chem* **2021**, *22*, 100622.
[182] J. Moritz, A. Abram, M. Čekada, U. Gabor, M. Garvas, I. Zdovc, A. Dakskobler, J. Cotič, K. Ivičak-Kocjan, A. Kocjan, *J. Eur. Ceram. Soc.* **2019**, *39*, 4347.

[183] X. Ge, J. Zhao, K. D. Esmeryan, X. Lu, Z. Li, K. Wang, F. Ren, Q. Wang, M. Wang, B. Qian, *Mater. Des.* **2020**, *193*, 108790.
[184] I. Izquierdo-Barba, J. M. García-Martín, R. Álvarez, A. Palmero, J. Esteban, C. Pérez-Jorge, D. Arcos, M. Vallet-Regí, *Acta Biomater.* **2015**, *15*, 20.
[185] C. Sengstock, M. Lopian, Y. Motemani, A. Borgmann, C. Khare, P. J. S. Buenconsejo, T. A. Schildhauer, A. Ludwig, M. Köller, *Nanotechnology* **2014**, *25*, 195101.
[186] P. Mandal, J. Ivvala, H. S. Arora, S. K. Ghosh, H. S. Grewal, *Colloids Surf., B* **2022**, *211*, 112311.
[187] G.-H. Wang, H. Fu, Y.-Z. Zhao, K.-C. Zhou, S.-H. Zhu, S. H. Zhu, *Trans. Nonferrous Met. Soc. China* **2017**, *27*, 2007.
[188] A. Hayles, J. Hasan, R. Bright, J. Wood, D. Palms, P. Zilm, D. Barker, K. Vasilev, *ACS Appl. Nano Mater.* **2021**, *5*, 12051.
[189] J. Singh, S. Jadhav, S. Avasthi, P. Sen, *ACS Appl. Mater. Interfaces* **2020**, *12*, 20202.
[190] J. I. Lim, S. l. Kim, Y. Jung, S. H. Kim, *Polymer* **2013**, *37*, 411.
[191] T. Wang, L. Huang, Y. Liu, X. Li, C. Liu, S. Handschuh-Wang, Y. Xu, Y. Zhao, Y. Tang, *ACS Appl. Mater. Interfaces* **2020**, *12*, 24432.
[192] Y. Lv, C. Song, Y. Hou, M. Shi, Q. Li, T. Zhang, *J. Dispersion Sci. Technol.* **2020**, *41*, 1690.
[193] Â. Luís, F. Domingues, A. Ramos, *Microorganisms* **2019**, *7*, 267.
[194] S. Zouaghi, S. Bellayer, V. Thomy, T. Dargent, Y. Coffinier, C. Andre, G. Delaplace, M. Jimenez, *Food Bioprod. Process.* **2019**, *113*, 32.
[195] S. Li, A. Chen, Y. Chen, Y. Yang, Q. Zhang, S. Luo, M. Ye, Y. Zhou, Y. An, W. Huang, T. Xuan, Y. Pan, X. Xuan, H. He, J. Wu, *Chem. Eng. J.* **2020**, *402*, 126202.
[196] W. Kim, D. Kim, S. Park, D. Lee, H. Hyun, J. Kim, *J. Ind. Eng. Chem.* **2018**, *61*, 39.
[197] N. J. Shirtcliffe, G. Mchale, M. I. Newton, G. Chabrol, C. C. Perry, *Adv. Mater.* **2004**, *16*, 1929.
[198] M. Yamamoto, N. Nishikawa, H. Mayama, Y. Nonomura, S. Yokojima, S. Nakamura, K. Uchida, *Langmuir* **2015**, *31*, 7355.
[199] H.-X. Huang, X. Wang, *Mater. Today Commun.* **2019**, *19*, 487.
[200] G. B. Hwang, K. Page, A. Patir, S. P. Nair, E. Allan, I P. Parkin, *ACS Nano* **2018**, *12*, 6050.
[201] M. Santander-Borrego, E. Taran, A. M. A. Shadforth, A. K. Whittaker, T. V. Chirila, I. Blakey, *Langmuir* **2017**, *33*, 485.
[202] K. J. Cha, K.-S. Park, S.-W. Kang, B.-H. Cha, B.-K. Lee, I.-B. Han, D. A. Shin, D. S. Kim, S.-H. Lee, *Macromol. Biosci.* **2011**, *11*, 1357.
[203] M. Klicova, Z. Oulehlova, A. Klapstova, M. J. Hejda, M. Krejcik, O. Novak, J. Mullerova, J. Erben, J. Rosendorf, R. Palek, V. Liska, A. Fucikova, J. Chvojka, I. Zvercova, J. Horakova, *Mater. Des.* **2022**, *217*, 110661.
[204] Y. Li, W. Sun, A. Zhang, S. Jin, X. Liang, Z. Tang, X. Liu, H. Chen, *J. Colloid Interface Sci.* **2021**, *603*, 501.
[205] J. I. Lim, S. Il Kim, S. H. Kim, *Colloids Surf., B* **2013**, *103*, 463.
[206] A. de Leon, R. C. Advincula, *ACS Appl. Mater. Interfaces* **2014**, *6*, 22666.
[207] R. Nowak, M. Olech, Å. U. Pecio, W. Aw Oleszek, R. Los, A. Malm, J. Rzymowska, *J. Sci. Food Agric.* **2014**, *94*, 560.
[208] W. Zhang, F. H. Abdel-Rahman, M. A. Saleh, *J. Environ. Sci. Health, Part B* **2011**, *46*, 381.
[209] L. Feng, Y. Zhang, J. Xi, Y. Zhu, N. Wang, F. Xia, L. Jiang, *Langmuir* **2008**, *24*, 4114.
[210] A. Mukhopadhyay, A. Das, S. Mukherjee, M. Rajput, A. Gope, A. Chaudhary, K. Choudhury, A. Barui, J. Chatterjee, R. Mukherjee, *ACS Appl. Bio Mater.* **2021**, *4*, 4328.
[211] D. I. Yu, S. W. Doh, H. J. Kwak, H. C. Kang, H. S. Ahn, H. S. Park, M. Kiyofumi, M. H. Kim, *Appl. Phys. Lett.* **2015**, *106*, 171602.
[212] G. S. Watson, D. W. Green, L. Schwarzkopf, X. Li, B. W. Cribb, S. Myhra, J. A. Watson, *Acta Biomater.* **2015**, *21*, 109.
[213] S. Pogodin, J. Hasan, V. A. Baulin, H. K. Webb, V. K. Truong, T. H. P. Nguyen, V. Boshkovikj, C. J. Fluke, G. S. Watson, J. A. Watson, R. J. Crawford, E. P. Ivanova, *Biophys. J.* **2013**, *104*, 835.
[214] A. Velic, J. Hasan, Z. Li, P. K. D. V. Yarlagadda, *Biophys. J.* **2021**, *120*, 217.
[215] S. Sun, H. Li, Y. Guo, H.-Y. Mi, P. He, G. Zheng, C. Liu, C. Shen, *Prog. Org. Coat.* **2021**, *151*, 106090.
[216] R. D. Mukhopadhyay, B. Vedhanarayanan, A. Ajayaghosh, *Angew. Chem.* **2017**, *129*, 16234.
[217] Y. Shao, J. Zhao, Y. Fan, Z. Wan, L. Lu, Z. Zhang, W. Ming, L. Ren, *Chem. Eng. J.* **2020**, *382*, 122989.
[218] F. Gao, Y. Yao, W. Wang, X. Wang, L. Li, Q. Zhuang, S. Lin, *Macromolecules* **2018**, *51*, 2742.
[219] X. Luo, L. Lu, M. Yin, X. Fang, X. Chen, D. Li, L. Yang, G. Li, J. Ma, *Mater. Res. Bull.* **2019**, *109*, 183.
[220] I. Navarro-Baena, A. Jacobo-Martã, J. J. Hernãndez, J. R. C. Smirnov, F. Viela, M. A. Monclus, M. R. Osorio, J. M. Molina-Aldareguia, I. Rodriguez, *Nanoscale* **2018**, *10*, 15496.
[221] G. D. Bixler, B. Bhushan, *Adv. Funct. Mater.* **2013**, *23*, 4507.
[222] Y. L. Peng, C. G. Lin, L. Wang, *Adv. Mater. Res.*, Trans Tech Publications Ltd., **2009**, *79–82*, pp. 977–980.
[223] H. M. Wong, Y. Y. Zhang, Q. L. Li, *Bioact. Mater.* **2022**, *7*, 491.
[224] A. Oyane, I. Sakamaki, K. Koga, M. Nakamura, K. Shitomi, H. Miyaji, *Mater. Sci. Eng., C* **2020**, *116*, 111170.
[225] A. J. Nathanael, A. Oyane, M. Nakamura, M. Mahanti, K. Koga, K. Shitomi, H. Miyaji, *Acta Biomater.* **2018**, *79*, 148.
[226] L. Zhang, Q.-L. Li, H. M. Wong, *Composites, Part B* **2022**, *233*, 109651.
[227] Z. Jia, X. Lv, Y. Hou, K. Wang, F. Ren, D. Xu, Q. Wang, K. Fan, C. Xie, X. Lu, *Bioact. Mater.* **2021**, *6*, 2676.
[228] A. Valiei, M. Okshevsky, N. Lin, N. Tufenkji, *ACS Appl. Mater. Interfaces* **2018**, *10*, 41207.
[229] G. Feng, Y. Cheng, S.-Y. Wang, D. A. Borca-Tasciuc, R. W. Worobo, C. I. Moraru, *npj Biofilms Microbiomes* **2015**, *1*, 15022.
[230] H. H. Tuson, D. B. Weibel, *Soft Matter* **2013**, *9*, 4368.
[231] T.-F. Mah, *Future Microbiol.* **2012**, *7*, 1061.
[232] T.-F. C. Mah, G. A. O'toole, *Trends Microbiol.* **2001**, *9*, 34.
[233] D. Davies, *Nat Rev Drug Discov* **2003**, *2*, 114.
[234] J. E. Patrick, D. B. Kearns, *Mol. Microbiol.* **2012**, *83*, 14.
[235] T. E. P. Kimkes, M. Heinemann, *FEMS Microbiol. Rev.* **2019**, *44*, 106.
[236] B.-J. Laventie, U. Jenal, *Annu. Rev. Microbiol.* **2020**, *74*, 735.
[237] L. D. Renner, D. B. Weibel, *MRS Bull.* **2011**, *36*, 347.
[238] N. P. Boks, H. J. Kaper, W. Norde, H. J. Busscher, H. C. Van Der Mei, *Colloids Surf., B* **2008**, *67*, 276.
[239] K. C. Marshall, R. Stout, R. Mitchell, *J. Gen. Microbiol.* **1971**, *68*, 337.
[240] J. W. Mcclaine, R. M. Ford, *Appl. Environ. Microbiol.* **2002**, *68*, 1280.
[241] M. A.-S. Vigeant, R. M. Ford, M. Wagner, L. K. Tamm, *Appl. Environ. Microbiol.* **2002**, *68*, 2794.
[242] G. S. Watson, D. W. Green, B. W. Cribb, C. L. Brown, C. R. Meritt, M. J. Tobin, J. Vongsvivut, M. Sun, A.-P. Liang, J. A. Watson, *ACS Appl. Mater. Interfaces* **2017**, *9*, 24381.
[243] K. Modaresifar, S. Azizian, M. Ganjian, L. E. Fratila-Apachitei, A. A. Zadpoor, *Acta Biomater.* **2019**, *83*, 29.
[244] G. S. Watson, D. W. Green, J. A. Watson, Z. Zhou, X. Li, G. S. P. Cheung, M. Gellender, *Adv. Mater. Interfaces* **2019**, *6*, 1801646.
[245] M. Ganjian, K. Modaresifar, M. R. O. Ligeon, L. B. Kunkels, N. Tumer, L. Angeloni, C. W. Hagen, L. G. Otten, P. L. Hagedoorn, I. Apachitei, L. E. Fratilaâ-Apachitei, A. A. Zadpoor, *Adv. Mater. Interfaces* **2019**, *6*, 1900640.
[246] Y. Ammar, D. Swailes, B. Bridgens, J. Chen, *Surf. Coat. Technol.* **2015**, *284*, 410.
[247] X. Li, *Phys. Chem. Chem. Phys.* **2015**, *18*, 1311.
[248] A. Velic, A. Jaggessar, T. Tesfamichael, Z. Li, P. K. D. V. Yarlagadda, *Nanomaterials* **2021**, *11*, 2472.

[249] F. Xue, J. Liu, L. Guo, L. Zhang, Q. Li, *J. Theor. Biol.* **2015**, *385*, 1.
[250] W. Choi, C. Lee, C. H. Yoo, M. G. Shin, G. W. Lee, T.-S. Kim, H. W. Jung, J. S. Lee, J.-H. Lee, *J. Memb. Sci.* **2020**, *595*, 117602.
[251] E. P. Ivanova, D. P. Linklater, M. Werner, V. A. Baulin, X. Xu, N. Vrancken, S. Rubanov, E. Hanssen, J. Wandiyanto, V. K. Truong, A. Elbourne, S. Maclaughlin, S. Juodkazis, R. J. Crawford, *Proc. Natl. Acad. Sci. USA* **2020**, *117*, 12598.
[252] M. Miyazaki, A. Miyauchi, *Effect on Suppression of Biofilm Growth Using Microstructures Inspired by Living Organism*, **n.d.**
[253] N. Encinas, C.-Y. Yang, F. Geyer, A. Kaltbeitzel, P. Baumli, J. Reinholz, V. Mailänder, H.-J. Butt, D. Vollmer, *ACS Appl. Mater. Interfaces* **2020**, *12*, 21192.
[254] K. Modaresifar, L. B. Kunkels, M. Ganjian, N. Tümer, C. W. Hagen, L. G. Otten, P.-L. Hagedoorn, L. Angeloni, M. K. Ghatkesar, L. E. Fratila-Apachitei, A. A. Zadpoor, *Nanomaterials* **2020**, *10*, 347.
[255] A. Velic, T. Tesfamichael, Z. Li, P. K. D. V. Yarlagadda, *Procedia Manuf* **2019**, *30*, 514.
[256] S. M. Kelleher, O. Habimana, J. Lawler, B. O'reilly, S. Daniels, E. Casey, A. Cowley, *ACS Appl. Mater. Interfaces* **2016**, *8*, 14966.
[257] M. Michalska, F. Gambacorta, R. Divan, I. S. Aranson, A. Sokolov, P. Noirot, P. D. Laible, *Nanoscale* **2018**, *10*, 6639.
[258] A. Valiei, N. Lin, G. McKay, D. Nguyen, C. Moraes, R. J. Hill, N. Tufenkji, *ACS Appl. Mater. Interfaces* **2022**, *14*, 27564.
[259] A. Valiei, N. Lin, J.-F. Bryche, G. Mckay, M. Canva, P. G. Charette, D. Nguyen, C. Moraes, N. Tufenkji, *Nano Lett.* **2020**, *20*, 5720.
[260] V. T. H. Pham, V. K. Truong, M. D. J. Quinn, S. M. Notley, Y. Guo, V. A. Baulin, M. Al Kobaisi, R. J. Crawford, E. P. Ivanova, *ACS Nano* **2015**, *9*, 8458.
[261] A. M. Andreotti, C. A. de Sousa, M. C. Goiato, E. V. F. da Silva, C. Duque, A. Moreno, D. M. dos Santos, *Eur. J. Dent.* **2018**, *12*, 176.
[262] Y. Yuan, Y. Zhang, *Nanomedicine* **2017**, *13*, 2199.
[263] X. Lu, X. Feng, J. R. Werber, C. Chu, I. Zucker, J. H. Kim, C. O. Osuji, M. Elimelech, *Proc. Natl. Acad. Sci. USA* **2017**, *114*, E9793.
[264] Y. Du, J. L. Guo, J. Wang, A. G. Mikos, S. Zhang, *Biomaterials* **2019**, *218*, 119334.
[265] J. Lewandowski, in *Physical Control Methods in Plant Protection* (Eds: C. Vincent, B. Panneton, F. Fleurat-Lessard), Springer Berlin Heidelberg, Berlin, Heidelberg **2001**, pp. 111–124.
[266] C. Li, F. Lin, W. Sun, F.-G. Wu, H. Yang, R. Lv, Y.-X. Zhu, H.-R. Jia, C. Wang, G. Gao, Z. Chen, *ACS Appl. Mater. Interfaces* **2018**, *10*, 16715.
[267] F. L. Davis, O. B. Williams, *J. Bacteriol.* **1948**, *56*, 555.
[268] R. Pagan, P. Manas, J. Raso, S. Condon, *Appl. Environ. Microbiol.* **1999**, *65*, 297.
[269] H. Van Acker, T. Coenye, *Trends Microbiol.* **2017**, *25*, 456.
[270] M. Song, Y. Cheng, Y. Tian, C. Chu, C. Zhang, Z. Lu, X. Chen, X. Pang, G. Liu, *Adv. Funct. Mater.* **2020**, *30*, 2003587.
[271] A T. Dharmaraja, *J. Med. Chem.* **2017**, *60*, 3221.
[272] G. T. Nguyen, E. R. Green, J. Mecsas, *Front. Cell. Infect. Microbiol.* **2017**, *7*, 373.
[273] A. P. West, G. S. Shadel, S. Ghosh, *Nat. Rev. Immunol.* **2011**, *11*, 389.
[274] K. Zarse, M. Ristow, *Nat Metab* **2021**, *3*, 588.
[275] B. Pinegin, N. Vorobjeva, M. Pashenkov, B. Chernyak, *J. Cell. Physiol.* **2018**, *233*, 3745.
[276] X. Li, J. F. Lovell, J. Yoon, X. Chen, *Nat. Rev. Clin. Oncol.* **2020**, *17*, 657.
[277] Q. Jia, Q. Song, P. Li, W. Huang, *Adv. Healthcare Mater.* **2019**, *8*, 1900608.
[278] X. Hu, H. Zhang, Y. Wang, B. C. Shiu, J. H. Lin, S. Zhang, C. W. Lou, T. T. Li, *Chem. Eng. J.* **2022**, *450*, 138129.
[279] M. Qi, M. Chi, X. Sun, X. Xie, M. D. Weir, T. W. Oates, Y. Zhou, L. Wang, Y. Bai, H. H. K. Xu, *Int. J. Nanomed.* **2019**, *14*, 6937.
[280] X. Sun, J. Sun, Y. Sun, C. Li, J. Fang, T. Zhang, Y. Wan, L. Xu, Y. Zhou, L. Wang, B. Dong, *Adv. Funct. Mater.* **2021**, *31*, 2101040.
[281] Z. M. Marković, M. Kováčová, P. Humpolíček, M. D. Budimir, J. Vajďák, P. Kubát, M. Mičušík, H. Švajdlenková, M. Danko, Z. Capáková, M. Lehocký, B. M. T. Marković, Z. Špitalský, *Photodiagn. Photodyn. Ther.* **2019**, *26*, 342.
[282] K. Grzech-Leśniak, B. Gaspirc, A. Sculean, *Photodiagn. Photodyn. Ther.* **2019**, *27*, 44.
[283] G. Hong, A. L. Antaris, H. Dai, *Nat. Biomed. Eng.* **2017**, *1*, 0010.
[284] N. Maldonado-Carmona, T.-S. Ouk, M. J. F. Calvete, M. M. Pereira, N. Villandier, S. Leroy-Lhez, *Photochem. Photobiol. Sci.* **2020**, *19*, 445.
[285] J. Sun, Y. Fan, P. Zhang, X. Zhang, Q. Zhou, J. Zhao, L. Ren, *J. Colloid Interface Sci.* **2020**, *559*, 197.
[286] S. Liu, G. Feng, B. Z. Tang, B. Liu, *Chem. Sci.* **2021**, *12*, 6488.
[287] Y.-Y. Xie, Y.-W. Zhang, X.-Z. Liu, X.-F. Ma, X.-T. Qin, S.-R. Jia, C. Zhong, *Chem. Eng. J.* **2021**, *413*, 127542.
[288] H. M. Yadav, J.-S. Kim, S. H. Pawar, *Korean J. Chem. Eng.* **2016**, *33*, 1989.
[289] K. Qi, B. Cheng, J. Yu, W. Ho, *J. Alloys Compd.* **2017**, *727*, 792.
[290] Z. Liu, X. Yu, L. Li, *Chin. J. Catal.* **2020**, *41*, 534.
[291] Y. Liu, R. Qin, S. A. J. Zaat, E. Breukink, M. Heger, *J. Clin. Transl. Res.* **2015**, *1*, 140.
[292] X. Cai, J. Tian, J. Zhu, J. Chen, L. Li, C. Yang, J. Chen, D. Chen, *Chem. Eng. J.* **2021**, *426*, 131919.
[293] W. Wang, M.-S. Song, X.-N. Yang, J. Zhao, I. S. Cole, X.-B. Chen, Y. Fan, *ACS Appl. Mater. Interfaces* **2020**, *12*, 46862.
[294] C. J. Murphy, H.-H. Chang, P. Falagan-Lotsch, M. T. Gole, D. M. Hofmann, K. N. L. Hoang, S. M. Mcclain, S. M. Meyer, J. G. Turner, M. Unnikrishnan, M. Wu, X. Zhang, Y. Zhang, *Acc. Chem. Res.* **2019**, *52*, 2124.
[295] F. Nawaz, Y. Yang, S. Zhao, M. Sheng, C. Pan, W. Que, *J. Mater. Chem. A* **2021**, *9*, 16233.
[296] K. Bhattacharya, F. T. Andon, R. El-Sayed, B. Fadeel, *Adv. Drug Delivery Rev.* **2013**, *65*, 2087.
[297] H. Zhou, K. Zhao, W. Li, N. Yang, Y. Liu, C. Chen, T. Wei, *Biomaterials* **2012**, *33*, 6933.
[298] X. Hu, M. Zhou, Q. Zhou, *Environ. Sci. Technol.* **2015**, *49*, 3410.
[299] K.-H. Liao, Y.-S. Lin, C. W. Macosko, C. L. Haynes, *ACS Appl. Mater. Interfaces* **2011**, *3*, 2607.
[300] Y. Qiu, Y. Dong, S. Zhao, J. Zhang, P. Huang, W. Wang, A. Dong, L. Deng, *J. Appl. Polym. Sci.* **2021**, *138*, 50572.
[301] F. Yang, Y. Feng, X. Fan, M. Zhang, C. Wang, W. Zhao, C. Zhao, *Colloids Surf., B* **2019**, *173*, 266.
[302] P. Wei, L. Wang, F. Xie, J. Cai, *Chem. Eng. J.* **2022**, *431*, 133964.
[303] J. Wang, Y. Li, L. Deng, N. Wei, Y. Weng, S. Dong, D. Qi, J. Qiu, X. Chen, T. Wu, *Adv. Mater.* **2017**, *29*, 1603730.
[304] S. Wu, Z. Weng, X. Liu, K. W. K. Yeung, P. K. Chu, *Adv. Funct. Mater.* **2014**, *24*, 5464.
[305] Z. Yuan, B. Tao, Y. He, J. Liu, C. Lin, X. Shen, Y. Ding, Y. Yu, C. Mu, P. Liu, K. Cai, *Biomaterials* **2019**, *217*, 119290.
[306] M. Li, L. Li, K. Su, X. Liu, T. Zhang, Y. Liang, D. Jing, X. Yang, D. Zheng, Z. Cui, Z. Li, S. Zhu, K. W. K. Yeung, Y. Zheng, X. Wang, S. Wu, *Adv. Sci.* **2019**, *6*, 1900599.
[307] H. Chen, X. He, Z. Zhou, Z. Wu, H. Li, X. Peng, Y. Zhou, C. Tan, J. Shen, *J. Nanobiotechnol.* **2022**, *20*, 136.
[308] R. Chen, L. Wei, Y. Yan, G. Chen, X. Yang, Y. Liu, M. Zhang, X. Liu, Y. Cheng, J. Sun, L. Wang, *Biomater. Sci.* **2022**, *10*, 467.
[309] T. Zhang, Y. Wan, H. Xie, Y. Mu, P. Du, D. Wang, X. Wu, H. Ji, L. Wan, *J. Am. Chem. Soc.* **2018**, *140*, 7561.
[310] B. Yang, J. Yin, Y. Chen, S. Pan, H. Yao, Y. Gao, J. Shi, *Adv. Mater.* **2018**, *30*, 1705611.
[311] J. Shao, H. Xie, H. Huang, Z. Li, Z. Sun, Y. Xu, Q. Xiao, X.-F. Yu, Y. Zhao, H. Zhang, H. Wang, P. K. Chu, *Nat. Commun.* **2016**, *7*, 12967.
[312] Y.-L. Hsieh, W.-H. Su, C.-C. Huang, C.-Y. Su, *ACS Appl. Mater. Interfaces* **2020**, *12*, 37375.
[313] L. Wu, J. Wang, J. Lu, D. Liu, N. Yang, H. Huang, P. K. Chu, X.-F. Yu, *Small* **2018**, *14*, 1801405.
[314] Z. Li, L. Wu, H. Wang, W. Zhou, H. Liu, H. Cui, P. Li, P. K. Chu, X.-F. Yu, *ACS Appl. Nano Mater.* **2019**, *2*, 1202.

[315] Y. Zhao, H. Wang, H. Huang, Q. Xiao, Y. Xu, Z. Guo, H. Xie, J. Shao, Z. Sun, W. Han, X.-F. Yu, P. Li, P. K. Chu, *Angew. Chem.* **2016**, *128*, 5087.
[316] L. Tong, Q. Liao, Y. Zhao, H. Huang, A. Gao, W. Zhang, X. Gao, W. Wei, M. Guan, P. K. Chu, H. Wang, *Biomaterials* **2019**, *193*, 1.
[317] S. Eustis, M. A. El-Sayed, *Chem. Soc. Rev.* **2006**, *35*, 209.
[318] L. Jauffred, A. Samadi, H. Klingberg, P. M. Bendix, L. B. Oddershede, *Chem. Rev.* **2019**, *119*, 8087.
[319] Y. Zou, Y. Zhang, Q. Yu, H. Chen, *Biomater. Sci.* **2021**, *9*, 10.
[320] R. S. Norman, J. W. Stone, A. Gole, C. J. Murphy, T. L. Sabo-Attwood, *Nano Lett.* **2008**, *8*, 302.
[321] J. Chen, J. Feng, Z. Li, P. Xu, X. Wang, W. Yin, M. Wang, X. Ge, Y. Yin, *Nano Lett.* **2018**, *19*, 400.
[322] A. Wang, Q. Zhu, Z. Xing, *Chem. Eng. J.* **2020**, *393*, 124781.
[323] N. Li, D. Yin, L. Xu, H. Zhao, Z. Liu, Y. Du, *Mater. Chem. Front.* **2019**, *3*, 394.
[324] C. Fasciani, M. J. Silvero, M. A. Anghel, G. A. Arguello, M. C. Becerra, J. C. Scaiano, *J. Am. Chem. Soc.* **2014**, *136*, 17394.
[325] D. Hu, H. Li, B. Wang, Z. Ye, W. Lei, F. Jia, Q. Jin, K.-F. Ren, J. Ji, *ACS Nano* **2017**, *11*, 9330.
[326] Y. Peng, Y. Liu, X. Lu, S. Wang, M. Chen, W. Huang, Z. Wu, G. Lu, L. Nie, *J. Mater. Chem. B* **2018**, *6*, 2813.
[327] G. Guan, K. Y. Win, X. Yao, W. Yang, M. Y. Han, *Adv. Healthcare Mater.* **2021**, *10*, 2001158.
[328] P. Pallavicini, A. Donã, A. Taglietti, P. Minzioni, M. Patrini, G. Dacarro, G. Chirico, L. Sironi, N. Bloise, L. Visai, L. Scarabelli, *Chem. Commun.* **2014**, *50*, 1969.
[329] P. Pallavicini, B. Bassi, G. Chirico, M. Collini, G. Dacarro, E. Fratini, P. Grisoli, M. Patrini, L. Sironi, A. Taglietti, M. Moritz, I. Sorzabal-Bellido, A. Susarrey-Arce, E. Latter, A. J. Beckett, I. A. Prior, R. Raval, Y. A. D. Fernandez, *Sci. Rep.* **2017**, *7*, 5259.
[330] O. Khantamat, C.-H. Li, F. Yu, A. C. Jamison, W.-C. Shih, C. Cai, T. R. Lee, *ACS Appl. Mater. Interfaces* **2015**, *7*, 3981.
[331] T. Yang, D. Wang, X. Liu, *Colloids Surf., B* **2019**, *173*, 833.
[332] S. Cabana, C. S. Lecona-Vargas, H. I. Meléndez-Ortiz, A. Contreras-García, S. Barbosa, P. Taboada, B. Magariños, E. Bucio, A. Concheiro, C. Alvarez-Lorenzo, *J. Drug Delivery Sci. Technol.* **2017**, *42*, 245.
[333] Y. Qu, T. Wei, J. Zhao, S. Jiang, P. Yang, Q. Yu, H. Chen, *J. Mater. Chem. B* **2018**, *6*, 3946.
[334] B. Anasori, M. R. Lukatskaya, Y. Gogotsi, *Nat. Rev. Mater.* **2017**, *2*, 16098.
[335] Y. Gogotsi, B. Anasori, *ACS Nano* **2019**, *13*, 8491.
[336] F. Shahzad, M. Alhabeb, C. B. Hatter, B. Anasori, S. Man Hong, C. M. Koo, Y. Gogotsi, *Science* **2016**, *353*, 1137.
[337] X. Fan, L. Liu, X. Jin, W. Wang, S. Zhang, B. Tang, *J. Mater. Chem. A* **2019**, *7*, 14319.
[338] K. Chaudhuri, M. Alhabeb, Z. Wang, V. M. Shalaev, Y. Gogotsi, A. Boltasseva, *ACS Photonics* **2018**, *5*, 1115.
[339] D. Xu, Z. Li, L. Li, J. Wang, *Adv. Funct. Mater.* **2020**, *30*, 2000712.
[340] L. Cheng, X. Wang, F. Gong, T. Liu, Z. Liu, *Adv. Mater.* **2020**, *32*, 1902333.
[341] J. Yin, Q. Han, J. Zhang, Y. Liu, X. Gan, K. Xie, L. Xie, Y. Deng, *ACS Appl. Mater. Interfaces* **2020**, *12*, 45891.
[342] Z. Yu, L. Jiang, R. Liu, W. Zhao, Z. Yang, J. Zhang, S. Jin, *Chem. Eng. J.* **2021**, *426*, 131914.
[343] Q. Li, W. Wang, H. Feng, L. Cao, H. Wang, D. Wang, S. Chen, *J. Colloid Interface Sci.* **2021**, *604*, 810.
[344] Q. Wu, L. Tan, X. Liu, Z. Li, Y. Zhang, Y. Zheng, Y. Liang, Z. Cui, S. Zhu, S. Wu, *Appl. Catal. B* **2021**, *297*, 120500.
[345] J. Li, Z. Li, X. Liu, C. Li, Y. Zheng, K. W. K. Yeung, Z. Cui, Y. Liang, S. Zhu, W. Hu, Y. Qi, T. Zhang, X. Wang, S. Wu, *Nat. Commun.* **2021**, *12*, 1224.
[346] H. Zheng, S. Wang, F. Cheng, X. He, Z. Liu, W. Wang, L. Zhou, Q. Zhang, *Chem. Eng. J.* **2021**, *424*, 130148.
[347] M. Gong, L. Yue, J. Kong, X. Lin, L. Zhang, J. Wang, D. Wang, *ACS Appl. Mater. Interfaces* **2021**, *13*, 9053.
[348] J. Li, L. Ma, Z. Li, X. Liu, Y. Zheng, Y. Liang, C. Liang, Z. Cui, S. Zhu, S. Wu, *Small* **2022**, *18*, 2104448.
[349] Y. Li, M. Han, Y. Cai, B. Jiang, Y. Zhang, B. Yuan, F. Zhou, C. Cao, *Biomater. Sci.* **2022**, *10*, 1068.
[350] Y. Zheng, Y. Yan, L. Lin, Q. He, H. Hu, R. Luo, D. Xian, J. Wu, Y. Shi, F. Zeng, C. Wu, G. Quan, C. Lu, *Acta Biomater.* **2022**, *142*, 113.
[351] R. Nie, Y. Sun, H. Lv, M. Lu, H. Huangfu, Y. Li, Y. Zhang, D. Wang, L. Wang, Y. Zhou, *Nanoscale* **2022**.
[352] A. Szuplewska, D. Kulpinska, M. Jakubczak, A. Dybko, M. Chudy, A. Olszyna, Z. Brzozka, A. M. Jastrzebska, *Adv. Drug Delivery Rev.* **2022**, *182*, 114099.
[353] D. Zhang, W. Zheng, X. Li, A. Li, N. Ye, L. Zhang, Y. Liu, X. Liu, R. Zhang, M. Wang, J. Cheng, H. Yang, M. Gong, *Carbon* **2021**, *178*, 810.
[354] W. Lei, K. Ren, T. Chen, X. Chen, B. Li, H. Chang, J. Ji, *Adv. Mater. Interfaces* **2016**, *3*, 1600767.
[355] L. Tan, J. Li, X. Liu, Z. Cui, X. Yang, S. Zhu, Z. Li, X. Yuan, Y. Zheng, K. W. K. Yeung, H. Pan, X. Wang, S. Wu, *Adv. Mater.* **2018**, *30*, 1801808.
[356] X. Ai, J. Mu, B. Xing, *Theranostics* **2016**, *6*, 2439.
[357] Z. Ansi, *Laser Institute of America, Orlando* **2000**.
[358] H. Yuan, A. M. Fales, T. Vo-Dinh, *J. Am. Chem. Soc.* **2012**, *134*, 11358.
[359] Y. Ran, Z. Xu, M. Chen, W. Wang, Y. Wu, J. Cai, J. Long, Z. S. Chen, D. Zhang, B. O. Guan, *Adv. Sci.* **2022**, *9*, 2200456.
[360] M. Postema, O. Gilja, *Curr. Pharm. Biotechnol.* **2007**, *8*, 355.
[361] E. S. Ebbini, G. Ter Haar, *Int. J. Hyperthermia* **2015**, *31*, 77.
[362] S. R. Sirsi, M. A. Borden, *Adv. Drug Delivery Rev.* **2014**, *72*, 3.
[363] X. Wang, F. Yan, X. Liu, P. Wang, S. Shao, Y. Sun, Z. Sheng, Q. Liu, J. F. Lovell, H. Zheng, *J. Controlled Release* **2018**, *286*, 358.
[364] A. L. Klibanov, T. I. Shevchenko, B. I. Raju, R. Seip, C. T. Chin, *J. Controlled Release* **2010**, *148*, 13.
[365] W. Sun, H. Jiang, X. Wu, Z. Xu, C. Yao, J. Wang, M. Qin, Q. Jiang, W. Wang, D. Shi, Y. Cao, *Nano Res.* **2019**, *12*, 115.
[366] L. J. Delaney, D. Macdonald, J. Leung, K. Fitzgerald, A. M. Sevit, J. R. Eisenbrey, N. Patel, F. Forsberg, C. K. Kepler, T. Fang, S. M. Kurtz, N. J. Hickok, *Acta Biomater.* **2019**, *93*, 12.
[367] X. Pang, Q. Xiao, Y. Cheng, E. Ren, L. Lian, Y. Zhang, H. Gao, X. Wang, W. Leung, X. Chen, G. Liu, C. Xu, *ACS Nano* **2019**, *13*, 2427.
[368] X. Pang, X. Liu, Y. Cheng, C. Zhang, E. Ren, C. Liu, Y. Zhang, J. Zhu, X. Chen, G. Liu, *Adv. Mater.* **2019**, *31*, 1902530.
[369] J. Wu, W. L. Nyborg, *Adv. Drug Delivery Rev.* **2008**, *60*, 1103.
[370] T. G. Leighton, M. J. W. Pickworth, A. J. Walton, P. P. Dendy, *Phys. Med. Biol.* **1988**, *33*, 1239.
[371] X. Pan, H. Wang, S. Wang, X. Sun, L. Wang, W. Wang, H. Shen, H. Liu, *Sci. China: Life Sci.* **2018**, *61*, 415.
[372] X. Pang, D. Li, J. Zhu, J. Cheng, G. Liu, *Nanomicro Lett.* **2020**, *12*, 144.
[373] W. D. O'brien, C. X. Deng, G. R. Harris, B. A. Herman, C. R. Merritt, N. Sanghvi, J. F. Zachary, *J. Ultrasound Med.* **2008**, *27*, 517.
[374] A. C. Andre, M. Laborde, B. S. Marteyn, *Trends Microbiol.* **2022**, *30*, 643.
[375] S. Swain, R. N. Padhy, T. R. Rautray, *Mater. Chem. Phys.* **2020**, *239*, 122002.
[376] R. Das, S. Langou, T. T. Le, P. Prasad, F. Lin, T. D. Nguyen, *Front. Bioeng. Biotechnol.* **2022**, *9*, 795300.
[377] P. Allawadhi, A. Khurana, S. Allwadhi, U. S. Navik, K. Joshi, A. K. Banothu, K. K. Bharani, *Med. Hypotheses* **2020**, *144*, 110259.
[378] R. Luo, J. Dai, J. Zhang, Z. Li, *Adv. Healthcare Mater.* **2021**, *10*, 2100557.
[379] C. Wang, X. Jiang, H. J. Kim, S. Zhang, X. Zhou, Y. Chen, H. Ling, Y. Xue, Z. Chen, M. Qu, L. Ren, J. Zhu, A. Libanori, Y. Zhu, H. Kang, S. Ahadian, M. R. Dokmeci, P. Servati, X. He, Z. Gu, W. Sun, *Biomaterials* **2022**, *285*, 121479.

[380] B. Liu, R. Fu, Z. Duan, C. Zhu, J. Deng, D. Fan, *Composites, Part B* **2022**, *236*, 109804.
[381] C. Watters, M. Kay, in *Antibiofilm Agents: From Diagnosis to Treatment and Prevention* (Eds: K. P. Rumbaugh, I. Ahmad), Springer, Berlin **2014**, pp. 425–447.
[382] A. H. Delcour, *Annu. Rev. Microbiol.* **2013**, *67*, 179.
[383] Z. Schofield, G. N. Meloni, P. Tran, C. Zerfass, G. Sena, Y. Hayashi, M. Grant, S. A. Contera, S. D. Minteer, M. Kim, A. Prindle, P. Rocha, M. B. A. Djamgoz, T. Pilizota, P. R. Unwin, M. Asally, O. S. Soyer, *J. R. Soc., Interface* **2020**, *17*, 20200013.
[384] H. Strahl, L. W. Hamoen, *Proc. Natl. Acad. Sci. USA* **2010**, *107*, 12281.
[385] J. M. Jones, J. W. Larkin, *Bioelectricity* **2021**, *3*, 116.
[386] C. T. Bot, C. Prodan, *Biophys. Chem.* **2010**, *146*, 133.
[387] S. Pirbadian, M. S. Chavez, M. Y. El-Naggar, *Proc. Natl. Acad. Sci. USA* **2020**, *117*, 20171.
[388] A. Hirose, T. Kasai, M. Aoki, T. Umemura, K. Watanabe, A. Kouzuma, *Nat. Commun.* **2018**, *9*, 1083.
[389] J. P. Stratford, C. L. A. Edwards, M. J. Ghanshyam, D. Malyshev, M. A. Delise, Y. Hayashi, M. Asally, *Proc. Natl. Acad. Sci. USA* **2019**, *116*, 9552.
[390] G. N. Vemuri, M. A. Eiteman, J. E. Mcewen, L. Olsson, J. Nielsen, *Proc. Natl. Acad. Sci. USA* **2007**, *104*, 2402.
[391] M. R. Asadi, G. Torkaman, *Adv. Wound Care* **2014**, *3*, 91.
[392] N. Wellman, S. M. Fortun, B. R. Mcleod, *Antimicrob. Agents Chemother.* **1996**, *40*, 2012.
[393] J. W. Costerton, B. Ellis, K. Lam, F. Johnson, A. E. Khoury, *Antimicrob. Agents Chemother.* **1994**, *38*, 2803.
[394] P. S. Stewart, W. Wattanakaroon, L. Goodrum, S. M. Fortun, B. R. Mcleod, *Antimicrob. Agents Chemother.* **1999**, *43*, 292.
[395] W. d. C. M. A. de Melo, R. Celiešiūtė-Germanienė, P. Šimonis, A. Stirkė, *Virulence* **2021**, *12*, 2247.
[396] J. Qin, X. Sun, Y. Liu, T. Berthold, H. Harms, L. Y. Wick, *Environ. Sci. Technol.* **2015**, *49*, 5663.
[397] R. Kaur, S. Liu, *Prog. Surf. Sci.* **2016**, *91*, 136.
[398] R. Kügler, O. Bouloussa, F. Rondelez, *Microbiology* **2005**, *151*, 1341.
[399] H. Murata, R. R. Koepsel, K. Matyjaszewski, A. J. Russell, *Biomaterials* **2007**, *28*, 4870.
[400] J. Huang, R. R. Koepsel, H. Murata, W. Wu, S. B. Lee, T. Kowalewski, A. J. Russell, K. Matyjaszewski, *Langmuir* **2008**, *24*, 6785.
[401] J. Svenson, R. Karstad, G. E. Flaten, B.-O. Brandsdal, M. Brandl, J. S. Svendsen, *Mol. Pharm.* **2009**, *6*, 996.
[402] Y. Jiao, L.-N. Niu, S. Ma, J. Li, F. R. Tay, J.-H. Chen, *Prog. Polym. Sci.* **2017**, *71*, 53.
[403] L. A. T. W. Asri, M. Crismaru, S. Roest, Y. Chen, O. Ivashenko, P. Rudolf, J. C. Tiller, H. C. Van Der Mei, T. J. A. Loontjens, H. J. Busscher, *Adv. Funct. Mater.* **2014**, *24*, 346.
[404] M. C. Jennings, K. P. C. Minbiole, W. M. Wuest, *ACS Infect. Dis.* **2016**, *1*, 288.
[405] S. Buffet-Bataillon, P. Tattevin, M. Bonnaure-Mallet, A. Jolivet-Gougeon, *Int. J. Antimicrob. Agents* **2012**, *39*, 381.
[406] K. P. C. Minbiole, M. C. Jennings, L. E. Ator, J. W. Black, M. C. Grenier, J. E. Ladow, K. L. Caran, K. Seifert, W. M. Wuest, *Tetrahedron* **2016**, *72*, 3559.
[407] M. E. Forman, M. H. Fletcher, M. C. Jennings, S. M. Duggan, K. P. C. Minbiole, W. M. Wuest, *ChemMedChem* **2016**, *11*, 958.
[408] R. Spohn, L. Daruka, V. Lázár, A. Martins, F. Vidovics, G. Grézal, O. Méhi, B. Kintses, M. Számel, P. K. Jangir, B. Csörgő, Á. Györkei, Z. Bódi, A. Faragó, L. Bodai, I. Földesi, D. Kata, G. Maróti, B. Pap, R. Wirth, B. Papp, C. Pál, *Nat. Commun.* **2019**, *10*, 4538.
[409] K. U. Schallreuter, K. H. Schulz, *Clin. Exp. Dermatol.* **1986**, *11*, 460.
[410] H. L. Shane, E. Lukomska, M. L. Kashon, S. E. Anderson, *Toxicol. Sci.* **2019**, *168*, 508.
[411] B. Yu, C. He, W. Wang, Y. Ren, J. Yang, S. Guo, Y. Zheng, X. Shi, *ACS Appl. Bio Mater.* **2020**, *3*, 5383.
[412] M. E. Hernandez, D. K. Newman, *Cell. Mol. Life Sci.* **2001**, *58*, 1562.
[413] G. Reguera, K. D. Mccarthy, T. Mehta, J. S. Nicoll, M. T. Tuominen, D. R. Lovley, *Nature* **2005**, *435*, 1098.
[414] D. R. Lovley, K. P. Nevin, *Curr. Opin. Biotechnol.* **2013**, *24*, 385.
[415] T. Zhang, T. S. Bain, K. P. Nevin, M. A. Barlett, D. R. Lovley, *Appl. Environ. Microbiol.* **2012**, *78*, 8304.
[416] D. E. Rawlings, D. Dew, C. Du Plessis, *Trends Biotechnol.* **2003**, *21*, 38.
[417] J. Li, G. Wang, H. Zhu, M. Zhang, X. Zheng, Z. Di, X. Liu, X. Wang, *Sci. Rep.* **2014**, *4*, 4359.
[418] G. Wang, H. Feng, A. Gao, Q. Hao, W. Jin, X. Peng, W. Li, G. Wu, P. K. Chu, *ACS Appl. Mater. Interfaces* **2016**, *8*, 24509.
[419] J. Li, H. Zhou, S. Qian, Z. Liu, J. Feng, P. Jin, X. Liu, *Appl. Phys. Lett.* **2014**, *104*, 261110.
[420] A. Halim, A. D. Ariyanti, Q. Luo, G. Song, *Stem Cell Rev. Rep.* **2020**, *16*, 661.
[421] CDC, *Antibiotic Resistance Threats in the United States*, U.S. Department of Health and Human Services, Atlanta, GA **2019**.
[422] M. E. Falagas, A. P. Grammatikos, A. Michalopoulos, *Expert Rev. Anti-Infect. Ther.* **2008**, *6*, 593.
[423] D. M. Livermore, *Clin. Microbiol. Infect.* **2004**, *10*, 1.
[424] Z. K. Zander, M. L. Becker, *ACS Macro Lett.* **2018**, *7*, 16.
[425] G. Thrivikraman, S. K. Boda, B. Basu, *Biomaterials* **2018**, *150*, 60.

Babak Mehrjou received his PhD in materials science and engineering at 2020 from City University of Hong Kong on biomimicked silk-based antibacterial surface and its application on corrosion improvement of magnesium alloy. He is now postdoctoral fellow in the Department of Physics of City University of Hong Kong and his research interests include design of antibacterial surfaces, biopolymers, plasma surface treatment of biomaterials, metal organic frameworks, corrosion improvement of bio-metallics and cartilage tissue engineering.

Yuzheng Wu studied physical chemistry and obtained his research master's degree at University of Chinese Academy of Sciences, China in 2020. He joined the group of Prof. Paul Chu at City University of Hong Kong in 2020 as a Ph.D. student. His research interests include the fabrications of antibacterial surfaces and their application in biomedical field.

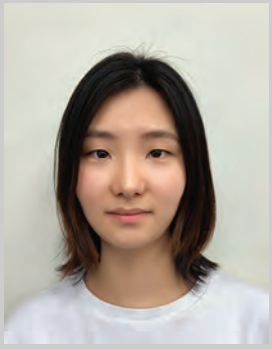

Pei Liu is a Ph.D. student at the department of Physics, City University of Hongkong, and supervised under Prof. Paul K Chu. Her research interest focuses on the design of biomaterials, nanomaterials for antibacterial application.

Guomin Wang received her B.S., M.S. and Ph.D. from Nankai University, Peking University and the City University of Hong Kong, respectively. Guomin's research interests focus on antibacterial materials and multifunctional biomaterials design, with more than 30 publications in journals including *Nature Communications, Advanced Materials, Advanced Science, Advanced Functional Materials and Biomaterials*, etc.

Paul K Chu received his B.S. in mathematics from The Ohio State University and M.S./Ph.D. in chemistry from Cornell University. He is Chair Professor of Materials Engineering in City University of Hong Kong. His research activities are quite diverse spanning plasma and materials science and engineering. He is a highly cited researcher and has received more than 20 scientific/technical awards. He is a fellow of the APS, AVS, IEEE, MRS, and HKIE. He is also a fellow and council member of the Hong Kong Academy of Engineering Sciences (HKAES).